University of Szeged

Faculty of Pharmacy

Doctoral School of Pharmaceutical Sciences

Institute of Pharmacognosy

PhD Thesis

Isolation and structure elucidation of phenanthrenes from *Juncus* species

Dóra Stefkó Pharm.D.

Supervisors:

Andrea Vasas PhD

Szeged, Hungary

2023

LIST OF PUBLICATIONS RELATED TO THE THESIS

I. **Stefkó D**, Kúsz N, Csorba A, Jakab G, Bérdi P, Zupkó I, Hohmann J, Vasas A.
Phenanthrenes from *Juncus atratus* with antiproliferative activity
Tetrahedron **2019**, *75*:116–120.

II. **Stefkó D**, Kúsz N, Barta A, Kele Z, Bakacsy L, Szepesi Á, Fazakas Cs, Wilhelm I, Krizbai I. A, Hohmann J, Vasas A.
Gerardiins A–L and structurally related phenanthrenes from the halophyte plant *Juncus gerardii* and their cytotoxicity against triple-negative breast cancer cells
Journal of Natural Products **2020**, *83*:3058–3068.

III. Kúsz N, **Stefkó D***, Barta A, Kincses A, Szemeredi N, Spengler G, Hohmann J, Vasas A.
Juncaceae species as promising sources of phenanthrenes: antiproliferative compounds from *Juncus maritimus* Lam.
Molecules **2021**, *26*:999.

IV. **Stefkó D**, Kúsz N, Szemerédi N, Barta A, Spengler G, Berkecz R, Hohmann J, Vasas A.
Unique phenanthrenes from *Juncus ensifolius* and their antiproliferative and synergistic effects with the conventional anticancer agent doxorubicin against human cancer cell lines
Pharmaceutics **2022**, *14*:608.

* shared first authorship

LIST OF PUBLICATIONS NOT RELATED TO THE THESIS

I. Orbán-Gyapai O, Liktor-Busa E, Kúsz N, **Stefkó D**, Urbán E, Hohmann J, Vasas A.
Antibacterial screening of *Rumex* species native to the Carpathian Basin and bioactivity-guided isolation of compounds from *Rumex aquaticus*
Fitoterapia **2017**, *118*:101–106.

II. Bús Cs, Tóth B, **Stefkó D**, Hohmann J, Vasas A.
Family Juncaceae: promising source of biologically active natural phenanthrenes
Phytochemistry Reviews, **2018**, *17*:833–851.

TABLE OF CONTENTS

ABBREVIATIONS AND SYMBOLS

1D	one-dimensional
2D	two-dimensional
APCI	atmospheric pressure chemical ionization
CI	Combination Index
COSY	correlated spectroscopy
cryst	crystallization
δ	chemical shift
fr	fraction
GF	gel filtration
HMBC	heteronuclear multiple-bond correlation spectroscopy
HSQC	heteronuclear single-quantum coherence spectroscopy
HPLC	high-performance liquid chromatography
HRE(S)IMS	high-resolution electron (spray) ionization mass spectroscopy
JMOD	*J*-modulated spin-echo experiment
NMR	nuclear magnetic resonance
MS	mass spectroscopy
MPLC	medium pressure liquid chromatography
MTT	3-(4,5-dimethylthiazol-2yl)-2,5-diphenyltetrazolium bromide
NOE	nuclear *Overhauser* effect
NOESY	nuclear *Overhauser* enhancement spectroscopy
NP	normal-phase
OCC	open-column chromatography
PLC	preparative thin-layer chromatography
R_f	retention factor
RP	reversed-phase
RPC	rotation planar chromatography
SD	standard deviation
Seph	Sephadex LH-20 gel chromatography
SI	selectivity index
TLC	thin-layer chromatography
TMS	tetramethylsilane
t_R	retention time
UV	ultraviolet
VLC	vacuum-liquid chromatography

1. INTRODUCTION

Cancer is one of the leading causes of death globally and development of new anticancer agents are in the focus of research worldwide. Natural products are still the best options for finding novel agents/active templates and offer the potential to discover novel structures and new templates that can lead to effective agents in a variety of cancers.[1] Novel biomolecules have an advantage in terms of biosafety, and they can serve as leads for synthetic chemists and pharmacologists. The effective anticancer drugs often work by inhibiting angiogenesis, inducing apoptosis, and blocking cancer cell proliferation. A common feature of phytochemicals is attenuating cancer progression by inhibition of inflammation and induction of apoptosis through caspase-dependent mechanisms or induction of intracellular oxidative stress. Moreover, natural compounds can target multiple key regulators, e.g., in tumor angiogenesis by downregulation of the *in vitro* expression of HIF-1α, VEGF, VEGFR2, p-AKT, p-ERK1/2, MMP9, p-FAK, and p-STAT3.[2] Several molecular targets and the mechanisms of action of natural compounds are already explored and great efforts are performed to increase their efficiency by using structure-based drug design strategies. Ligand based drug design is used when the target is unknown in order to identify the features of potential receptors. The molecular docking of natural compounds with the receptor targets followed by ADMET (Absorption Distribution Metabolism Excretion Toxicity) analysis could also help to increase the hit probability of effective drugs.[3]

Conventional chemotherapy plays an important role in the treatment of cancers, but clinical limitations exist because of dose-limiting side effects and drug resistance. Therefore, combination treatment of chemotherapeutic agents and natural compounds are considered to be a promising therapeutic strategy with a higher clinical efficacy. Doxorubicin is routinely used as a single drug for the treatment of patients with different types of cancer. It intercalates into DNA, stabilizes the topoisomerase II protein, and causes cell death via inhibition of topoisomerase II and generation of reactive oxygen species and free radicals by redox reactions.[4] Although doxorubicin is an effective antineoplastic agent and has cytotoxic effects, resistance limits its use in chemotherapy.[5] A growing body of combination treatments with natural products has been reported to synergistically prevent tumor growth.[4] Besides combination with standard drugs, the efficacy and bioavailability of natural compounds can further increase by applying different formulation techniques. Recent advances in drug delivery systems describe the use of nanoemulsions, nanoparticles, liposomes, and films to carry various phytochemicals such as berberine, curcumin, resveratrol, camptothecins, and celastrol, showing a promising improved anticancer action.[6,7]

A promising group of natural small molecules are phenanthrenes. Phenanthrenes possess noteworthy pharmacological activities, such as antiproliferative, anti-inflammatory, and antimicrobial properties.[8] Among Juncaceae phenanthrenes, dehydroeffusol, juncusol, and juncuenin B seems to be the most promising ones. All of them showed noteworthy antiproliferative effect against different

human cancer cell lines. Dehydroeffusol inhibited dose dependently (12–48 μM) the gastric cancer cell mediated vasculogenic mimicry on SGC-7901 cells. It also decreased the VE-cadherin expression and exposure, suppressed the MMP2 protease expression and activity, and inhibited the gastric cancer cell adhesion, migration, and invasion.[9] Moreover, it inhibited the gastric cell growth and the tumorigenicity through inducing tumor suppressive ER stress responses.[10] The flow cytometric cell-cycle analysis of juncusol showed that juncusol treatment of HeLa cells for 24 h increased the cell population in the G2/M and sub-G1 phases. It also showed pro-apoptotic properties through the presence of active caspase-3, -8, and -9 in HeLa cells, suggesting that juncusol is caused cell death by apoptosis induction and by inhibition of tubulin polymerization *in vitro*.[11] Juncuenin B possessed promising antiproliferative activity (IC_{50} 2.9 μM) against HeLa cells. One of its semisynthetic derivatives, differing only in the presence of a methoxy group at C-8a and a carbonyl group at ring C, showed even higher inhibitory effect (IC_{50} 0.9 μM).[12] In a superoxide anion generation assay, remarkable anti-inflammatory activity was determined for juncusol (IC_{50} 3.1 μM) and juncuenin B (IC_{50} 4.9 μM). The latter also inhibited the elastase release on human neutrophils (IC_{50} of 5.5 μM) in response to fMLP/CB activation.[13]

In 2014, a research program was initiated in the Department of Pharmacognosy, University of Szeged with the aim of investigating the special metabolites of Juncaceae species. This program involves the phytochemical and pharmacological investigation of Juncaceae species occurring mainly in the Carpathian Basin, isolation of biologically active phenanthrenes, and semisynthetic derivatization of the most promising ones. To date, more than 20 species were screened in the framework of this project; biologically active phenanthrenes were isolated from *Juncus compressus*, *J. inflexus*, *J. tenuis*, and *Luzula luzuloides* and semisynthetic derivatives were prepared from juncuenin B, juncusol and effusol. The present thesis summarizes the results of the preparative work on *J. atratus*, *J. ensifolius*, *J. gerardii* and *J. maritimus*.

2. AIMS OF THE STUDY

The family Juncaceae is a plentiful source of phenanthrenes. A few years ago, a research program has been started in the Department of Pharmacognosy, University of Szeged with the aim of investigating the secondary metabolites of plants belonging to the family Juncaceae. The objectives of the present work were the isolation and structural characterization of phenanthrenes, and investigation of their pharmacological effects.

In order to achieve the aims, the main tasks of the presented study were:

- Collection of Juncaceae plant samples (altogether four species).
- Preparation and fractionation of plant extracts.
- Isolation of compounds of *Juncus atratus*, *J. gerardii*, *J. maritimus*, and *J. ensifolius* using a combination of different chromatographic methods.
- Structure determination of the isolated compounds by spectroscopic methods (1D and 2D NMR, HR-MS).
- Investigation of the antiproliferative effect of isolated compounds in different test systems.

3. LITERATURE OVERVIEW

3.1. BOTANY OF THE INVESTIGATED SPECIES

Taxonomically, the family Juncaceae belong in Juncales, and is closely allied with the grasses (Poaceae) and the sedges (Cyperaceae). Juncaceae includes eight genera (*Juncus, Luzula, Oxychloe, Distichia, Patosia, Marsippospermum, Rostkovia, Prionium*) and about 300 species worldwide, mainly in temperate regions. They all have glumaceous, usually complete; pentacyclic, trimerous flowers, and the vast majority are grass-like herbs.[14] The largest genera are *Juncus*, with more than 200 species of which 53 occur in Europe, and *Luzula*, with approx. 75 species of which 31 are represented in Europe.[15] The genus *Juncus* is cosmopolitan but most of its species occur in the northern hemisphere. The genus *Luzula* is also mostly northern in distribution. Main botanical characteristics of the investigated *Juncus* species are summarized in **Table 1**.[15]

Juncus atratus Krock. belongs to the Subgen. *Septati*.[14] It is named for its dark brown, almost black flowers. *J. atratus* is a rare herbaceous perennial in Central European floodplains that has long been known to occur in disturbed habitat patches and in marshy and saline marshes. It blooms from June to August.[16]

Juncus gerardii (Subgen. *Polophylli*) Loisel. (black needle rush) is a high latitude cosmopolitan, and extremely salt tolerant (halophyte) species occurring in saline areas. Within salt marshes of the U.S. mid-Atlantic and New England coasts, it occupies a narrow belt along the marsh-upland border.[17] Halophytes are specialized plants able to survive and thrive in saline soils. Apart from their physiological adaptation, improved biochemical strategies such as improved antioxidant capacity and transporters determine the tolerance against oxidative stress caused by high salinity conditions.[18]

The common name of *Juncus maritimus* (Subgen. *Thalassici*) Lam. is sea rush. It is a perennial herbaceous plant, widespread along salt marshes and meadows. It is widely distributed in Europe, West Africa and North Asia, and commonly occurs along the littoral salt marshes on permanently wet soils. This species is an important component of halophyte meadows in Mediterranean salt and brackish marshes. It has a potential importance in the trophic structure of marsh and estuarine ecosystems.[19] In Hungary, it occurs on the northern part of Lake Balaton.[16]

Juncus ensifolius Wikstr. (Subgen. *Ensifolii*) (swordleaf rush) is an evergreen rhizomatous herb with dark brown flowers. *J. ensifolius* is a ruderal species of rush that occurs as a widespread, frequent to common native wetland plant from near sea level to subalpine elevations throughout western North America and East Asia, readily establishes in disturbed wet soils, often from buried seeds.[14] In Europe, Australia, New Zealand and Hawaii, *J. ensifolius* has apparently become naturalized in the 20th century following gardening and as a contaminant in seed mixes and peat introductions. *J. ensifolius* is a popular and attractive plant in garden ponds.[20] It is produced in horticulture in Hungary.

Table 1. Main botanical characteristics of the investigated *Juncus* species[15]

	J. atratus	*J. gerardii*	*J. maritimus*	*J. ensifolius*
Occurrence	floodplains, marshes and salt marhes C. and E. Europe, northwards to Latvia	salt marshes and damp usually, saline grassland most of Europe	salt marshes and saline meadows coasts of Europe, northwards to Scotland and Sweden locally inland in E. C. Europe and the Mediterranean region	locally naturalized in Finland (North America)
Rhizome	sparingly branched	plant caespitose or with a creeping	creeping sometimes laxly caespitose intravaginal shoots absent	laxly caespitose or with a creeping
Stems	40-120 cm	5-50 cm sometimes compressed	50-100 cm usually, 1.5-2 mm in diameter	25-80 cm compressed and narrowly winged
Sheaths	basal sheaths absent	0-2 basal sheaths		few basal sheaths
Leaves	3-5 cauline 7 to 11 angled adaxial side the widest unitubulose perfectly septate	4-5 basal and 0-2 upper cauline leaves 2-30 cm x 0.5-2.5 mm flat to subterete	2-4 leaves	4-6 cauline 2-5 mm wide
Inflorescence	15-50(-200) heads each 5-10 dark brown flowers	usually, lax	many flowered usually, lax first bract long, forming an apparent prolongation of the stem	1-6 globose many-flowered heads
Perianth segments	2.5-3.5 mm equal or the inner longer than the outer narrowly ovate acuminate	2.5-4 mm equal ovate obtuse	unequal outer ovate more or less boat-shaped acute shortly mucronate inner shorter narrowly elliptical obtuse without auricles	3-4 mm equal or the inner slightly shorter outer narrowly ovate, acuminate inner oblong-lanceolate, acute
Stamens	shorter than perianth	c. 2/3 as long to almost as long as perianth	c. 2/3 as long as perianth	3(-6) c. 1/2 as long as perianth
anthers	0.8-1.3 mm about as long as the filaments	1-2.2 mm 2-6 times as long as the filaments	about twice as long as filaments	0.5-0.8 mm about as long as filaments
Capsule	exceeding the perianth trigonous ovoid abruptly contracted into a long, usually oblique beak	about equaling perianth ovoid to broadly ellipsoid usually trigonous at apex obtuse and mucronate or rarely acute	2.5-3.5 mm trigonous ovoid obtuse or subacute mucronate equaling or slightly exceeding the perianth	equaling or slightly exceeding perianth trigonous-prismatic attenuate into a short mucro
Seeds	0.5-0.7 mm 2*n* = 40	0.4-0.5 mm without appendages 2*n* = 84	0.8-1.2 mm 2*n* = 48	0.6-0.7 mm turbinate to ellipsoid dark and acute at both ends reticulate 2*n* = 40

3.2. CHEMICAL CONSTITUENTS OF THE FAMILY JUNCACEAE

To date, only a small amount (approx. 5%) of Juncaceae species was investigated thoroughly from phytochemical point of view. Earlier phytochemical works were focused on the phenolic content of the plants, as it was observed that in the monocotyledons each family generally has a characteristic pattern of flavonoids; therefore, such analysis can be helpful in assessing both phenetic and phylogenetic relationships within these plants.[21]

Bate-Smith detected caffeic acid in *Juncus ensifolius*, *J. effusus*, *J. inflexus* and *Luzula sylvatica* and quercetin in *L. sylvatica*.[22] Luteolin and its 7-glucoside were identified in different *Juncus* (*J. articulatus*, *J. conglomeratus*, *J. effusus*, *J. filiformis*, *J. gerardii*, *J. tenuis*), and *Luzula* (*L. arcuata*, *L. campestris*, *L. confusa*, *L. forsteri*, *L. lactea*, *L. multiflora*, *L. nivea*, *L. nodulosa*, *L. nutans*, *L. pilosa*, *L. spicata*, and *L. sylvatica*,) species.[23,24] Furthermore, other flavonoids, e.g. apigenin, apigenin 7-*O*-glucoronide, chrysoeriol, hydnocarpin, nobiletin, isorhamnetin-3-*O*-α-L-rhamnopyranosyl(1→6)-β-D-glucopyranoside, narcissin, quercetin, quercetin-3-*O*-α-L-rhamnopyranosyl(1→6)-β-D-glucopyranoside, rutin, kaempferol-3-*O*-α-L-rhamnopyranosyl(1→6)-β-D-glucopyranoside, quercetin-3-*O*-α-L-rhamnopyranoside, quercitrin, quercetin-3-O-β-D-xylopyranoside, luteolin 5-methyl ether, luteolin 5-methyl ether 7-*O*-glucoside, and procyanidin were also identified in some *Juncus* and *Luzula* species. Therefore, flavonoids were considered as the main secondary metabolites, and the most characteristic components of these two genera.[23-27]

Besides flavonoids, *Juncus* species (e.g. *J. bufonius*, *J. effusus*, and *J. gerardii*) contain other types of special metabolites, e.g. phenolic compounds (*p*-coumaric acid, vanillic acid, markhamioside F, canthoside B), coumarins [juncusyl ester A, (2*S*)-1-*O*-*p*-coumaroyl glyceride, 6-hydroxy-7-methyl-5α,8α-benzocoumarin], steroids (β-sitosterol, stigmasterol, α-spinasterol), terpenoids (effusenone A, juncusides I–V), and carotenoids.[28-33]

Besides flavonoids, coumarins, terpenoids and phenolic acid derivatives, nowadays, phenanthrenes and 9,10-dihydrophenanthrenes are considered the most specific chemical constituents of Juncaceae. To date, approx. 100 phenanthrenes were isolated from the members of *Juncus* and *Luzula* genera.[36] Although most probably stilbenes are considered to be the biosynthetic precursors of phenanthrenes and 9,10-dihydrophenanthrenes, up to now only two such compounds (oxyresveratrol 2-*O*-β-D-glucopyranoside and resveratrol 3',4'-*O*,*O*'-di-β-D-glucopyranoside) were identified from a Juncaceae species, *J. acutus*.[33]

3.2.1. Chemical characteristics of natural phenanthrenes isolated in the period of 2018–2022

Occurrence of phenanthrenes in nature is limited to only a few plant families. Among them Orchidaceae and Juncaceae are the most abundant sources of these specific metabolites.[8,34] Phenanthrenes have chemotaxonomical significance, since the presence of certain substituents in

them are apparently restricted to certain families.[35,36] As in 2018 an article was published about the structure and pharmacology of natural phenanthrenes, this section review phenanthrenes isolated from that time.

3.2.1.1. Chemical characteristics of phenanthrenes

In general, phenanthrenes are known as polycyclic aromatic hydrocarbons (PAHs), a class of organic compounds containing two or more fused aromatic rings (linear, cluster, or angular arrangement). They originated from incomplete combustion or pyrolysis of organic matter.[37,38] In particular, the term PAHs refers to compounds solely consist of carbon and hydrogen atoms, whereas the more general term "polycyclic aromatic compounds" also includes the functional derivatives and the heterocyclic analogs. Nowadays, hundreds of PAHs are known; e.g. over 100 PAHs have been identified in atmospheric particulate matter and about 200 in tobacco smoke.[39] This group of compounds have potential harmful effects on ecosystems as well as human health, as many of them have been shown to be carcinogenic, teratogenic and mutagenic.[40] In many cases, plants and associated soil microorganisms are used for phytoremediation, the process that can result in the reduction of the concentrations or toxic effects of these contaminants in the environment.[41]

Besides PAHs, phenanthrenes are synthesized naturally in plants and form a rather uncommon class of aromatic special metabolites with approx. 500 compounds possessing promising biological activities. Their biosynthetic route is not entirely determined; they are presumably formed during oxidative coupling of aromatic rings of stilbene precursors, and they solve as protecting agents for plants against different microorganisms.[42] Other biosynthetic pathways of phenanthrenes are also likely, e.g., diterpenoid origin in case of Euphorbiaceae phenanthrenes or the alkaloids of opium (e.g., morphine, codeine, and thebaine).[43-45]

Natural phenanthrenes may be divided into three major groups: mono-, di- and triphenanthrenes. Monophenanthrenes are further divided according to the saturation of bond between C-9 and C-10 (phenanthrenes and dihydrophenanthrenes), and the number and type of functional groups joining to the skeleton, while di- and triphenanthrenes can be classified by the type of monomers and connection positions of the phenanthrene units.[46] Phenanthrenes have a limited occurrence; the identified compounds were determined from the members of Annonaceae, Aristolochiaceae, Berberidaceae, Cannabaceae, Combretaceae, Dioscoreaceae, Euphorbiaceae, Juncaceae, Lauraceae, Malpighiaceae, Menispermaceae, Orchidaceae and Stemonaceae families.[44,46]

In the past four years, more than 50 new phenanthrenes were isolated mainly from Orchidaceae species, but Dioscoreaceae, Aristolochiaceae, Euphorbiaceae, Berberidaceae, Stemonaceae, Menispermaceae and Juncaceae species also served as sources of this type of compounds (**Figs. 1, 2**, and **Table 2**). The identified compounds are listed based on their structures: monophenanthrenes

(phenanthrenes and dihydrophenanthrenes) and diphenanthrenes (phenanthrenes and dihydrophenanthrenes). The numbers of the compounds are written in italic in order to differentiate from those listed in the Results section of the Thesis. From the identified 53 phenanthrenes, 30 were isolated from Orchidaceae species. The dihydrophenanthrenofuran bleochranols A–D (***34***, ***35***, ***36***, ***45***) were identified from the rhizomes of *Bletilla ochracea*.[47] Phytochemical investigation of *Bletilla striata* resulted in the identification of 10 new phenanthrene derivatives, blestanols A–M (***48***, ***49***, ***50***, ***38***, ***39***, ***40***, ***41***, ***42***, ***44***, ***43***).[48] Two new dihydrophenanthrofurans, dendronbibislines A (***32***) and B (***33***) were isolated from the stems of *Dendrobium nobile*,[49] two further 9,10-dihydroderivatives, dendrocandins P1 (***8***) and P2 (***37***) containing dioxane ring were determined from *Dendrobium officinale*,[50] and finally, dendroinfundins A (***13***) and B (***14***) were isolated from the whole plant of *Dendrobium infundibulum*.[51] The phenanthrene bobulretin A (***6***) and the 9,10-dihydrophenanthrene bobulretin B (***22***) were identified from the whole plants of *Bulbophyllum retusiusculum*.[52] Spiranthesphenanthrenes A–F (***15***, ***23***, ***24***, ***25***, ***26***, ***27***) were isolated from the whole plant of *Spiranthes sinensis*.[53]

Three new phenanthrenes, among them two monomers (***1***, ***3***) and one dimer (***46***) were isolated from the ethyl acetate extract of *Dioscorea bulbifera*.[54] Neomacrodione (***19***), a phenanthroquinone was isolated from an Euphorbiaceae species *Neoboutonia macrocalyx*.[55] Two new phenanthrenes, epicornunis C (***21***) and D (***51***) were isolated from ethanol extract of *Epimedium brevicornu* leaves.[56] Phytochemical investigation of *Stemona parviflora* roots resulted in the identification of six new phenanthrenes (parviphenanthrines A–F, ***4***, ***9***, ***10***, ***11***, ***12***, ***20***).[57] Three new phenanthrenes (epigaeas A–C, ***5***, ***7***, ***47***) were isolated from the roots of *Stephania epigaea*. Epigaea A (***7***) can be considered as an alkaloid containing a phenanthrol-oxazole moiety.[58] Phenanthrenequinone enantiomers, namely bulbocodioidins A–D (***28***, ***29***, ***30***, ***31***) were isolated from the tubers of *Pleione bulbocodioides*.[59] The biphenanthrene atropisomers cremaphenanthrenes F (***52***) and G (***53***) were isolated from the tubers of *Cremastra appendiculata*.[60] Finally, four new phenanthrenes, dehydrojuncunol (***2***), and sylvaticins A–C (***16***, ***17***, ***18***) were isolated from *Luzula sylvatica*.[61]

More than 40% of the currently known naturally occurring phenanthrenes were identified during the past three decades. Tubers, roots, rhizomes, stems, medulla and the whole plants are equally served as sources of phenanthrenes. The majority of these metabolites have been identified from species belonging to the Orchidaceae and Juncaceae families.[8]

The limited occurrence of phenanthrenes gives their importance as chemotaxonomic markers. The presence of certain substitutions could be restricted to specific families; hydroxybenzyl- and stilbene-substituted compounds can be found in Orchidaceae species, vinyl substituted phenanthrenes were reported only from Juncaceae plants, while prenylated derivatives occur mainly in spurges.[8,35]

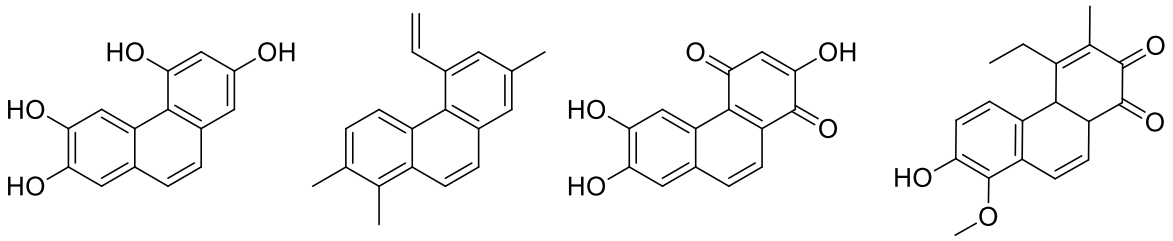

1 ***2*** ***3*** ***4***

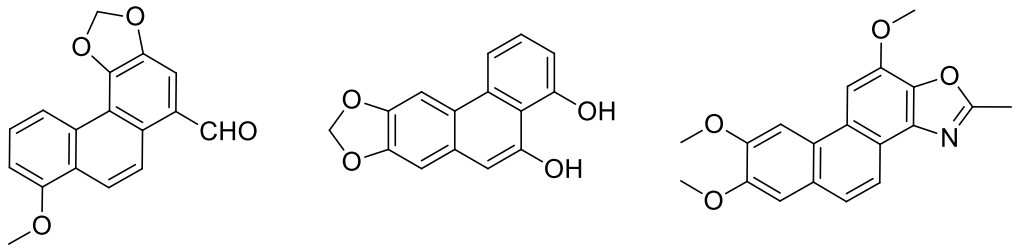

5 ***6*** ***7***

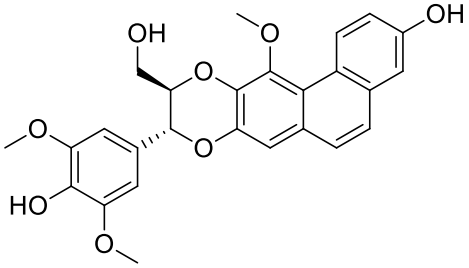

8

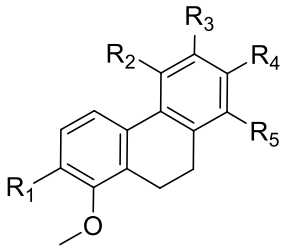

	R_1	R_2	R_3	R_4	R_5
9	OH	OMe	H	OH	H
10	OH	Me	OMe	OMe	H
11	OH	H	OMe	H	OMe
12	OMe	OMe	Me	OH	Me

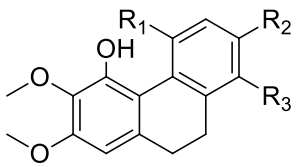

	R_1	R_2	R_3
13	H	OMe	H
14	OH	H	OMe

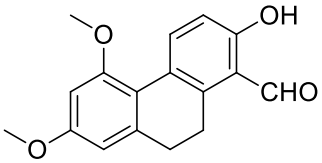

15

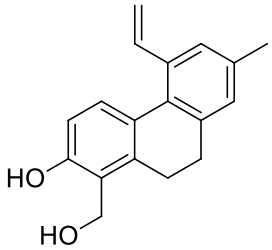

16

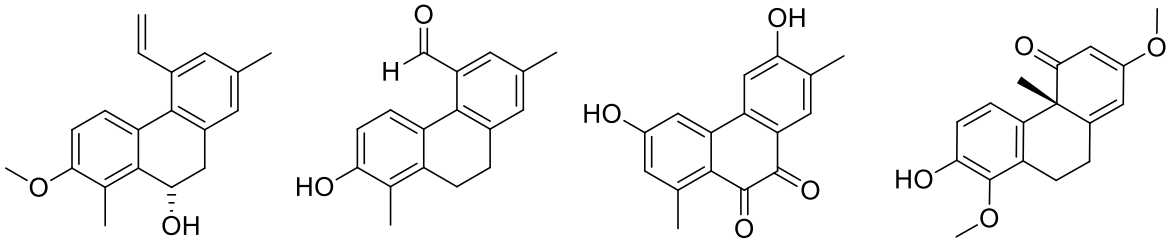

17 ***18*** ***19*** ***20***

Figure 1. Monophenanthrenes isolated from plants between 2018–2022 *Cont*.

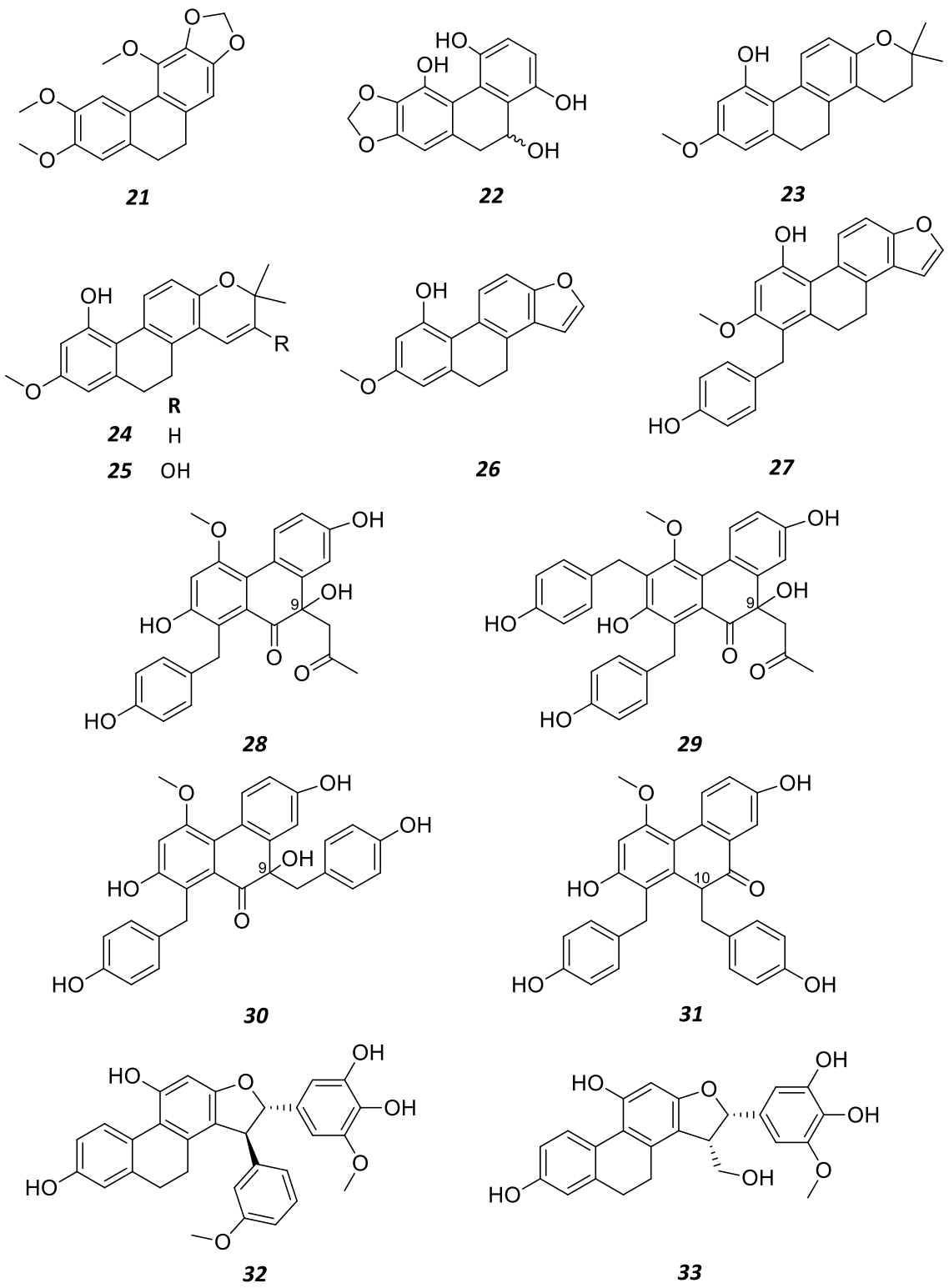

Figure 1. Monophenanthrenes isolated from plants between 2018–2022 *Cont*.

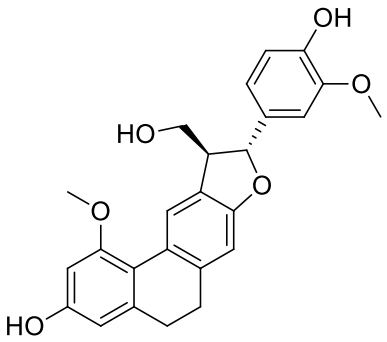

34

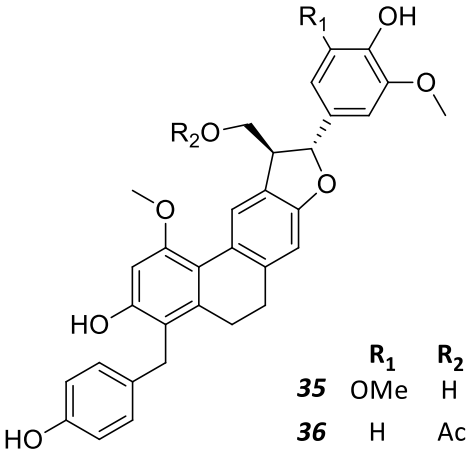

	R_1	R_2
35	OMe	H
36	H	Ac

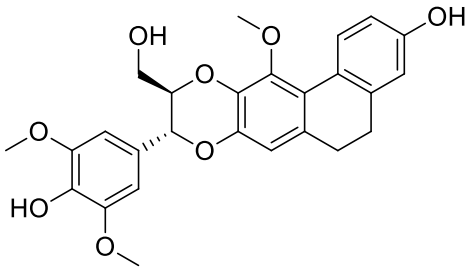

37

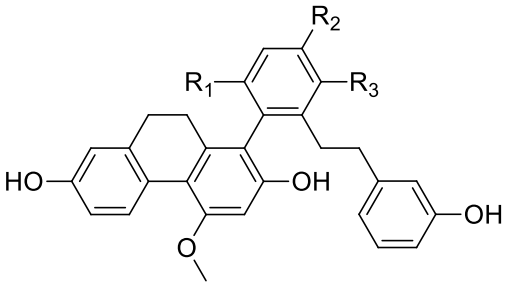

	R_1	R_2	R_3
38	OH	OMe	H
39	OH	OMe	CH_2-*p*-hydroxybenzyl
40	OMe	OH	CH_2-*p*-hydroxybenzyl

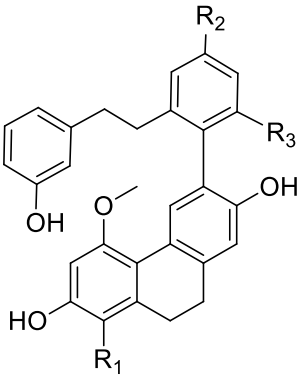

	R_1	R_2	R_3
41	H	OMe	OH
42	CH_2-*p*-hydroxybenzyl	OH	OMe

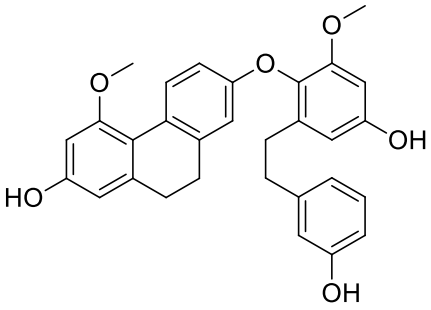

43

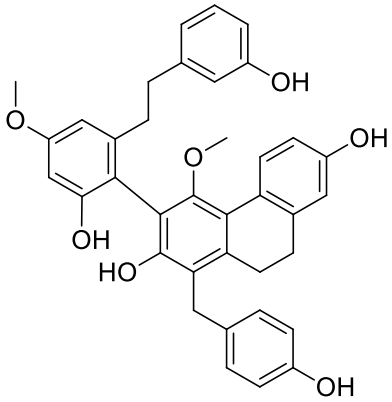

44

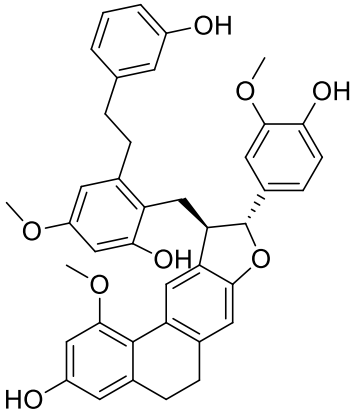

45

Figure 1. Monophenanthrenes isolated from plants between 2018–2022

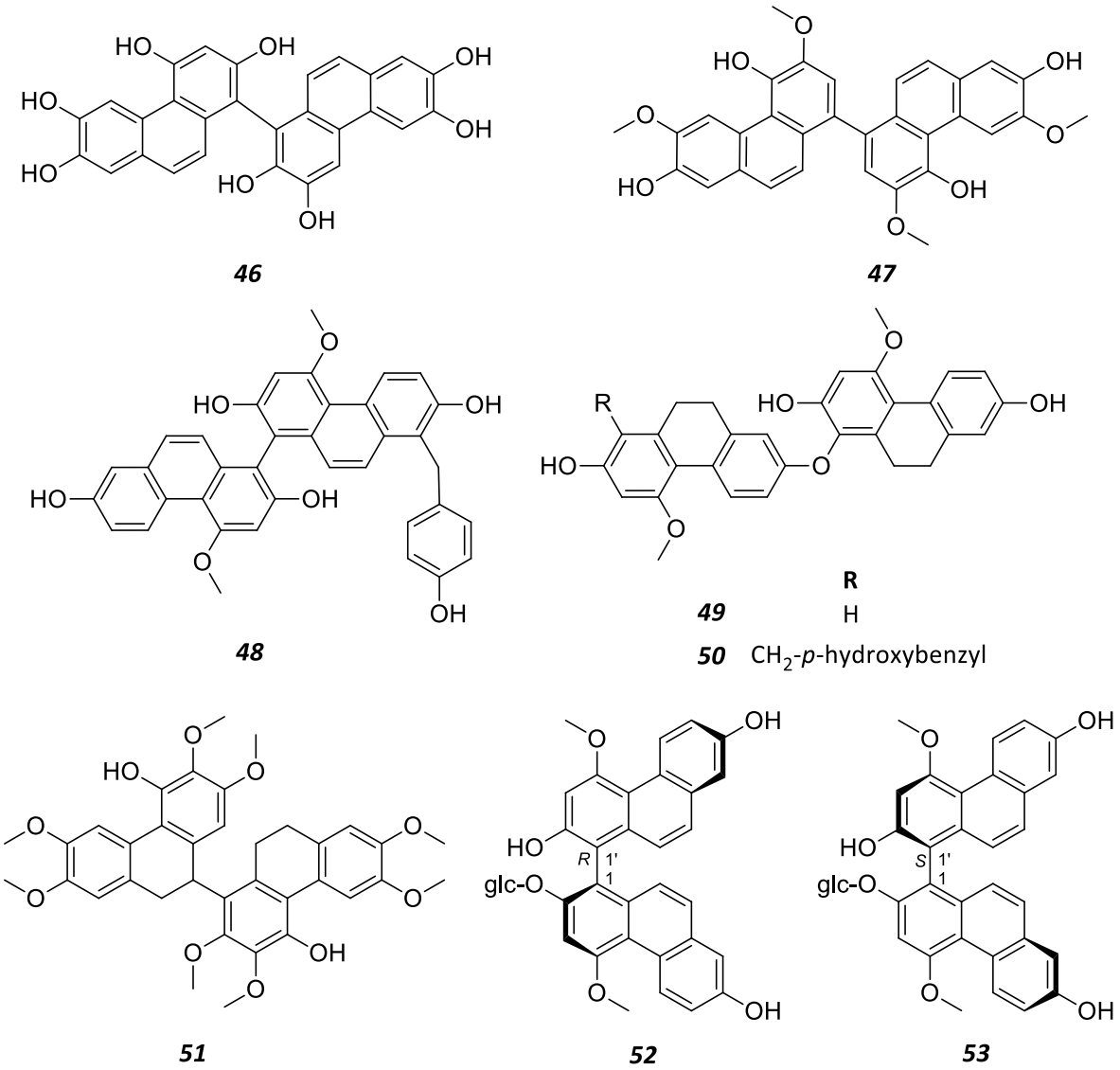

Figure 2. Diphenanthrenes isolated from plants between 2018–2022

Table 2. Plant families and species phenanthrenes isolated from in the period 2018–2022

Family	Species	Compound	Ref.
Berberidaceae	*Epimedium brevicornu*	***21***, ***51***	[56]
Dioscoreaceae	*Dioscorea bulbifera*	***1***, ***3***, ***46***	[54]
Euphorbiaceae	*Neoboutonia macrocalyx*	***19***	[55]
Juncaceae	*Luzula sylvatica*	***2***, ***16***–***18***	[61]
Menispermaceae	*Stephania epigaea*	***5***, ***7***, ***47***	[58]
Orchidaceae	*Bletilla ochracea*	***34***–***36***, ***45***	[47]
	Bletilla striata	***38***–***44***, ***48***–***50***	[48]
	Bulbophyllum retusiusculum	***6***, ***22***	[52]
	Cremastra appendiculata	***52***, ***53***	[60]
	Dendrobium infundibulum	***13***, ***14***	[51]
	Dendrobium nobile	***32***, ***33***	[49]
	Dendrobium officinale	***8***, ***37***	[50]
	Spiranthes sinensis	***15***, ***23***–***27***	[53]
Stemonaceae	*Stemona parviflora*	***4***, ***9***–***12***, ***20***	[57]

3.2.2. Chemical constituents of *Juncus atratus*

This plant has not been invetstigated previously from phytochemical and pharmacological points of view.

3.2.3. Chemical constituents of *Juncus gerardii*

J. gerardii is a halophyte species, possesses specialized antioxidant system, including enzymes and bioactive compounds, allow to produce a plethora of further interesting biological activities.[62] Extensive phytochemical investigations of this plant have not been reported previously.

3.2.4. Chemical constituents of *Juncus maritimus*

A bioactivity-guided separation resulted in the isolation of effusol, juncusol and dehydrojuncusol from the methanol extract prepared from the rhizomes of the plant.[63,64]

3.2.5. Chemical constituents of *Juncus ensifolius*

Extensive phytochemical investigations of this plant have not been reported previously. Bate-Smith reported the presence of caffeic acid in *J. ensifolius*.[22]

3.3. PHARMACOLOGY OF PHENANTHRENES

Several naturally derived phenanthrenes were tested for their biological activities, and many of them showed remarkable antiproliferative, antimicrobial, anti-inflammatory, spasmolytic, and anxiolytic effects *in vitro*. Among them denbinobin, isolated from an orchid, *Dendrobium nobile* can be considered as the most promising one, because of its complex mechanisms of action, involving apoptosis-induction through caspase-dependent and -independent ways; activation of proapoptotic Bax protein, and inactivation of Bcl-2; blocking of the NF-κB activation; enhancing the synthesis of reactive oxygen species (ROS); reducing Src kinase activity; inhibition of calcium-binding cell migration protein (S100A8), and downregulation of matrix metalloproteinases MMP-2 and MMP-9.[65-67]

Enzyme inhibitory activity:

A biphenanthrene (***46***), isolated from *D. bulbifera*, exhibited promising dual inhibitory activity towards α-glucosidase and protein-tyrosine phosphatase 1B (PTP1B) with IC_{50} values of 2.08 and 3.36 μM, respectively.[54] Phenanthrenes isolated from the fresh rhizomes of *Tamus communis* (syn. *Dioscorea communis*) were investigated for their acetylcholinesterase (AChE) and butyrylcholinesterase (BChE) inhibitory activities. 2,4-Dimethoxy-7,8-methylendioxy-3-phenanthrenol and 2,4,8-trimethoxy-3,7-phenanthrenediol inhibited BChE with IC_{50} values 11.4 and 14.6 μg/mL, respectively (positive control galantamine IC_{50} 34.8 μg/mL).[68] The biphenanthrene glycoside cremaphenanthrene F (***52***) showed potent BChE inhibitory effect with IC_{50} of 14.62 μM. Interestingly, its atropisomer ***53*** exhibited only weak activity. Both compounds were inactive for AChE inhibition.[60]

Anti-inflammatory activity:

2,7-Dihydroxy-4,6-dimethoxyphenanthrene and 6,7-dihydroxy-2,4-dimethoxyphenanthrene from the peel of *Dioscorea batatas* were proved to be active against particulate matter 2.5 ($PM_{2.5}$)-induced pulmonary injury in mice. The compounds exhibited significant scavenging activity against $PM_{2.5}$-induced ROS and inhibited ROS-induced activation of p38 mitogen-activated protein kinase. Moreover, they reduced vascular protein leakage, leukocyte infiltration, and proinflammatory cytokine release in the bronchoalveolar lavage fluid obtained from $PM_{2.5}$-induced lung tissues.[69] Dehydrojuncunol (***2***) and sylvaticin B (***17***) inhibited ROS production of blood leucocytes significantly in a dose-dependent manner.[61] Blestanols D (***38***), F (***40***) and H (***42***) showed anti-neuroinflammatory activity against LPS-stimulated BV-2 cells with IC_{50} values 5.6, 9.3 and 5.0 μM, respectively (positive control curcumin IC_{50} 3.8 μM). The dimeric 9,10-dihydrophenanthrenes blestriarene A and gymconopin C, also isolated from *B. striata* exhibited potent inhibitory activity against NO production with IC_{50} values 5.1 and 10.6 μM.[48] 6,7-dihydroxy-2,4-dimethoxyphenanthrene obtained from *Dioscorea opposita* (syn. Chinese yam) was tested against DSS-induced (dextran sulfate sodium) intestinal mucosal injury in mice. It was observed that administration of the compound downregulated the oxidative stress-associated factors (MPO and NO) and improved tight junction protein occludin. Moreover, it also decreased the caspase-3 expression and the apoptosis rate of intestinal epithelial cells, ameliorated the production of inflammatory cytokines including TNF-α, IFN-γ, IL-10, and IL-23 in the colon, and suppressed the protein expression of ERK/2, NF-κB, and COX-2. Therefore, 6,7-dihydroxy-2,4-dimethoxyphenanthrene protected intestinal mucosa from damage.[70]

Antimicrobial activity:

Trigonostemone, isolated from the roots of *Strophioblachia fimbricalyx* (Euphorbiaceae), exhibited inhibitory effect on the growth of the Gram-positive methicillin-susceptible *Staphylococcus aureus* (MSSA), methicillin-resistant *Staphylococcus aureus* (MRSA) and *Bacillus cereus* with the MIC/MBC (minimum bactericidal concentration) values of 12.5/25.0, 6.25/25 and 6.26/6.25 mg/mL, respectively. The compound possessed time- and concentration-dependent bactericidal activity against *B. cereus*, and it caused bacteriostatic activity against *S. aureus* (MSSA) at the concentration of 2 × MIC by changing cell morphology and bactericidal activity against *B. cereus* at the concentration of 2 × MIC after 4 h by inducing cell size variation, respectively.[71] Neomacrodione (***19***) displayed moderate antibacterial activity against *S. aureus* (MIC = 12.5 μg/mL), *Enterococcus faecalis* (MIC = 25 μg/mL) and *Salmonella typhimurium* (MIC = 12.5 μg/mL).[55]

Parviphenanthrines A (***20***) and E (***11***) showed nematocidal activity against *Meloidogyne incognita* with IC_{50} values of 14.02 and 2.51 μM, respectively.[57]

Cytotoxic activity:

Dendronbibislines A (***32***) and B (***33***) shown cytotoxic activity against HepG2 human hepatic cell line with IC_{50} values 4.81 and 19.47 μM, respectively.[49] The dimer epicornunin D (***51***) exhibited higher cytotoxic activity (IC_{50} 32.7 μM), than the positive control 5-fluorouracil (IC_{50} 40.5 μM) against HepG2 cells.[56] The cytotoxic activity of blestanols A–M (***38***–***44***, ***48***–***50***) and other phenanthrenes, isolated from *B. striata*, were tested against colon (HCT-116), liver (HepG2), stomach (BGC-823), lung (A549), and glioma (U251) cancer cell lines using the MTT method. Blestanol H (***42***), blestriarene A, 4,4',7,7'-tetrahydroxy-2,2'-dimethoxy-1,1'-biphenanthrene, 4,4'-dimethoxy-9,10-dihydro-[6,1'-biphenanthrene]-2,2',7,7'-tetraol, and bulbocodiolidin H showed cytotoxicity against several of the cancer cell lines, with IC_{50} values ranging from 1.4 to 8.3 μM, respectively.[48] Bleochranol A (***45***) showed remarkable cytotoxic activity against HL-60, A-549, and MCF-7 cells with IC_{50} values of 0.24, 3.51 and 3.30 μM, respectively.[47] Spiranthesphenanthrene A (***23***) showed higher cytotoxic activity (IC_{50} 19.0 μM) against the B16–F10 (murine melanoma) cell line than the positive control cisplatin (IC_{50} 26.8 μM).[53] The compound was also inhibited the migration of B16–F10 cancer cells in a time- and dose-dependent manner. It increased the level of the E-cadherin protein and decreased the levels of the vimentin and N-cadherin proteins. Moreover, the level of the transcription factor Snail was also decreased by compound ***23*** in a dose-dependent manner.[53]

Pharmacology of Juncaceae phenanthrenes

Among Juncaceae phenanthrenes, dehydroeffusol, juncusol, and juncuenin B seem to be the most promising ones. All of them showed a noteworthy antiproliferative effect against different human cancer cell lines. Dehydroeffusol dose dependently (12–48 μM) inhibited gastric cancer cell-mediated vasculogenic mimicry in SGC-7901 cells. It also decreased VE-cadherin expression and exposure, suppressed the MMP2 protease expression and activity, and inhibited gastric cancer cell adhesion, migration, and invasion.[9] Moreover, it inhibited the gastric cell growth and the tumorigenicity by inducing tumor-suppressive ER stress responses.[10] The flow cytometric cell-cycle analysis of juncusol showed that juncusol treatment of HeLa cells for 24 h increased the cell population in the G2/M and sub-G1 phases. It also showed pro-apoptotic properties through the presence of active caspase-3, 8, and 9 in HeLa cells, suggesting that juncusol causes cell death by apoptosis induction and inhibition of tubulin polymerization *in vitro*.[11] Juncuenin B possessed promising antiproliferative activity (IC_{50} 2.9 μM) against HeLa cells. One of its semisynthetic derivatives, differing only in the presence of a methoxy group at C-8a and a carbonyl group at ring C, showed an even higher inhibitory effect (IC_{50} 0.9 μM).[12] In a superoxide anion generation assay, remarkable anti-inflammatory activity was determined for juncusol (IC_{50} 3.1 μM) and juncuenin B (IC_{50} 4.9 μM). The latter also inhibited elastase release in human neutrophils (IC_{50} of 5.5 μM) in response to fMLP/CB activation.[13]

In the past few years, only a few pharmacological investigations were performed with Juncaceae species. The crude extract of *Juncus maritimus* was proved to exhibit high antiviral activity against HCV cells *in vitro*. Its phenanthrene constituent dehydrojuncusol was responsible for this effect as it significantly inhibited HCV infection when added after virus inoculation of HCV genotype 2a (EC_{50} = 1.35 μM) and was also efficient on HCV genotype 3a. Dehydrojuncusol was able to inhibit RNA replication of two frequent daclatasvir-resistant mutants (L31M and Y93H in NS5A) showing that NS5A (nonstructural protein 5A) protein is the target of the molecule.[64]

Effusol showed strong antifungal activity (MIC value 19 μg/mL) against *Zymoseptoria tritici*, the most important pathogen of wheat, responsible for Septoria tritici blotch.[63]

The crude extract of *J. maritimus* was shown to exhibit high antiviral activity against HCV in cell culture. Dehydrojuncusol was determined as the active compound of the extract. This compound was able to inhibit infection of different HCV genotypes (2a and 3a with EC_{50}s 1.35 μM and 9.91 μM, respectively) by targeting the NS5A protein and is active against resistant HCV variants frequently found in patients with treatment failure.[63]

Cytotoxic effect of dehydrojuncunol (***2***), and sylvaticins A–C (***16***–***18***) were tested in THP-1 human monocytic leukemia cell line, and compounds ***2***, ***16*** and ***17*** showed remarkable effect with IC_{50} values 3, 11 and 10 μM, respectively.[61]

4. MATERIALS AND METHODS

4.1. PLANT MATERIAL

Juncus atratus Krock. (dried whole plant, 3.1 kg) was collected during the flowering period in 2015, near Békéscsaba (GPS coordinates: 46°38’0.80”N; 21°8’26.71”E) (Hungary). Botanical identification of the plant material was performed by Gusztáv Jakab (Institute of Environmental Sciences, Szent István University, Szarvas, Hungary).

Juncus gerardii Loise. (dried whole plant, 3.6 kg) was collected during the flowering period in 2017, near Mórahalom (GPS coordinates: 46°12.017”N; 019°58.955”E) (Hungary). Botanical identification of the plant material was performed by László Bakacsy (Department of Plant Biology, University of Szeged, Szeged, Hungary).

Juncus maritimus Lam. (dried whole plant, 2.2 kg) was collected in June 2018, near Vir (coordinates: 44°31’80.74” N; 15°05’72.00” E) (Croatia), and identified by László Bakacsy (Department of Plant Biology, University of Szeged, Szeged, Hungary).

*Juncus ensifoliu*s Wikstr. samples (dried whole plant, 3.1 kg) were bought from a horticulture (Mocsáry Évelőkertészet, Tárnok, Hungary) in August 2019.

Voucher specimens [No. 877 (*J. atratus*), 881 (*J. gerardii*), 884 (*J. maritimus*) and 890 (*J. ensifolius*)] have been deposited at the Department of Pharmacognosy, University of Szeged, Szeged, Hungary.

4.2. General extraction and isolation procedures

Open-column chromatography: OCC was performed on polyamide (MP Biomedicals).

Vacuum-liquid chromatography: For normal phase VLC, silica gel 60 G (15 μm, Merck) was used. LiChroprep RP-18 (40–63 μm, Merck) stationary phase was used for reversed phase VLC.

Gel filtration chromatography: Sephadex LH-20 (25–100 μm, Sigma-Aldrich) was used for gel filtration.

Medium pressure liquid chromatography: MPLC was performed by a Combi Flash Rf$^+$ Lumen instrument (Teledyne Isco) on a reversed-phase RediSep Rf HP Gold (50 g) column.

High-performance liquid chromatography: HPLC was carried out on a Shimadzu LC-10AT pump interface equipped with a Shimadzu SPD-20A UV-Vis detector using Luna® Phenyl-Hexyl column (250 × 10 mm, 5 μm) and on a Waters HPLC, using normal [Phenomenex Luna Silica (3 μm, 100 A)] and reversed-phase [Phenomenex, Kinetex 5 μm, C18 100 A, and LiChrospher LiChroCART 250-4 RP-18 (5 μm)] columns. For the investigation of compounds with chiral carbon atoms, a Lux amylose-1 column (250 × 21.2 mm) (Phenomenex, USA) was used with cyclohexane–isopropanol (85:15) as the mobile phase.

Thin-layer chromatography: Preparative thin-layer chromatography (PLC) was performed on silica gel 60 F_{254} plates (Merck) as well as on reversed-phase silica gel 60 RP-18 F_{254} plates (Merck). Separation was monitored in UV light at 254 nm and 366 nm. Compounds were eluted from the scraped adsorbent with CH_2Cl_2–MeOH (4:1). The OCC, VLC, PLC, MPLC fractions obtained were monitored by TLC on silica gel 60 F_{254} (Merck 105554) and on reversed phase silica gel 60 F_{254} (Merck 105559).

Visualization methods: UV light at 254 nm and 366 nm, and at daylight after spraying with vanillin-sulfuric acid reagent and heating at 120 °C for 5 min.

4.3. Structure determination of the isolated compounds

Optical rotations were determined in MeOH or in $CHCl_3$ at room temperature with a Perkin-Elmer 341 and JASCO P-2000 polarimeter.

NMR spectra were recorded in CD_3OD, $CDCl_3$, and DMSO-d_6 on a Bruker Avance DRX 500 spectrometer at 500 MHz (^{1}H) and 125 MHz (^{13}C). The signals of the deuterated solvents were considered reference points. Chemical shift values (δ) of the reported compounds were given in ppm, and coupling constant values (J) were reported in Hz. Two-dimensional (2D) experiments were

performed with standard JEOL or standard Bruker software. In the ^{1}H-^{1}H COSY, HSQC and HMBC experiments, gradient-enhanced versions were applied.

The high-resolution MS spectra were acquired on a Thermo Scientific Q-Exactive Plus orbitrap mass spectrometer equipped with ESI ion source in positive ionization mode. The data were acquired and processed with MassLynx software.

APCI-MS measurements were performed on an API 2000 Triple Quad mass spectrometer (AB SCIEX, Framingham, MA, USA) with an atmospheric pressure chemical ionization (APCI) interface, using positive and negative polarity. The source temperature was 350 °C and the samples were dissolved in CH_3CN.

4.4. PHARMACOLOGICAL TESTS

Pharmacological investigations (antiproliferative, synergism with doxorubicin) were performed in cooperation with the Department of Pharmacodynamics and Biopharmacy, University of Szeged, the Department of Medical Microbiology, Albert Szent-Györgyi Medical School, University of Szeged and Institute of Biophysics, ELKH Biological Research Centre, Szeged. The synergism test was performed by the author.

The antiproliferative properties of the isolated phenanthrenes were determined on a panel of human malignant cell lines:

- *J. atratus*: HeLa, SiHa (cervix), MDA-MB-231 (breast)
- *J. gerardii*: 4T1 (mouse triple-negative breast), MDA-MB-231 (human triple-negative breast), D3 (nontumor human cerebral microvascular endothelial cells)
- *J. maritimus*: HeLa (cervix), MCF-7, KCR, HTM-26 (breast), T-47D (ductal), A2780, A2780cis (ovarian), MRC-5 (normal human fetal lung fibroblast)
- *J. ensifolius*: HeLa (cervix), COLO 205, COLO 320 (colon), MRC-5 (normal human fetal lung fibroblast cells)

Antiproliferative effects were measured by means of the MTT assay. Cisplatin and doxorubicin were used as positive controls. The reduced MTT was assayed at 545 nm, using a microplate reader, and the IC_{50} values were calculated utilizing GraphPad Prism 4.0. All *in vitro* experiments were carried out on two microplates with five parallel wells. Stock solutions of the tested compounds (10 mM) were prepared in DMSO. The highest DMSO content of the medium (0.3%) did not have any substantial effect on the cell proliferation. In case of *J. ensifolius*, the active compounds were tested in combination with doxorubicin on HeLa cell lines.

5. RESULTS

5.1. ISOLATION OF PHENANTHRENES

In all four cases, the air-dried and ground plant material were percolated with MeOH at room temperature. The crude methanol extracts were concentrated under reduced pressure, dissolved in 50% aqueous methanol, and subjected to solvent–solvent partitioning with *n*-hexane (*J. gerardii* and *J. ensifolius*, and *J. maritimus*), CH_2Cl_2 (*J. atratus*) or $CHCl_3$ (*J. gerardii*, *J. maritimus* and *J. ensifolius*) and EtOAc.

5.1.1. Isolation of phenanthrenes from *J. atratus*

The concentrated CH_2Cl_2-soluble fraction (98.3 g) was separated on a polyamide column (OCC) with gradient system of MeOH–H_2O [1:1, 2:1 (8 L and 10 L, respectively), each eluent was collected as a fraction (I. and II.)] (**Annex I**). Phenanthrenes were enriched in fraction II. (27.7 g), therefore, it was subjected to NP-VLC on silica gel with a gradient system of cyclohexane–EtOAc–MeOH [from 98:2:0 to 1:1:1 (1500 mL/eluent), and finally with MeOH; volume of collected fractions were 100 mL] to yield 15 major fractions (II/1–15). The fractions were combined according to their TLC patterns. Fraction II/4 (1.59 g) was separated by RP-VLC with a gradient system of MeOH–H_2O [from 1:1 to 98:2 (500 mL/eluent), and finally MeOH (200 mL); each fractions was 50 mL] to yield fractions eight subfractions II/4/1–8. Subfraction II/4/8 was pure and resulted in compound **6** (10.2 mg). Fraction II/8 (494.0 mg) was also purified by RP-VLC, using a gradient system of MeOH–H_2O [from 1:1 to 95:5 (500 mL/eluent), and finally MeOH (200 mL); volume of collected fractions was 50 mL)] and seven subfractions (II/8/1–7) were obtained. Subfraction II/8/2 resulted in pure compound **3** (3.5 mg).

RP-VLC was used for the separation of fraction II/9 (928.3 mg). The fraction was eluted by a gradient system of MeOH–H_2O [from 1:1 to 98:2 (500 mL/eluent), and finally MeOH (150 mL); volume of collected fractions was 50 mL] to afford nine subfractions (II/9/1–9). Further purification of subfraction II/9/2 was made by RP-HPLC under gradient conditions, using MeOH–H_2O (3:2 to 9:1 in 10 min) as mobile phase, at a flow rate of 1.0 mL/min to yield compound **1** (t_R = 8.6 min, 3.2 mg). By the use of PLC on silica gel with cyclohexane–EtOAc–EtOH (60:30:3) as solvent system compound **4** (3.2 mg) was isolated. Subfraction II/9/5 resulted in the pure compound **2** (48.1 mg). Subfraction II/9/6 contained the pure compound **5** (122.6 mg). Fraction II/11 (194.1 mg) was also separated by RP-VLC [MeOH–H_2O gradient system from 1:1 to 98:2 (150 mL/eluent), and finally MeOH (100 mL); volume of collected fractions was 20 mL] to afford five combined fractions (II/11/1–5). Fraction II/11/3 (7.1 mg) was purified by PLC on silica gel using cyclohexane–EtOAc–EtOH (60:30:3) as solvent system to yield compound **7** (4.8 mg). Finally, fraction II/13 (1.05 g) was purified by RP-VLC, using a gradient system of MeOH–H_2O [from 1:1 to 9:1 (500 mL/eluent), and finally MeOH (100 mL); volume of collected fractions

was 50 mL] to afford six combined fractions (II/13/1–6). Fraction II/13/3 (65.9 mg) was further purified by Sephadex LH-20 gel chromatography using CH_2Cl_2–MeOH (1:1) as solvent system to yield compounds **8** (22.3 mg) and **9** (24.9 mg).

5.1.2. Isolation of phenanthrenes from *J. gerardii*

The concentrated chloroform-soluble fraction (52 g) was separated by polyamide OCC with gradient system of MeOH–H_2O {2:3 (**A**), 3:2 (**B**), 2:1 [10 L (**C**), 8 L (**D**) and 8 L (**E**), respectively], each eluent was collected as a fraction} (**Annex I**). Fraction **B** (12 g) was subjected to VLC on silica gel with a gradient system of cyclohexane–EtOAc–MeOH [from 98:2:0 to 1:1:1 (1500 mL/eluent) and finally with MeOH; volume of collected fractions was 100 mL], to yield 16 major fractions (B/1−16). The fractions were combined according to their TLC patterns.

Fractions B/1–3 (45.5, 21.5, and 38.9 mg, respectively) were purified using Sephadex LH-20 gel chromatography with CH_2Cl_2–MeOH (1:1) as eluent to yield compounds **17** (1.2 mg) and **22** (5.8 mg) and from B/1, **23** (6.8 mg) from B/2, and compound **11** (11.8 mg) from B/3. Fraction B/4 (1.64 g) was separated by RP-MPLC using a gradient system of MeOH–H_2O [from 1:1 to 1:0 (40 mL/min); volume of collected fractions was 20 mL], to yield eight subfractions (B/4/1−8). Subfractions B/4/2 and B/4/4 were pure for compounds **4** (1.3 g) and **24** (185 mg), respectively. Fraction B/6 (494.0 mg) was also separated by RP-MPLC, using a gradient system of MeOH–H_2O [from 1:1 to 1:0 (40 mL/min); volume of collected fractions was 20 mL)], to afford eight subfractions (B/6/1−8). Subfractions B/6/2 (31.8 mg) and B/6/5 (42.6 mg) were purified by PLC on silica gel using cyclohexane–EtOAc–EtOH (20:10:1) as solvent system to yield compounds **10** (2.1 mg) and **5** (3.9 mg). Subfraction B/6/6 contained compound **25** (109 mg). Fraction B/7 (771.1 mg) was separated by RP-MPLC with a gradient system of MeOH−H_2O [from 1:1 to 1:0 (40 mL/min); volume of collected fractions was 20 mL] to yield 11 subfractions (B/7/1−11). Fraction B/7/2 (179.5 mg) was purified by Sephadex LH-20 gel chromatography using CH_2Cl_2–MeOH (1:1) as solvent system to afford five subfractions (B/7/2/1−5). Further purification of subfraction B/7/2/4 by NP-HPLC under gradient conditions, using cyclohexane–EtOAc (9:1 to 1:9 in 10 min at a flow rate of 1.5 mL/ min) as a mobile phase, yielded two fractions (t_R = 7.5 min and t_R = 7.9 min), which were purified by PLC on silica gel using cyclohexane–EtOAc–EtOH (20:10:1) as solvent system to yield compounds **26** (3.1 mg) and **27** (2.0 mg). Fraction B/7/6 (8.6 mg) was purified by PLC on silica gel using cyclohexane–EtOAc–EtOH (20:10:1) as mobile phase to yield compound **20** (6.2 mg). Fractions B/8 (63 mg), B/9 (230.2 mg), B/12 (421.3 mg) and B/14 (548.6 mg) were separated by Sephadex LH-20 gel chromatography using CH_2Cl_2−MeOH (1:1) as solvent system to yield compounds **21** (5.5 mg, from B/8), **29** (8.2 mg, from B/9/2), **6** (18.7 mg, from B/12/2), and **7** (22.8 mg, from B/14/2). Fraction B/10 (154.5 mg) was purified by Sephadex LH-20 gel chromatography using CH_2Cl_2−MeOH (1:1) as solvent system to afford six subfractions (B/10/1−6). Fraction B/10/4 (30.1 mg) was purified by

preparative TLC on silica gel using CH_2Cl_2−MeOH (9:1) as solvent system to yield compound **14** (9.2 mg). Fraction B/11 (474.1 mg) was purified by Sephadex LH-20 gel chromatography using CH_2Cl_2−MeOH (1:1) as solvent system to afford four subfractions (B/11/1−4). Fractions B/11/2 (112.2 mg) and B/11/ 3 (54.6 mg) were further purified by preparative TLC on silica gel using CH_2Cl_2−MeOH (9:1) as solvent system, to yield compounds **31** (9.2 mg) and **28** (11.8 mg). Fractions B/12 (421.3 mg) and B/14 (548.6 mg) were purified on Sephadex LH-20 gel column using CH_2Cl_2–MeOH as eluent. Subfractions B/12/2 and B/14/2 afforded pure compounds **6** and **7**.

The fraction obtained from the polyamide column with MeOH−H_2O 2:1 (3 g) was subjected to VLC on silica gel with a gradient system of cyclohexane−EtOAc−MeOH [from 95:5:0 to 1:1:1 (200 mL/eluent), and finally with MeOH; the volumes of the collected fractions were 50 mL], to yield six major fractions (D/1−6). Fraction D/4 (130.1 mg) was purified by Sephadex LH-20 gel chromatography applying CH_2Cl_2−MeOH (1:1) as eluent to afford four subfractions (D/4/1−4). Subfraction D/4/4 (15.8 mg) was purified by PLC on silica gel using CH_2Cl_2−MeOH (9:1) as solvent system to yield **18** (5.9 mg). Fraction D/5 (124 mg) was purified by Sephadex LH-20 gel chromatography using CH_2Cl_2−MeOH (1:1) as eluent to afford four subfractions (D/5/1−4). Further purification of subfraction D/5/3 was performed by RP-HPLC under gradient conditions, using CH_3CN−H_2O (from 55:44 to 7:3 in 11 min as mobile phase, flow rate 1.5 mL/min), resulted in the isolation of compound **30** (t_R = 8.1 min, 4.6 mg). Fraction D/5/4 (20.1 mg) was purified by PLC on silica gel using CH_2Cl_2−MeOH (95:5) as a solvent system, to yield compound **19** (4.0 mg).

The concentrated EtOAc-soluble fraction (**F**, 37 g) was separated by VLC on silica gel with a gradient system of $CHCl_3$−MeOH [from 98:2 to 6:4 (1500 mL/eluent), and finally with MeOH; volume of collected fractions were 100 mL], to yield 15 major fractions (F/1−15). The fractions were combined according to their TLC patterns. Fraction F/8 (705.3 mg) was purified on Sephadex LH-20 column using CH_2Cl_2−MeOH (1:1) as eluent, and then by RP-TLC on RP silica gel using MeOH−H_2O (1:1) as mobile phase. Further purification of subfraction F/8/2/1 by RP-HPLC under gradient conditions, using CH_3CN−H_2O (from 21:79 to 26:74 in 10 min as mobile phase, flow rate 1.5 mL/min), resulted in the isolation of compounds **12** (t_R = 8.35 min, 1.8 mg) and **13** (t_R = 9.4 min, 2.0 mg). Fraction F/10 (720.4 mg) was separated by Sephadex LH-20 gel chromatography using CH_2Cl_2−MeOH (1:1) as eluent and RP-TLC on RP silica gel using MeOH−H_2O (2:3) as solvent system. Further purification of subfraction F/10/2/1 by RP-HPLC under gradient conditions, using CH_3CN−H_2O (from 1:9 to 35:65 in 12 min, flow rate 1.5 mL/min) as mobile phase, afforded compounds **15** (t_R = 11.3 min, 6.8 mg) and **16** (t_R = 12.1 min, 1.8 mg).

5.1.3. Isolation of phenanthrenes from *J. maritimus*

After extraction and solvent-solvent partition, the concentrated $CHCl_3$-soluble fraction (32 g) was separated by VLC on silica gel with a gradient system of cyclohexane–EtOAc–MeOH [from 98:2:0 to 1:1:1 (1500 mL/eluent); volume of collected fractions was 150 mL] (**Annex I**). This separation yielded 14 main fractions (1–14). All major fractions were purified by Sephadex LH-20 gel chromatography using CH_2Cl_2–MeOH (1:1) as eluent. Fraction 2/2 was separated by NP-HPLC under gradient conditions, using cyclohexane–EtOAc (19:1 to 9:1 in 10 min and 9:1 to 65:35 in 1 min; flow rate 1.5 mL/min) as mobile phase to obtain compounds **25** (t_R = 8.3 min, 1.2 mg) and **33** (t_R = 10.4 min, 2.9 mg). Purification of fractions 4/4 and 4/5 by PLC afforded compounds **4** (4.3 mg) and **27** (3.4 mg).

Fraction 5/2 was chromatographed by RP-MPLC using MeOH–H_2O (from 8:2 to 1:0). Subfraction 5/1 was then purified by RP-HPLC under gradient conditions, using MeOH–H_2O (from 45:55 to 82:18 in 10 min; flow rate 1.2 mL/min) as mobile phase, to yield compound **38** (t_R = 5.6 min, 2.4 mg). Subfraction 5/2 was separated by PLC on silica gel using cyclohexane–EtOAc–EtOH (20:10:1) as solvent system to yield compounds **36** (3.5 mg) and **34** (4.5 mg). Fractions 8/3 and 9/4 were combined because of their similar chemical composition and were purified by RP-MPLC using a stepwise gradient solvent system composed of MeOH–H_2O (from 8:2 to 1:0). Subfraction 8-9/3-4/1 was separated by PLC on silica gel using cyclohexane–EtOAc–EtOH (20:10:1) as an eluent to isolate compound **37** (10.4 mg). Then Fr. 8-9/3-4/1/2 was purified by RP-HPLC under gradient conditions, using MeOH–H_2O (from 45:55 to 82:18 in 10 min; flow rate 1.2 mL/min) as mobile phase, and compound **32** (t_R = 9.0 min, 5.6 mg) was isolated. Subfraction 8-9/3-4/7 was further fractionated by NP-HPLC with gradient system of cyclohexane–EtOAc (from 80:20 to 65:35 in 12 min; flow rate 1.7 mL/min) as mobile phase, to afford compound **22** (t_R = 13.2 min, 2.3 mg). Subfraction 8-9/3-4/9 was separated by PLC on silica gel using cyclohexane–EtOAc–EtOH (20:10:1) as an eluent, and then 8-9/3-4/9/3 was purified by RP-HPLC under gradient conditions, using CH_3CN–H_2O mixtures (from 56:44 to 70:30 in 10 min; flow rate 1.2 mL/min) to yield compound **35** (t_R = 7.5 min, 2.0 mg).

5.1.4. Isolation of phenanthrenes from *J. ensifolius*

After extraction of the plant material with MeOH and solvent-solvent partition with *n*-hexane, $CHCl_3$ and EtOAc, the concentrated $CHCl_3$-soluble fraction (12 g) was separated by VLC on silica gel using a gradient solvent system of cyclohexane–EtOAc–MeOH [from 98:2:0 to 1:1:1] to collect 14 major fractions (1–14) (**Annex I**). In the second step, all major fractions were purified by Sephadex LH-20 gel chromatography using CH_2Cl_2–MeOH (1:1) as eluent. Fractions 1/2, 6/3, and 8/4 yielded pure compounds **17** (5.8 mg), **3** (51 mg), and **47** (8.4 mg), respectively. Fraction 2/4 was separated by RP-HPLC under isocratic conditions, using MeOH–H_2O (78:22 in 10 min; flow rate 1 mL/min) as the mobile phase, and obtained compound **42** (t_R = 6.8 min, 2.5 mg). Purification of fraction 4/2 was performed

by RP-HPLC with gradient system of MeOH–H_2O (from 8:2 to 93:3 in 10 min, then washed with MeOH in 1 min; flow rate 1 mL/min) to yield compounds **49** (t_R = 8.4 min, 1.8 mg), **40** (t_R = 9.8 min, 3.0 mg), and **48** (t_R = 10.4 min, 1.5 mg). After gel filtration on Sephadex LH-20, fraction 5/4 was separated by RP-MPLC by MeOH–H_2O gradient elution (from 1:9 to 1:0), and then subfraction 5/4/3 was further purified by RP-HPLC using a MeOH–H_2O solvent system (from 82:18 to 86:14 in 10 min; flow rate 1 mL/min) as the mobile phase to yield compound **50** (t_R = 10.6 min, 1.1 mg). Fraction 5/5 was separated by RP-HPLC under gradient conditions using MeOH–H_2O (from 75:25 to 81:19 in 10 min; flow rate 1 mL/min) as mobile phase to yield compounds **53** (t_R = 5.5 min, 100.3 mg) and **43** (t_R = 6.4 min, 13.0 mg). Fraction 5/6 was also purified by RP-HPLC using MeOH–H_2O (from 78:22 to 1:0 in 10 min; flow rate 1 mL/min) as eluent to yield compound **51** (t_R = 7.2 min, 1.0 mg). Fraction 6/2 was separated by RP-MPLC using MeOH–H_2O (from 1:9 to 1:0), and then subfraction 6/2/3 was further purified by RP-HPLC under gradient conditions using CH_3CN–H_2O (from 1:1 to 7:3 in 10 min; flow rate 1 mL/min) as the mobile phase to yield compounds **41** (t_R = 3.7 min, 7.3 mg) and **52** (t_R = 5.2 min, 8.2 mg).

Fraction 7/3 was separated by RP-HPLC with CH_3CN–H_2O gradient system (from 4:6 to 55:45 in 10 min; flow rate 1 mL/min) to yield compound **45** (t_R =5.3 min, 2.1 mg). Fraction 7/4 was also separated by RP-HPLC using MeOH–H_2O (from 4:6 to 65:35 in 10 min; flow rate 1 mL/min) as the mobile phase to yield compound **2** (t_R = 7.75 min, 2.1 mg). Purification of fraction 9/3 by RP-HPLC under gradient conditions (CH_3CN–H_2O from 1:1 to 8:2 in 10 min; flow rate 1 mL/min) yielded compound **46** (t_R = 2.7 min, 2.5 mg). Fraction 12/3 was separated by RP-HPLC using CH_3CN–H_2O gradient system (from 35:65 to 7:3 in 12 min; flow rate 1 mL/min) as the mobile phase to yield compounds **44** (t_R = 5.15 min, 4.7 mg) and **39** (t_R = 10.75 min, 2.0 mg). After gel filtration, fraction 14/2 yielded pure compound **7** (4.2 mg).

5.2. CHARACTERIZATION AND STRUCTURE DETERMINATION OF THE ISOLATED COMPOUNDS

The structure elucidation of the compounds was performed by means of MS and NMR measurements and comparison of the spectral data with literature values. HRESIMS measurements revealed the molecular masses and molecular compositions of the novel compounds. Information from 1D (^{1}H NMR and JMOD) and 2D (^{1}H–^{1}H COSY, NOESY, HSQC and HMBC) NMR experiments proved to be the most valuable for the structure determination. In order to differentiate compounds mentioned in section 3 from those isolated in our experiments, former ones marked with bold and italic, the later ones with bold.

5.2.1. Compounds from *Juncus atratus*

From the CH_2Cl_2 fraction of *J. atratus* nine compounds (**1**–**9**) were obtained.

Compound **1** was obtained as yellow amorphous powder. Its HRESIMS suggested the molecular formula $C_{18}H_{18}O_3$, through the presence of a peak at *m/z* 283.1327 $[M+H]^+$ (calcd. for $C_{18}H_{19}O_3$, 283.1329). The ^{1}H NMR spectrum (**Table A1** in **Annex II**) showed signals of two *ortho*-coupled aromatic protons (δ_H 6.70 d and 7.35 d), one aromatic proton as a singlet (δ_H 7.11), three methyls (δ_H 2.48 s, 2.17 s and 2.07 s), and two methylenes (δ_H 2.73 m and 2.53 m, each 2H). These methylene resonances (H_2-9, H_2-10) indicated this compound to be a 9,10-dihydrophenanthrene derivative. In the JMOD spectrum, 18 carbon signals was detected closely resembling to juncuenin B, isolated previously from other *Juncus* species (*J. effusus*, *J. inflexus*, and *J. setchuensis*) (**Table A1** in **Annex II**).[72,73] The only difference found was that an acetyl group instead of the vinyl group is linked to the skeleton at position C-8. In the ^{1}H-^{1}H COSY spectrum, correlations were observed between δ_H 6.70 d and δ_H 7.35 d (H-3–H-4), and δ_H 2.53 m and 2.73 m (H-9–H-10). The location of the methyl groups was concluded from the HMBC spectrum, as proton signal at δ_H 2.17 (H_3-11) showed correlations with δ_C 122.5 (C-1), 138.2 (C-1a), and 156.2 (C-2), and the proton signal at δ_H 2.07 (H_3-12) was found to be in correlation with δ_C 117.7 (C-7), 155.5 (C-6) and 143.7 (C-8). The position of the acetyl group was determined by the HMBC cross-peaks between methyl signal at δ_H 2.48 (H_3-14) with δ_C 211.4 (C-13) and 143.7 (C-8) (**Fig. 3**). The position of the hydroxy groups were indicated by the δ_C values of C-2 (156.2) and C-6 (155.5). HMBC correlations of H-5 with C-4a and C-8a also evidenced the subtitution of ring C in positions C-6, C-7, and C-8.

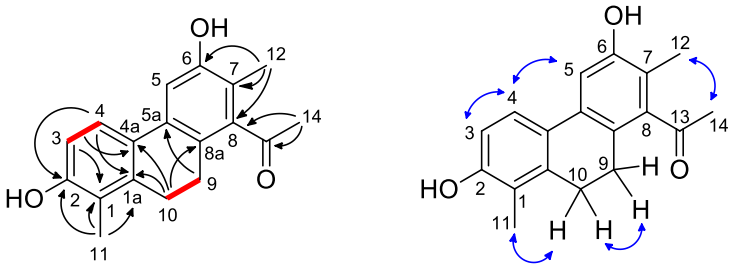

Figure 3. Diagnostic COSY (—), HMBC (H→C) and NOESY (↔) correlations of compound **1**

The NOESY correlations further confirmed the structure of compound **1**. Overhauser effects were detected between H-3/H-4, H-4/H-5, H_2-10/H_3-11, and H_3-14/H_3-12 (**Fig. 3**). All of the above evidence confirmed the structure of **1** named as juncatrin A.

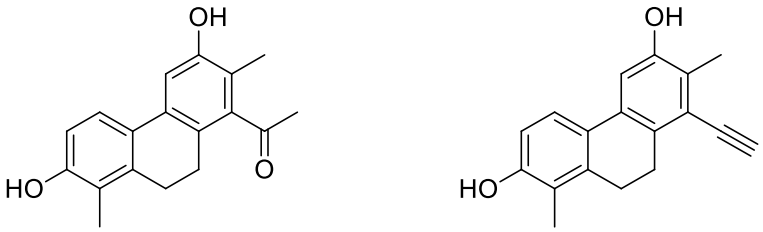

1 **2**

Compound **2** was obtained as yellow amorphous powder. The ^{1}H NMR spectrum of compound **2** was very similar to that of **1**, the only differences were the absence of a methyl signal and the appearance of proton resonance at δ_H 3.78 in **2** proving the presence of a methine (**Table A1** in **Annex II**). Its HRESIMS suggested the molecular formula $C_{18}H_{16}O_2$, through the presence of a peak at *m/z* 265.1222 $[M+H]^+$ (calcd. for $C_{18}H_{17}O_2$, 265.1223). Its JMOD spectrum (**Table A1** in **Annex II**) showed 18 signals close similar to juncuenin B and compound **1**, with exception of two signals at δ_C 82.2 and 86.0 which suggested the presence of an acetylene functionality in the molecule, instead of a vinyl (juncuenin B) or an acetyl group (**1**). The location of the methyl groups was concluded from the HMBC spectrum, as proton signal at δ_H 2.16 (H_3-11) showed correlations with δ_C 122.5 (C-1), 138.4 (C-1a), and 156.0 (C-2), whereas the proton signal at δ_H 2.33 (H_3-12) was found to be in correlation with δ_C 126.1 (C-7), 154.7 (C-6) and 122.8 (C-8). The position of the acetylene group was also determined from the HMBC spectrum, as proton signal at δ_H 3.78 (H-14) correlated with δ_C 122.8 (C-8). The position of the hydroxy groups (at C-2 and C-6) were determined by the δ_C values of C-2 (156.0) and C-6 (154.7). Moreover, HMBC correlations of H-5 with C-4a and C-8a also proved the subtitution of ring C in positions C-6, C-7, and C-8.

The NOESY cross-peaks between H-3/H-4, H-4/H-5, H-9/H-10, and H-10/H_3-11 confirmed the proposed structure of the molecule. Based on the above findings, the structure of this compound (juncatrin B) was established as depicted in structural formula **2**.

Besides new compounds, juncatrin A (**1**) and juncatrin B (**2**), two dihydrophenanthrenes [juncuenin B (**3**) and effusol (**4**)], one phenanthrene [dehydroeffusol (**5**)], two flavones [apigenin (**6**) and luteolin (**7**)], the acyclic diterpene phytol (**8**) and 13(*R*)-hydroxy-octadeca-(9*Z*,11*E*,15*Z*)-trienoic acid (**9**) were also isolated from *J. atratus*. Their structures were determined by analysis of MS, 1D and 2D NMR spectra, and by comparison with literature data.[72,73,74-79]

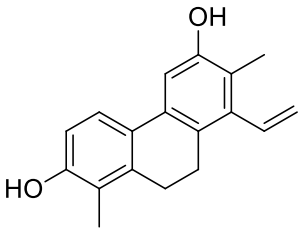

3

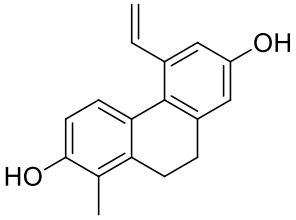

4

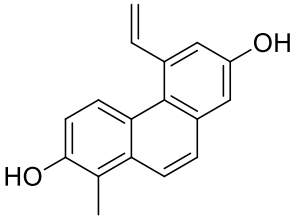

5

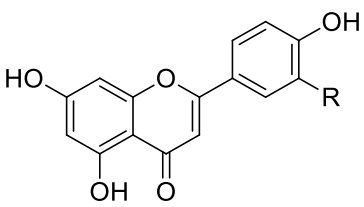

6 (R=H)

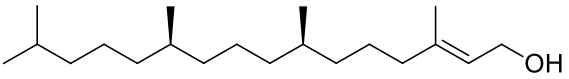

8

7 (R=OH)

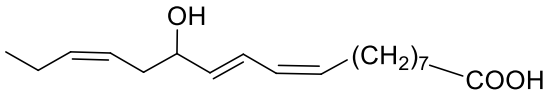

9

5.2.2. Compounds from *Juncus gerardii*

The $CHCl_3$ and EtOAc phases were purified by a combination of different techniques, including CC, VLC, MPLC, gel filtration, preparative TLC and HPLC, to afford 26 compounds (**4**–**7**, **10**–**21**, **22**–**31**).

Compound **10** was obtained as an amorphous solid. Its HRESIMS provided the molecular formula $C_{18}H_{18}O_3$ through the presence of a peak at *m/z* 251.1068 ($[M + H - CH_3OH]^+$, calcd $C_{17}H_{18}O_2$, 251.1072). The ^{1}H NMR spectrum (**Table A2** in **Annex II**) displayed signals of two *ortho*- (δ_H 6.69 and 7.32, each 1H, d, *J* = 8.5 Hz) and two *meta*-coupled (δ_H 6.64 and 6.84, each 1H, d, *J* = 2.4 Hz) aromatic protons, three methylenes (δ_H 2.62, 2.75 m, and 4.65 s, each 2H), a vinyl moiety (δ_H 6.91, 5.21, and 5.65, each 1H, dd), and a methoxy group (δ_H 3.40, 3H, s). The JMOD spectrum contained 18 carbon resonances attributable to a vinyl- and methoxy-substituted phenanthrene derivative (**Table A2** in **Annex II**). The presence of two adjacent methylene signals (H_2-9, H_2-10) in the COSY spectrum suggested that compound **10** is a 9,10-dihydrophenanthrene derivative. Further COSY correlations were observed between the signals at δ_H 6.69 and δ_H 7.32 (H-3/H-4), as well as δ_H 6.91 and δ_H 5.21 and 5.65 (H-12/H-13). The connectivities of the COSY fragments were determined by means of relevant HMBC correlations (**Fig. 4**).

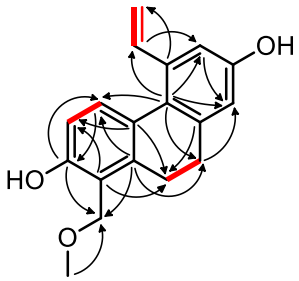

Figure 4. ^{1}H-^{1}H COSY (—) and diagnostic HMBC (C→H) correlations of **10**

Heteronuclear long-range correlations of C-4a with H-3 and H_2-10, C-5a with H-4, H-6, H-8, and H_2-9, C-1a with H-4, H_2-9, and H_2-11, as well as C-9 with H-8, and C-8a with H_2-10 were used to establish a 9,10-dihydrophenanthrene skeleton for compound **10**. HMBC cross peaks of C-2 (δ_C 156.0) with H-3, H-4, and H_2-11, together with C-7 (δ_C 156.7) with H-6 and H-8 showed the presence of two hydroxy groups at C-2 and C-7. The vinyl moiety was placed at C-5 based on the C-5a/H-12, C-6/H-12, and C-5/H_2-13 correlations. In addition, the strong cross peak of the methoxy group and the hydroxymethylene at δ_C 66.5 confirmed its location on C-11. The NOE interactions of H-4/H-12, H-8/H_2-9, and H_2-10/H_2-11 corroborated the proposed structure of gerardiin A (**10**), as shown.

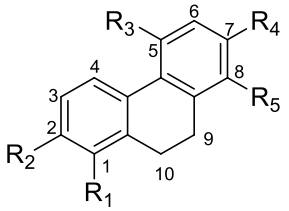

Compound	R_1	R_2	R_3	R_4	R_5	
10	CH_2OCH_3	OH	CH_2CH	OH	H	gerardiin A
11	CH_3	OH	H	CH_2OCH_3	CH_2CH	gerardiin B
12	CH_3	O-glc	CH_2CH	OH	H	gerardiin C
13	CH_3	OH	CH_2CH	O-glc	H	gerardiin D
14	CH_3	OH	$CH(CH_3)OH$	OH	H	gerardiin E
15	CH_3	O-glc	$CH(CH_3)OH$	OH	H	gerardiin F
16	CH_3	OH	$CH(CH_3)OH$	O-glc	H	gerardiin G

Compound **11** (gerardiin B) was obtained as an amorphous solid. The HRESIMS peak at *m/z* 249.1275 established the molecular formula as $C_{19}H_{20}O_2$ ($[M + H - CH_3OH]^+$, calcd $C_{18}H_{17}O$, 249.1279). In the ^{1}H NMR spectrum, signals of a methyl group (δ_H 2.18, 3H, s), four *ortho*-coupled aromatic protons (δ_H 7.53 and 7.25, each 1H, d, *J* = 8.0 Hz, 7.43 and 6.72, each 1H, d, *J* = 8.5 Hz), and a vinyl group (δ_H 6.85, 5.57, and 5.25, each 1H, dd *J* = 17.4 and 10.8 Hz, 17.4 and 1.3 Hz, and 10.8 and 1.3 Hz, respectively) were observed (**Table A2** in **Annex II**). The presence of saturated methylene protons at δ_H 2.70 and 2.82 (each 2H, m) indicated this compound to be a 9,10-dihydrophenanthrene. The HMBC cross peaks C-7/H-5, C-8a/H-5, C-8/H-6, C-12/H-6, C-8/H_2-12, C-7/H_2-12, C-7/H-13, C-8a/H-13, and C-8/H-14 demonstrated that the oxymethylene and vinyl groups are situated on the adjacent carbons C-7 and C-8, respectively. The three-bond correlation of the methoxy group with the carbon resonating at δ_C 74.3 unambiguously showed that it is attached to C-12. NOE correlations of H-4/H-5, H-6/H_2-12, H_2-12/H-14b, H_2-9/H-13, and H_2-10/H_3-11 supported the above findings, and afforded the stucture of gerardiin B (**11**), as shown.

According to the sodiated molecular ion exhibited at *m/z* 437.1565 $[M + Na]^+$ in the HRESIMS spectrum, compound **12** (gerardiin C) has the molecular formula of $C_{23}H_{26}O_7$ (calcd $C_{23}H_{26}O_7Na$, 437.1576). The ^{1}H NMR spectrum contained the signals of two *ortho*- (δ_H 7.18 and 7.00, each 1H, d, *J* = 8.6 Hz) and two *meta*-coupled (δ_H 6.80 and 6.66, both 1H) aromatic methines, a vinyl group (δ_H 6.84, 1H, dd, *J* = 17.3 and 10.8 Hz, and 5.64 and 5.27, each 1H, d, *J* = 17.3 and 10.8 Hz, respectively), and a methyl group (δ_H 2.21, 3H, s), two methylenes (δ_H 2.64 and 2.59, each 2H, m), and a sugar moiety (**Table A2** in **Annex II**). The monosaccharide was identified as D-glucose based on its ^{1}H and ^{13}C chemical shift values. The large coupling constant of the anomeric H-1' proton (*J* = 7.1 Hz) indicated that the glucose unit is attached to the phenanthrene skeleton through a β-glycosidic bond. The 1D and 2D NMR data of compound **3** were similar to those of effusol, and the HMBC cross peaks C-2/H-4, C-2/H_3-11, and C-2/H-1' revealed that gerardiin C (**12**) is a 2-*O*-glycoside of a known aglycon, as shown.

The same molecular formula, $C_{23}H_{26}O_7$ (*m/z* 437.1564 $[M + Na]^+$, calcd $C_{23}H_{26}O_7Na$, 437.1576) was assigned to gerardiin D (**13**) as to **12**, suggesting that these compounds are structural isomers. The markedly upfield shifted H-3 (δ_H 6.72, 1H, d, *J* = 8.4 Hz vs. 7.00, 1H, d, *J* = 8.6 Hz in **3**), and the deshielded *meta*-coupled protons assigned to ring C ($\delta_{H\text{-}6}$ 7.06 and $\delta_{H\text{-}8}$ 6.92, each 1H, d, *J* = 2.1 Hz vs. 6.80, 1H, d, *J* = 2.2 Hz, and 6.66, 1H, br s in **3**) implied that the glucose unit is attached to the C-7 hydroxy group of the aglycone (**Table A3** in **Annex II**). This conclusion was confirmed by HMBC cross peaks between C-7 (δ_C 155.4), H-6, and H-8, as well as by the NOE interactions of H-6 and H-8 with H-1', with the structure proposed for **13** as shown.

Compound **14** (gerardiin E) was obtained as a colorless amorphous solid. Its molecular formula was determined as $C_{17}H_{18}O_3$ by the HRESIMS data (*m/z* 253.1226 $[M + H - H_2O]^+$, calcd $C_{17}H_{17}O_2$, 253.1229). The presence of four aromatic methines (two *meta*- and two *ortho*-coupled), two saturated methylenes, and one methyl group in the ^{1}H NMR spectrum revealed that **14** is a 1,2,5,7-tetrasubstituted 9,10-dihydrophenanthrene derivative (**Table A3** in **Annex II**). However, the lack of any characteristic resonances of a vinyl moiety, and the additional oxymethine and methyl signals detected at δ_H 5.05 (1H, q, *J* = 6.2 Hz) and δ_H 1.39 (3H, d, *J* = 6.2 Hz) suggested the presence of an α-hydroxyethyl group in the molecule. HMBC cross peaks of C-12 (δ_C 64.2) with H-6 (δ_H 6.92), C-5a (δ_C 124.8) with H-4 (δ_H 7.13), H-6, and H-12 (δ_H 5.05), and C-5 (δ_C 144.2) with H-12 and H_3-13 (δ_H 1.39) revealed that the hydroxyethyl substituent is attached to C-5. From a biosynthetic point of view, this side chain is most likely formed from a vinyl group through hydration of the vinylic double bond. NOEs between H-4, H-12, and H_3-13, as well as between H-6 and H_3-13 were in line with the proposed structure of gerardiin E (**14**), as shown.

The molecular formula $C_{23}H_{28}O_8$ of gerardiin F (**15**) was deduced from the sodium adduct ion $[M + Na]^+$ observed at *m/z* 455.1671 (calcd $C_{23}H_{28}O_8Na$, 455.1682) in the HRESIMS. Apart from the signals of a D-glucose moiety, the ^{1}H NMR data closely resembled to those of compound **14**. On examining the chemical shifts, the deshielded nature of H-3 and H-4 (δ_H 7.00 and 7.26, each 1H, d, *J* = 8.6 Hz in **6** vs. 6.71 and 7.13, each 1H, d, *J* = 8.4 Hz in **5**) clearly suggested that the sugar unit is attached to the skeleton at C-2 (δ_C 153.9) (**Table A3** in **Annex II**). The position of the β-D-glucose was substantiated by HMBC correlations of C-2 (δ_C 153.9) with H-4, H_3-11, and the anomeric H-1', and by the NOE cross peak between H-3/H-1', and the structure of **15** was proposed as shown.

Gerardiin G (**16**) was shown to be a structural isomer of **15** by the sodium adduct HRESIMS ion at *m/z* 455.1675 $[M + Na]^+$ (calcd $C_{23}H_{28}O_8Na$, 455.1682). As in the case of gerardiin D, the position of the β-D-glucose at C-7 (δ_C 155.5) was determined with the aid of diagnostic HMBC and NOE cross peaks leading to the structure of **16** as shown.

HRESIMS data provided the molecular formula of $C_{18}H_{16}O$ for gerardiin H (**17**) through the presence of a peak at *m/z* 249.1274 ($[M + H]^+$, calcd $C_{18}H_{17}O$, 249.1279). The ^{1}H NMR data of **17** were

similar to those of the known 9,10-dehydrophenanthrene juncunol, except for the replacement of the H_2-9 and H_2-10 methylene signals by two *ortho*-coupled aromatic protons ($\delta_{H\text{-}10}$ 7.89 and $\delta_{H\text{-}9}$ 7.65, each 1H, d, *J* = 9.1 Hz) (**Table A4** in **Annex II**). The presence of a double bond between C-9 and C-10 was corroborated by the HMBC cross peaks of C-1a (δ_C 134.9), C-5a (δ_C 128.7), C-8 (δ_C 129.2) with H-9, and C-1 (δ_C 118.7), C-4a (δ_C 126.0), and C-8a (δ_C 133.3) with H-10, as well as by NOE interactions between H-8 (δ_H 7.59 s) and H-9, and H-10 and H_3-11 (δ_H 2.56).

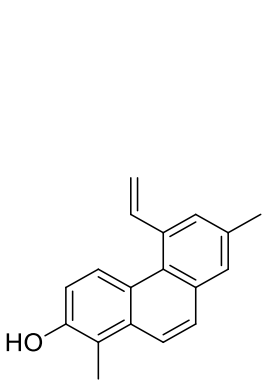

17

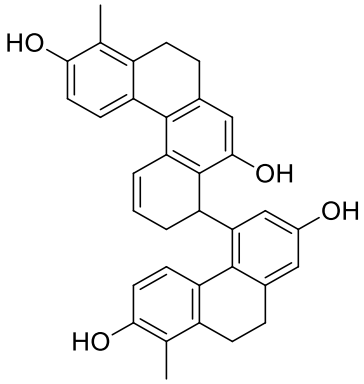

18

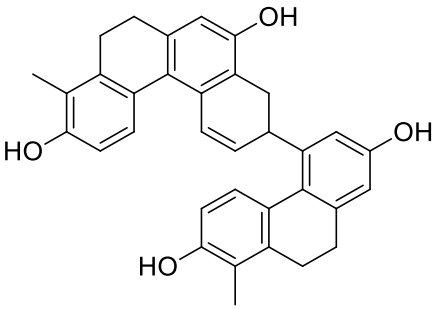

19

Compound **18** (gerardiin I) was isolated as an amorphous solid. The peak of the protonated molecule detected at *m/z* 503.2210 $[M + H]^+$ in the HRESIMS suggested a molecular formula of $C_{34}H_{30}O_4$ (calcd $C_{34}H_{31}O_4$, 503.2222). The 34 carbon signals, including five methylenes detected in the JMOD spectrum, indicated that **18** is a dimer consisting of two 9,10-dihdyrophenanthrene units (**Table A5** in **Annex II**). The ^1H-^1H COSY spectrum defined two $–CH_2–CH_2–$ fragments [δ_H 2.53 and 2.47, each 2H, m; 2.87, 2.59, 2.42 and 2.40, each 1H, m), two pairs of *ortho*-coupled aromatic protons (δ_H 7.62 and 6.74, each 1H, d, *J* = 8.4 Hz; δ_H 7.04 and 6.72, each 1H, d, *J* = 8.4 Hz), a pair of *meta*-coupled sp^2 methines (δ_H 6.40 and 6.12, each 1H, d, *J* = 2.0 Hz), and a further sequence of correlated protons as follows: –CH–CH_2–CH=CH– (δ_H 5.19, 1H, d, *J* = 9.3 Hz, 2.62 and 2.20, each 1H, m, 5.76, 1H, m, and 6.77, 1H, dd, *J* = 9.7 and 2.6 Hz) (**Fig. 5**). The latter structural portion was incorporated into a cyclohexadiene ring, and connected the two phenanthrene units between C-6'–C-12, and C-13'–C-13, as confirmed by the key HMBC correlations of C-12 (δ_C 30.8) with H-6 (δ_H 6.12) and C-5, C-5' and C-7' (δ_C 142.5, 130.5, and 152.3, respectively) with H-12 (δ_H 5.19) (**Fig. 2**). Further relevant HMBC correlations from C-5 (δ_C 142.5) and C-12' (δ_C 127.5) to H-13, from C-5' to H-13' (δ_H 5.76), and from C-6' (δ_C 123.9) to H-12' (δ_H 6.77) and H-8' (δ_H 6.56) were also observed (**Fig. 5**).

The substitution pattern of the monomers, excepting the connection sites at C-5, C-5', and C-6', were identical with the known effusol, which possesses a C-5 vinyl group. Thus, it is postulated that **18** is biosynthesized from two effusol monomers which are connected through their vinyl substituents and C-12–C-6'.

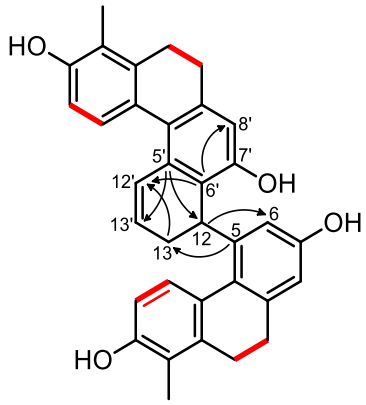

Figure 5. ^{1}H-^{1}H COSY (—) and diagnostic HMBC (C→H) correlations of **18**

NOESY cross peaks of H-12 with H-4, and H-4' with H-12' were in agreement with these conclusions. While the planar structure of gerardiin I (**18**) could be elucidated, the configuration of C-12 still remained uncertain. The specific rotation value $[\alpha]_D^{25}$ of the compound was 0 (*c* 0.1, MeOH). When gerardiin I was injected onto a chiral HPLC column, it eluted with two well-separated peaks with a peak ratio area of 1:1. The peaks also exhibited the same UV spectra, suggesting that **9** is a racemic mixture, with the structure shown.

The protonated molecular ion peak of compound **19** at *m/z* 503.2213 $[M + H]^+$ (calcd $C_{34}H_{31}O_4$, 503.2222) in the HRESIMS data provided the same molecular formula ($C_{34}H_{30}O_4$) as for **18**. Careful analysis of the 1D NMR spectra implied that compound **19** also comprises two effusol units (**Table A5** in **Annex II**). Based on the –CH(CH_2)–CH=CH– structural portion (δ_H 4.13, 1H, m, 3.17 and 2.59, each 1H, m, 5.93, 1H, br d, *J* = 9.8 Hz, 6.78, 1H, dd, *J* = 9.8 and 2.0 Hz), as defined by the ^{1}H-^{1}H COSY spectrum, it was assumed that the effusol monomers in **19** are connected via C-13' → C-12 and C-13 → C-6' linkages. This hypothesis was supported by HMBC cross peaks of C-12 (δ_C 35.4) with H-6 (δ_H 6.76), C-5 (δ_C 142.8), C-6' (δ_C 119.4), and C-7' (δ_C 151.9) with H-13 (δ_H 3.17), C-5 and C-5' (δ_C 129.5) with H-13' (δ_H 5.93), and C-5' and C-6'with H-12' (δ_H 6.78). The specific optical rotation of **19** was recorded as zero. When compound **19** was investigated by HPLC using the same chiral stationary phase as in case of **18**, only one peak was observed. Thus, the structure of gerardiin I (**19**) was assigned as shown.

Compound **20** (gerardiin K) was obtained as an amorphous solid. According to its protonated molecular ion peak seen at *m/z* 505.2375 $[M + H]^+$ (calcd $C_{34}H_{33}O_4$, 505.2379) in the HRESIMS, the molecular formula of $C_{34}H_{32}O_4$ was assigned to this compound. The JMOD spectrum displayed 34 signals, which suggested that compound **20** is also a phenanthrene dimer (**Table A6** in **Annex II**). The subunits were identified based on their 1D NMR data as effusol (**4**). The HMBC cross peak of C-7 (δ_C 156.9) with H-12' (δ_H 5.80), and a strong NOE from H-6 to H-12' revealed that the monomers are linked through an ether-bond formed between the OH-7 group of one of effusol monomers and the vinyl side chain of the other effusol molecule. Accordingly, the structure determined for gerardiin K (**20**) is as

shown. The specific optical rotation of **20** was recorded as zero. By HPLC investigation on chiral stationary phase, only one peak was observed.

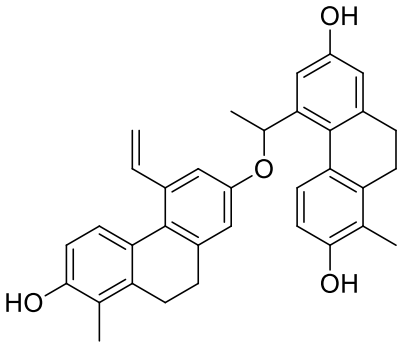

20

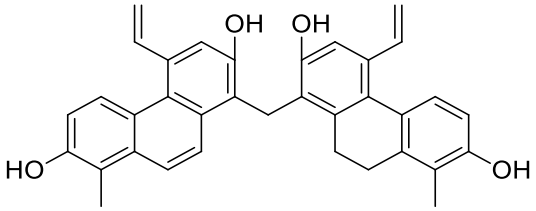

21

Gerardiin L (**21**) was obtained as an amorphous solid. Its HRESIMS provided the molecular formula $C_{35}H_{30}O_4$ through the presence of its protonated molecular ion peak at *m/z* 515.2213 $[M + H]^+$ (calcd $C_{35}H_{31}O_4$, 515.2222). The JMOD spectrum of **21** displayed 35 carbon resonances, which suggested that it is a dimer (**Table A6** in **Annex II**). Since two vinyl groups (δ_H 7.36, 5.74, and 5.33, each 1H, dd, *J* = 17.2, 10.7 Hz, 17.2, 1.3 Hz, and 10.7, 1.3 Hz, respectively, and 6.85, 5.65, and 5.13, each 1H, dd, *J* = 17.4 and 10.8 Hz, 17.4 and 1.2 Hz, 10.8 and 1.2 Hz, respectively) were identified in the ^{1}H NMR and ^{1}H-^{1}H COSY spectra, the phenanthrene monomers had to be linked together in a different manner as in the cases of gerardiin I–K (**18–20**). Moreover, the presence of a $–CH_2–CH_2–$ (δ_H 2.47 and 2.42, each 2H, m) subunit, and three pairs of *ortho*-coupled aromatic protons (δ_H 8.36 and 6.96, each 1H, d, *J* = 9.1 Hz, 8.02 and 7.68, each 1H, d, *J* = 9.6 Hz, and 6.98 and 6.50, each 1H, d, *J* = 8.4 Hz) showed that **21** is composed of a phenanthrene and a 9,10-dihydrophenantrene unit (**Fig. 6**). These monomers could be characterized as effusol (**4**) and dehydroeffusol (**5**) based on their ^{1}H and ^{13}C NMR chemical shifts. However, the signals of H-8 and H-8' were missing, and a downfield shifted, isolated methylene fragment appeared instead at δ_H 4.58 and δ_C 22.8. In order to clarify the exact structure, a series of 2D NMR experiments was recorded. Considering the HMBC cross peaks of C-7 and C-7' (δ_C 152.8 and 154.1), C-8 and C-8' (δ_C 122.9 and 127.5), and C-8a and C-8a' (δ_C 133.2 and 141.3) with the aforementioned methylene (H_2-14), it was conlcuded that the phenanthrene monomers are connected through the CH_2-14 group attached to the corresponding carbons C-8 and C-8' (**Fig. 6**).

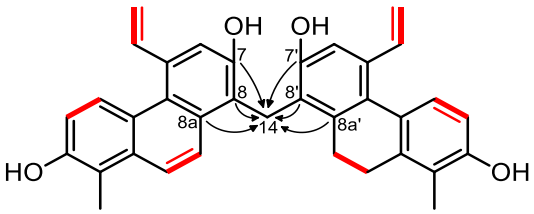

Figure 6. ^{1}H-^{1}H COSY (—) and diagnostic HMBC (C→H) correlations of **21**

These data, combined with NOE interactions of H-4/H-12, H-6/H-13, H-9/H-14, H-4'/H-12', H-6'/H-13' and H_2-9'/H-14 allowed the structure of **21** depicted in **Fig. 6**.

Besides the new compounds, gerardiins A–L (**10**–**21**), eleven known phenanthrenes, the monomers effusol (**4**), dehydroeffusol (**5**),[75] compressin A (**22**),[80] 7-hydroxy-2-methoxy-1-methyl-5-vinyl-9,10-dihydrophenanthrene (**23**),[81] juncusol (**24**),[74] 2-hydroxy-7-hydroxymethylene-1-methyl-5-vinyl-9,10-dihydrophenanthrene (**25**),[82] 2,7-dihydroxy-5-formyl-1-methyl-9,10-dihydrophenanthrene (**26**),[83] effususol A (**27**),[84] 2,7-dihydroxy-5-hydroxymethyl-1-methyl-9,10-dihydrophenanthrene (**28**),[81] jinflexin C (**29**),[73] and the diphenanthrene effususin A (**30**), 1-*O*-*p*-coumaroyl-3-*O*-feruloyl-glycerol (**31**),[85] and the flavones apigenin (**6**) and luteolin (**7**) were also isolated from *J. gerardii*.[76] Their identifications were made by analysis of their HRESIMS, 1D and 2D NMR spectra, and by comparison of their ^{1}H and ^{13}C NMR chemical shifts with literature values. Moreover, complete ^{1}H and ^{13}C NMR assignments are provided for **22**, **23**, **25**–**28**, **30**, and **31** measured in different solvents than those previously reported.

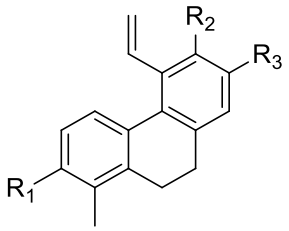

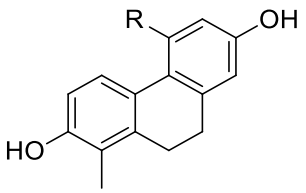

Compound	R_1	R_2	R_3
22	OCH_3	CH_3	OH
23	OCH_3	H	OH
24	OH	CH_3	OH
25	OH	H	CH_2OH

Compound	R
26	CHO
27	$CH(CH_3)OCH_3$
28	CH_2OH

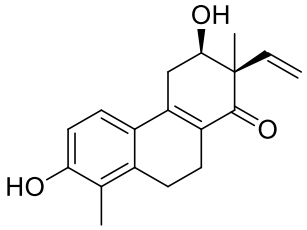

29

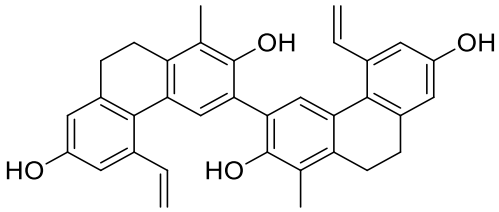

30

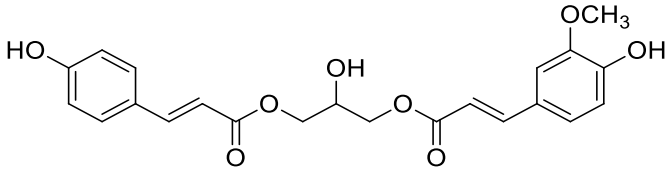

31

5.2.3. Compounds from *Juncus maritimus*

Compound **32** (maritin A) was isolated as a yellow amorphous solid. Its HRESIMS provided the molecular formula $C_{18}H_{18}O_3$ through the presence of a peak at *m/z* 281.1183 $[M - H]^-$ (calcd. for $C_{18}H_{17}O_3$, 281.1178). The ^{1}H-NMR spectrum displayed signals of two *ortho*-coupled aromatic methines (δ_H 7.13 d and 6.63 d, J = 8.4 Hz), an aromatic proton singlet (δ_H 6.92), two methylenes (δ_H 2.76 m and 2.68 m, each 2H), an oxymethylene (δ_H 4.79 s, 2H), a methyl group (δ_H 2.21 s, 3H), and a vinyl moiety (δ_H 6.90 dd, J = 17.4 and 10.9 Hz; δ_H 5.65 dd, J = 17.4 and 1.2 Hz; δ_H 5.18 dd, J = 10.9 and 1.2 Hz) (**Table A7** in **Annex II**). The 18 carbon resonances observed in the ^{13}C-JMOD NMR spectrum, including two oxygen-bearing sp^2 carbons at δ_C 155.1 and 155.3, were attributable to a pentasubstituted phenanthrene derivative.

The ^{1}H-^{1}H COSY correlations defined three sequences of correlated protons, namely, –CH_2–CH_2– (H_2-9–H_2-10), –CH=CH_2 (H-12–H-13a,b), and –CH=CH– (H-3–H-4) fragments (**Fig. 7**). The structure of compound **32** was assembled with the aid of an HMBC experiment. Heteronuclear long-range correlations of H-3 and H_2-10 with C-4a (δ_C 127.2), H-4, H-6, and H_2-9 with C-5a (δ_C 128.3), H_2-9, H_2-10, and H_2-14 with C-8a (δ_C 141.2), as well as of H-4, H_2-9, H_2-10, and H_3-11 with C-1a (δ_C 140.1) established a 9,10-dihydrophenanthrene skeleton. HMBC correlations from H-3, H-4, and H_3-11 to C-2 (δ_C 155.1), and from H-6 and H_2-14 to C-7 (δ_C 155.3) suggested that compound **32** contains two hydroxy groups at the positions of C-2 and C-7. The location of the H_3-11 methyl group at C-1 was dictated by its HMBC correlations with C-1, C-1a, and C-2. The two- and three-bond correlations between H_2-14 (δ_H 4.79), C-7, C-8 (δ_C 124.4), and C-8a demonstrated that the freely rotating hydroxymethyl substituent is attached to C-8. The location of the vinyl moiety at C-5 (δ_C 136.6) was confirmed by the H-6/C-12 and H-13/C-5 HMBC correlations. The NOE cross-peaks between H-4/H-12, H-13a/H-6, H_2-9/H_2-14, and H_2-10/H_3-11 were consistent with the proposed structure of **32**, as shown in **Fig. 7**.

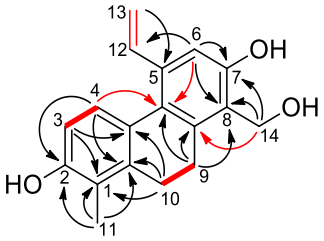

Figure 7. Key ^{1}H-^{1}H COSY (▬) and HMBC (C→H) interactions of maritin A (**32**)

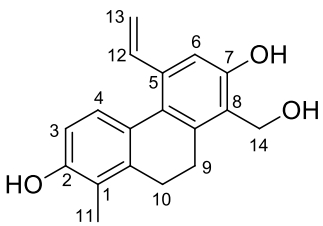

32

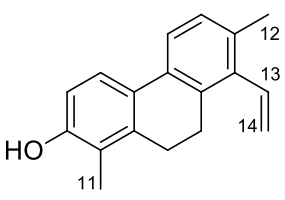

33

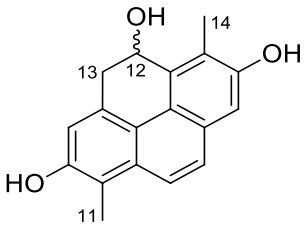

34

Compound **33** (maritin B) was obtained as a white amorphous solid. Its molecular formula was deduced to be $C_{18}H_{18}O$ based on the protonated molecule in the HRESIMS at *m/z* $[M + H]^+$ 251.1429 (calcd. for $C_{18}H_{19}O$, 251.1430). The ^{1}H-NMR spectrum contained signals of two pairs of *ortho*-coupled aromatic protons (δ_H 7.47 d and 6.73 d, J = 8.2 Hz; 7.49 d and 7.11 d, J = 8.4 Hz), two methylenes (δ_H 2.88 m and 2.74 m, each 2H), a vinyl substituent (δ_H 6.77 dd, J = 17.9 and 11.4 Hz; δ_H 5.59 dd, J = 11.4 and 2.0 Hz; δ_H 5.22 dd, J = 17.9 and 2.0 Hz), and two methyl groups (δ_H 2.32 s and 2.24 s, each 3H) (**Table A7** in **Annex II**). The HMBC correlations from H_3-11 (δ_H 2.24) to C-1 (δ_C 120.9), C-1a (δ_C 137.7), and C-2 (δ_C 153.3), and further correlations between H-3 (δ_H 6.73), H-4 (δ_H 7.47), and C-2 showed that a methyl and a hydroxy group are situated on the adjacent carbons C-1 and C-2, respectively. The locations of another methyl (δ_H 2.32) and a vinyl substituent at C-7 and C-8, respectively, were apparent from the HMBC correlations H_3-12/C-6, H_3-12/C-7, H_3-12/C-8, H-6/C-8, H_2-9/C-8, and H-14/C-8. Further heteronuclear correlations were detected between H-3, H-5 (δ_H 7.49), H_2-10 (δ_H 2.74), and C-4a (δ_C 128.4), H-4, H-6 (δ_H 7.11), H_2-9 (δ_H 2.88), and C-5a (δ_C 133.3), and from H-5, H_2-9, and H_2-10 to C-8a (δ_C 134.1). The NOE cross-peaks H-6/H_3-12, H_3-12/H-13, H_2-9/H-14b, and H_2-10/H_3-11 supported the proposed structure of compound **33**.

Compound **34** (maritin C) was isolated as an orange amorphous solid. According to a peak of the deprotonated molecule at *m/z* 279.1027 $[M - H]^-$ in the HRESIMS data, the molecular formula $C_{18}H_{16}O_3$ (calcd. for $C_{18}H_{15}O_3$, 279.1021) was assigned to **34**. The ^{1}H-NMR spectrum exhibited two aromatic methines coupled with each other (δ_H 7.79 and 7.56 d, J = 9.2 Hz), two aromatic singlets (δ_H 7.17 and 7.02), two methyl groups (δ_H 2.50 s and 2.49 s, each 3H), and signals of an oxymethine (δ_H 5.45, br s) and a saturated methylene (δ_H 3.38 and 3.29, each 1H) (**Table A7** in **Annex II**). The ^{1}H-^{1}H COSY spectrum afforded two structural elements, the aforementioned –CH=CH– (δ_H 7.79 and 7.56) and a –CH(OR)–CH_2– fragment (δ_H 5.45, 3.38, and 3.29). The proton signals at δ_H 7.02 (H-3) and δ_H 2.49 (H_3-11) gave HMBC correlations with a downfield shifted, nonprotonated carbon displayed at δ_C 153.4, while the aromatic singlet at δ_H 7.17 (H-8) and the methyl group at δ_H 2.50 (H_3-14) gave HMBC correlations to a carbon resonating at δ_C 155.1. Thus, it was deduced that this phenanthrene bears hydroxy groups at C-2 and C-7. The two methyls were placed onto C-1 and C-6 on the basis of the corresponding H_3-11/C-1, H_3-11/C-1a, H_3-11/C-2, H_3-14/C-5, H_3-14/C-6, and H_3-14/C-7 HMBC correlations. Further long-range correlations from H-9 (δ_H 7.56) to C-1a, C-5a, and C-8, as well as from H-10 (δ_H 7.79) to C-1, C-4a, and C-8a established a phenanthrene skeleton with an aromatic ring B. Considering the HMBC cross-peaks of H-13a (δ_H 3.38) with C-3 (δ_C 117.0), C-4 (δ_C 130.9), C-4a (δ_C 122.5), and C-5 (δ_C 134.6), it was clear that a vinyl group was incorporated into an oxygen-substituted cyclohexadiene ring. From a biosynthetic point of view, compound **34** was likely formed from a dehydrojuncusol precursor through the modification of its vinylic double bond, followed by a ring closure between C-4 and C-13. The depicted structure of maritin C was corroborated by NOE cross-peaks between H-3/H-13a and b, H-

12/H_3-14, H-8/H-9, and H-10/H_3-11. The specific optical rotation of **34** was recorded as zero, therefore, it was isolated as a racemic mixture.

Compound **35** (maritin D) has the molecular formula $C_{34}H_{30}O_4$ compatible with its protonated molecule at *m/z* 503.2203 $[M + H]^+$ (calcd. for $C_{34}H_{31}O_4$, 503.2222) in the HRESIMS data. The 34 carbon signals displayed in the ^{13}C-JMOD NMR spectrum suggested that compound **35** is a phenanthrene dimer. The ^{1}H-NMR spectrum, combined with homonuclear ^{1}H-^{1}H COSY correlations, showed the presence of two vinyl groups (H-12–H_2-13: δ_H 6.96 dd, J = 17.4 and 10.9 Hz; δ_H 5.67 d, J = 17.4 Hz; δ_H 5.23 d, J = 10.9 Hz; H-12′–H_2-13′: δ_H 6.64 dd, J = 17.3 and 11.4 Hz; δ_H 5.33 dd, J = 17.3 and 0.9 Hz; δ_H 4.78 d, J = 11.4 Hz), a –CH=CH– (H-3–H-4: δ_H 7.38 and 6.83 d, J = 8.4 Hz) and two –CH_2–CH_2– structural portions (H_2-9–H_2-10: δ_H 2.68 m and 2.78 m, each 2H; H_2-9′–H_2-10′: δ_H 2.63 m and 2.64 m, each 2H), and two methyls (H_3-11: δ_H 2.28 s; H_3-11′: δ_H 2.30 s, each 3H) in **35** (**Table A8** in **Annex II**). Two pairs of *meta*-coupled aromatic protons (H-6 and H-8: δ_H 6.88 d and 6.69 d, J = 2.2 Hz; H-6′ and H-8′: δ_H 6.68 br s and 6.61 br s) were also identified via weaker $^4J_{H\text{-}H}$ (*W*-type) COSY cross-peaks and three-bond HMBC correlations between the corresponding methine groups. Further analysis of the HMBC correlations unambiguously determined that **35** is comprised of two monomers of a known 9,10-dihydrophenanthrene, effusol, which was also isolated as an individual compound (**4**) from the plant. Taking into account the HMBC correlations from H-4′ and H_3-11′ to C-2′ (δ_C 144.6), it was concluded that oxygen atoms are connected to both of the vicinal carbons C-2′ and C-3′ (δ_C 156.6). Although no HMBC correlations were observed between the monomers, NOE cross-peaks H-4′/H_3-11 and H-13′b/H-12 indicated the close proximity of these protons, and consequently implied that the monomers must be attached through an ether bond between C-2/C-2′ or C-2/C-3′. In order to determine the exact structure, energy-minimized structures were generated for each of the hypothetical compounds by using the MM2 force field method. A minimum energy conformation provided by molecular dynamics calculations was in good agreement with the aforementioned NOE correlations and suggested that the ether bond was formed between C-2/C-3′. The proposed structure was further confirmed by the significantly shielded nature of H-4′ and vinyl resonances H-12′–H_2-13′ compared to H-4 and H-12–H_2-13 of the other monomer (**Table A8** in **Annex II**). This phenomenon was likely caused by the anisotropic effect of aromatic ring A since H-4′ and the vinyl moiety H-12′–H_2-13′ are located in the shielding cone of ring A. In case of the presence of a C-2/C-2′ linkage, H-4′ and H-12′–H_2-13′ would be located too far from ring A and, therefore, their chemical shifts would be less affected by the aromatic ring current effects. Considering the above findings, the structure of maritin D was formulated as (**35**).

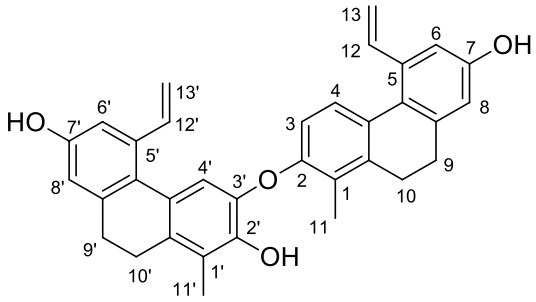

35

Besides the new compounds maritins A–D (**32**–**35**), seven known phenanthrenes, namely, effusol (**4**),[74] juncusol (**24**),[74] 2,7-dihydroxy-5-formyl-1-methyl-9,10-dihydrophenanthrene (**26**),[83] juncunol (**36**),[74] 2,7-dihydroxy-1,8-dimethyl-5-vinyl-9,10-dihydrophenanthrene (**37**),[74] jinflexin A (**38**),[73] and effususin A (**30**),[86] were also isolated from *J. maritimus*. Their structures were identified by 1D and 2D NMR spectroscopy, and by comparison of the ^{1}H and ^{13}C NMR chemical shift values with literature data. All compounds but effusol (**4**) were described for the first time from *J. maritimus*. Moreover, the ^{1}H and ^{13}C NMR assignments of jinflexin A (**38**) in methanol-d_4 were given for the first time.

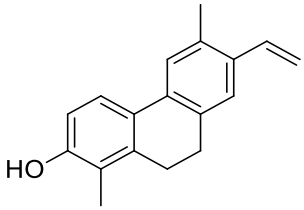

36

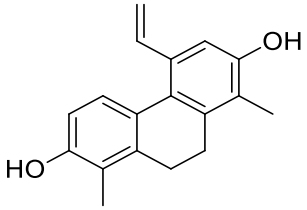

37

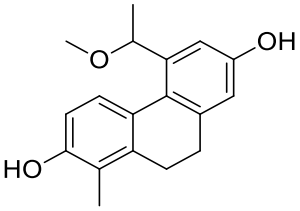

38

5.2.4. Compounds from *Juncus ensifolius*

Ensifolin A (**39**) was isolated as light yellow amorphous solid. Its HRESIMS peak at *m/z* 551.1708 $[M - H_2O + H]^+$ (calcd for 551.1706) suggested a molecular formula $C_{33}H_{26}O_8$. The ^{1}H NMR spectrum (**Table A9** in **Annex II**) exhibited resonances of an *ortho*- (δ_H 7.97 and 6.66, each 1H, d, J = 8.6 Hz) and a *meta*-coupled (δ_H 6.47 and 6.23, each 1H, d, J = 2.1 Hz) pair of aromatic protons, the signals of a 1,3,4-trisubstituted aromatic ring (δ_H 7.57, 1H, d, J = 2.2 Hz; δ_H 7.53, 1H, dd, J = 8.6 and 2.2 Hz; δ_H 7.06, 1H, d, J = 8.6 Hz), two aromatic singlets (δ_H 6.67 and 6.63), two methylenes (δ_H 2.87 and 2.77, each 1H, m; δ_H 2.64, 2H, m), two methyls (δ_H 2.38 and 2.18, each 3H, s), and a mutually coupled oxymethine (δ_H 5.65, 1H, dd, J = 9.9 and 2.9 Hz) and oxymethylene group (δ_H 4.42, 1H, dd, J = 11.9 and 9.9 Hz; δ_H 4.32, 1H, dd, J = 11.9 and 2.9 Hz). The 33 carbon resonances detected in the ^{13}C JMOD NMR spectrum were categorized based on their HSQC correlations and chemical shifts. A keto group at δ_C 183.9, the aforementioned *meta*-coupled aromatic methines (δ_H 6.47 d and 6.23 d, ring A) and a lone proton singlet (δ_H 6.63, ring C) attached to upfield shifted sp^2 carbons (δ_C 95.2, 100.3, and 104.9, respectively), as well as the presence of a 1,3,4-trisubstituted benzene ring (C-1”–C-6”, ring B) suggested that

compound **1** contains a 5,7,3',4'-tetrahydroxyflavone structural portion. The polyphenol was readily identified as luteolin, a common tetrahydroxyflavone previously described from various *Juncus* species [24,25]. Its ^{1}H and ^{13}C carbon assignments were in great agreement with literature values with the exception of small differences observed for ring B, implying that luteolin is connected to the other part of the molecule through its OH-3' or OH-4' group.[77]

The remaining 18 carbons, including two saturated methylenes at δ_C 27.8 and 26.5 were reminiscent of a 9,10-dihydrophenanthrene derivative. The ^{1}H–^{1}H COSY spectrum defined four sequences of correlated protons, namely, a –CH=CH– (δ_H 6.66 d and 7.97 d; H-3/H-4), a –CH_2–CH_2– (δ_H 2.87 m (1H), 2.77 m (1H), and 2.64 m (2H); H_2-9/H_2-10), and a –CH(OR)–CH_2(OR)– (δ_H 5.65 dd, 4.42 dd, and 4.32 dd; H-13/H_2-14) fragment (**Fig. 8**). The HMBC correlations from H-4, H_2-9, H_2-10, and H_3-11 to C-1a (δ_C 139.5), from H-3 and H_2-10 to C-4a (δ_C 125.8), and from H-4, H-6, and H_2-9 to C-5a (δ_C 123.2) established the phenanthrene skeleton (**Fig. 8**). According to the long-range heteronuclear correlations between H_3-11 and C-1a, C-1 (δ_C 121.1), C-2 (δ_C 155.0), and between H-4 and C-2, a methyl and a hydroxy group was placed onto C-1 and C-2, respectively. In a similar manner, HMBC interactions of H-6 with C-5 (δ_C 155.3), and of H_3-12 (δ_H 2.38) with C-6 (δ_C 118.5), C-7 (δ_C 136.8), and C-8 (δ_C 122.1) revealed the presence of a further hydroxy on C-5 and a methyl group on C-7. Additional HMBC correlations H-13/C-7, H-13/C-8, H-13/C-8a (δ_C 140.9), H-6/C-8, and H_2-9/C-8 dictated that the H-13–H_2-14 [–CH(OH)–CH_2(OR)–] moiety is situated on C-8. The side chain presumably originates from a vinyl group, which is characteristic of many phenanthrenes isolated from Juncaceae plants. The structure of this new phenanthrene found in compound **39** was determined as 2,5-dihydroxy-8-(1-hydroxyethyl)-1,7-dimethyl-9,10-dihydrophenanthrene. The NOE cross peaks H_3-11/H_2-10, H_3-12/H-6, H_3-12/H-13, and H-13/H_2-9 were consistent with the proposed structure, as depicted in **Fig. 8**. Furthermore, a three-bond HMBC correlation between H_2-14b (δ_H 4.32) and C-3" (δ_C 145.0) demonstrated that the phenanthrene and luteolin units are linked together by an ether bond formed between C-14 and C-3".

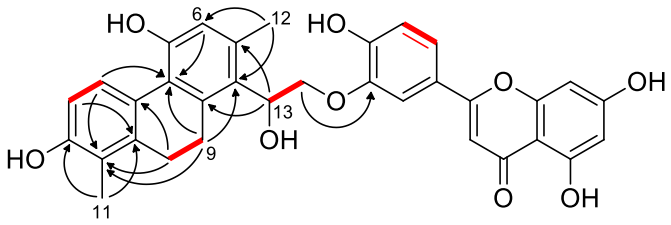

Figure 8. Key ^{1}H-^{1}H COSY (—) and HMBC (H→C) correlations of ensifolin A (**39**)

Compound **39** has an asymmetric carbon atom (C-14). The specific rotation value $[\alpha]_D^{25}$ of the compound was +9 (*c* 0.1, MeOH). When ensifolin A (**39**) was injected onto a chiral HPLC column, it eluted with two well-separated peaks with a peak ratio area of 1:1. The peaks exhibited the same UV spectra, suggesting that **39** is a racemic mixture, with the structure shown on **Fig. 9**. To the best of our

knowledge, this is the first time that a naturally occurring phenanthrene-flavonoid conjugate is reported.

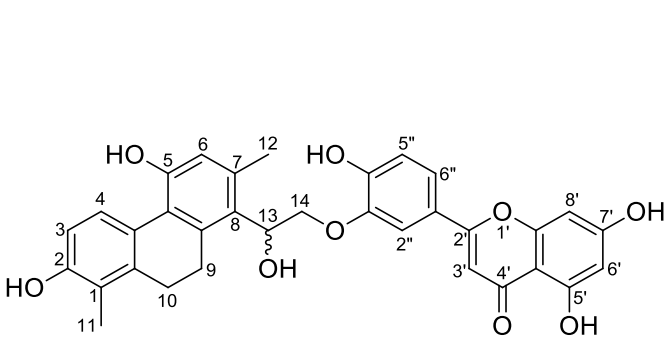

39

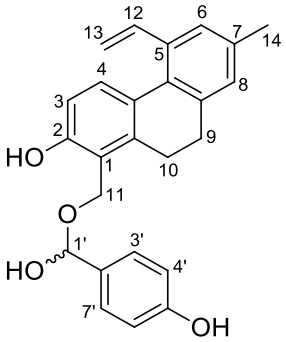

40

Ensifolin B (**40**) has the molecular formula $C_{25}H_{24}O_4$ compatible with the fragment ion in the HRESIMS at *m/z* 369.1497 $[M - H_2O - H]^-$ (calcd for 369.1491). The ^{1}H NMR spectrum displayed the typical signals of a vinyl-substituted 9,10-dihydrophenanthrene, together with resonances of an isolated oxymethylene (δ_H 5.19 and 5.09, each 1H, d, *J* = 14.5 Hz; δ_C 66.2), a hemiacetal group (δ_H 5.94, 1H, s; δ_C 98.7), and a *para*-disubstituted benzene ring (δ_H 7.50 and 6.89, each 2H, d, *J* = 8.5 Hz) (**Table A9** in **Annex II**). The structure of the phenanthrene skeleton was assembled through 2D NMR analysis. It was concluded that the phenanthrene core of compound **40** is identical to sylvaticin A, a 9,10-dihydrophenanthrene recently described from *Luzula sylvatica*.[61] However, NMR characteristics of the H_2-11 oxymethylene in **40** are different compared to those of sylvaticin A, including its upfield shifted carbon (δ_C 66.2 vs. 60.2) and magnetically inequivalent protons (δ_H 5.19 and 5.09, vs. δ_H 5.01, 2H, s). These findings, in conjunction with HMBC interactions from H_2-11 to the deshielded hemiacetal carbon (δ_C 98.7), from H-7' (δ_H 5.94) to C-3'/C-7' (δ_C 128.2), and from H-3'/H-7' (δ_H 7.50) to C-5' (δ_C 156.7) unequivocally demonstrated that OH-11 and a 4-hydroxybenzaldehyde unit participated in the formation of an acyclic hemiacetal moiety. Similarly to compound **39**, ensifolin B (**40**) also has an asymmetric carbon atom (C-1'). The specific rotation value $[\alpha]_D^{25}$ of the compound was +2 (*c* 0.1, MeOH). When compound **40** was injected onto a chiral HPLC column, it eluted with two well-separated peaks with a peak ratio area of 1:1. The peaks exhibited the same UV spectra, suggesting that **40** is a racemic mixture. Intermolecular hemiacetals are intrinsically unstable with respect to their parent alcohols and aldehydes. Indeed, the initially pure phenanthrene showed signs of decomposition, as two sets of proton signals (in an approximate 1:0.6 ratio) emerged in the ^{1}H NMR spectrum when measured again one day later. Considering that sylvaticin A (**52**) and 4-hydroxybenzaldehyde (**53**), the minor compounds of the mixture were also isolated from other fractions, it is unclear whether these phytochemicals originally presented in the harvested plant material, or they are just by-products of the decomposition of compound **40**.

Ensifolin C (**41**) was obtained as a white, amorphous solid. The HRESIMS peak of the protonated molecule at *m/z* 265.1265 $[M + H]^+$ ($C_{18}H_{19}O_2$, calcd for 265.1234) established a molecular formula $C_{18}H_{18}O_2$. Analysis of the NMR spectra afforded a 9,10-dihydrophenanthrene skeleton containing a rare 10-OH group (δ_{H10} 5.10, 1H, br t, J = 2.9 Hz; δ_{c10} 64.3) (**Table A9** in **Annex II**). Comparison with literature data showed that ensifolin C is the 2-demethyl derivative of sylvaticin B, which was isolated from *L. sylvatica*.[61] The structure of compound **41** was therefore determined to be 2,10-dihydroxy-1,7-dimethyl-5-vinyl-9,10-dihydrophenanthrene. Investigation of the compound on a chiral HPLC column resulted in only one peak. According to literature data on similar 10-hydroxyphenanthrenes, the configuration of C-10 can be supposed as (*S*).[61,87]

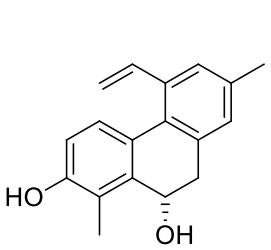

41

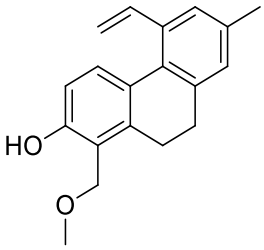

42

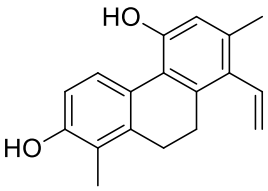

43

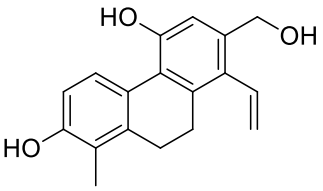

44

Ensifolin D (**42**) was isolated as a light yellow, amorphous powder, and the formula $C_{19}H_{20}O_2$ was assigned to it based on its protonated molecular peak at *m/z* 281.1540 $[M + H]^+$ (calcd for 281.1536) in the HRESIMS. The 1D NMR spectra implied that the chemical structure of compound **42** is very similar to that of sylvaticin A (**Table A10** in **Annex II**). The upfield shifted C-11 (δ_C 66.5 vs. 56.7 in methanol-d_4), as well as a diagnostic HMBC interaction between a methoxy function (δ_H 3.40, 3H, s; δ_C 66.5) and H_2-11 (δ_H 4.66, 2H, s) dictated that ensifolin D is the 11-methoxy derivative of sylvaticin A.

Ensifolin E (**43**) has the molecular formula $C_{18}H_{18}O_2$ according to its protonated molecular peak at *m/z* 267.1379 $[M + H]^+$ in the HRESIMS (calcd for 267.1380). The ^1H and ^{13}C JMOD NMR spectra displayed the characteristic signals of a 9,10-dihydrophenanthrene scaffold (δ_H 2.60 and 2.72, each 2H, m; δ_C 26.7 and 28.5) substituted with two methyls, a vinyl side-chain, and two hydroxy groups (δ_C 153.8 and 154.7) (**Table A10** in **Annex II**). Apart from these resonances, a lone aromatic singlet (δ_H 6.61, 1H) and two *ortho*-coupled aromatic protons (δ_H 6.65 and 7.98, each 1H, d, J = 8.6 Hz) were also detected in the ^1H NMR data. The HMBC correlations of H_3-11 with C-1, C-1a and C-2, and of H-4 with C-1a and C-2 assembled ring A. Correlations of the saturated methylenes H_2-9 and H_2-10 with C-1, C-1a, and C-4a connected rings A and B. The second methyl and the vinyl group are attached to the core at C-7 and C-8, respectively, as demonstrated by the H_3-12/C-6, H_3-12/C-7, H_3-12/C-8, H-13/C-8a, H-14/C-8, and H_2-9/C-8 heteronuclear long-range correlations. Further two- and three-bond HMBC interactions of H-6 (δ_H 6.61) with C-5a, C-5 (δ_C 154.7), and C-8 allowed the placement of an -OH group onto C-5 and established the final structure of **5** as 2,5-dihydroxy-1,7-dimethyl-8-vinyl-9,10-dihydrophenanthrene.

The NOE cross-peaks H_2-10/H_3-11, H-6/H_3-12, H-13/H_3-12, H-13/H_2-9, and H-14b/H_2-9 corroborated with the proposed structure of ensifolin E.

Ensifolin F (**44**) was a light yellow, amorphous powder. Its molecular formula $C_{18}H_{18}O_3$ was deduced from the HRESIMS peak at *m/z* 281.1214 $[M + H]^+$ (calcd for 281.1213). The 1D NMR data suggested that compounds **43** and **44** are closely related to each other, with the only difference being is the presence of a hydroxymethyl function in **44** (δ_H 4.58, 2H, s; δ_C 63.3) instead of a methyl (**Table A10** in **Annex II**). The oxymethylene protons gave HMBC correlations with C-6, C-7, and C-8, and NOE cross-peaks with H-6, H-13, and H-14b, therefore it must be situated on C-7.

Ensifolin G (**45**) was obtained as light yellow, amorphous granules. Its HRESIMS suggested the molecular formula $C_{18}H_{18}O_3$ through the presence of a peak at *m/z* 281.1213 $[M + H]^+$ (calcd for 281.1183). In the 1D NMR spectra the lack of resonances of a vinyl group, and the appearance of an upfield shifted methyl (δ_H 2.46, 3H, s) and a keto carbon at δ_C 211.4 demonstrated that the vinyl part of ensifolin E (**43**) was biosynthetically converted to an acetyl moiety (**Table A11** in **Annex II**). Its position at C-8 (δ_C 134.3) was shown by the HMBC correlations from H_3-14, H-6, H_3-12, and H_2-9 to this particular carbon. Careful analysis of the 2D NMR spectra led to the conclusion that ensifolin G is a structural isomer of juncatrin A (**1**), a 9,10-dihydrophenanthrene previously isolated from *Juncus atratus*, in which the H-6 proton and the OH-5 group are interchanged.[88]

HRESIMS data of ensifolin H (**46**) provided the molecular formula of $C_{18}H_{16}O_3$ for this compound through the peak of the protonated molecule at *m/z* 281.1174 (calcd for $C_{18}H_{17}O_3$ 281.1172). Upon comparison of its 1D NMR data with those of juncatrin B (**2**), a 9,10-dihydrophenanthrene described from *J. atratus* by our research group,[88] we found that the C-7 methyl group adjacent to an acetylene substituent was oxidized into a hydroxymethyl side chain. This assumption was substantiated by the HMBC correlations H_2-12/C-6, H_2-12/C-7, H_2-12/C-8, H-5/C-7, and H-14/C-8, and by the absence of 12-methyl.

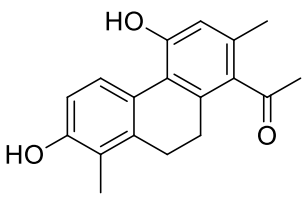

45

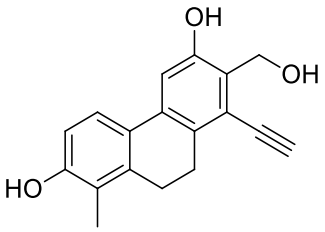

46

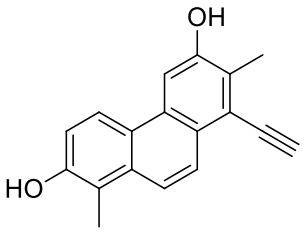

47

The molecular formula $C_{18}H_{14}O_2$ was assigned to ensifolin I (**47**) according to the HRESIMS peak of the protonated molecule at *m/z* 263.1069 $[M + H]^+$ (calcd for 263.1067). The signals in the ^1H NMR spectrum were similar to those of juncatrin B except for the replacement of its saturated H_2-9/H_2-10 structural part by two mutually coupled olefinic protons (δ_H 7.77 and 8.16, each 1H, J = 9.4 Hz) (**Table A11** in **Annex II**). The presence of a double bond between C-9 and C-10 was supported by the HMBC

correlations recorded between H-9 (δ_H 8.16) and C-1a, C-5a, and C-8, and between H-10 (δ_H 7.77) and C-1, C-4a, and C-8a. The H-4/H-5, H_3-12/H-14, H-9/H-14, and H-10/H_3-11 NOESY cross-peaks were in good agreement with the structure depicted for **47**.

Ensifolin J (**48**) possesses a molecular formula $C_{36}H_{34}O_4$ as suggested by its protonated molecule appearing at *m/z* 531.2516 $[M + H]^+$ (calcd for 531.2530) in the HRESIMS. The 1D NMR spectra of ensifolin J were almost superimposable with those of ensifolin E (**43**) (**Table A10** in **Annex II**). However, instead of an *ortho*-coupled aromatic protons it exhibited only one proton singlet in the aromatic region at δ_H 8.12, and an additional nonprotonated sp^2 carbon was also seen at δ_C 124.9 (**Table A12** in **Annex II**). These findings, in conjunction with the HRESIMS data clearly indicated that ensifolin J is a symmetric dimeric phenanthrene comprised of two ensifolin E units. In order to confirm the connection between them, a series of 2D NMR experiments were conducted. The upfield shifted singlet of H-4 (δ_H 8.12) gave three-bond heteronuclear correlations to C-1a, C-2, C-5a, and, most importantly, to the above-mentioned carbon (C-3') resonating at δ_C 124.9. In conclusion, it was determined that the two ensifolin E (**43**) monomers are linked together *via* their C-3 carbons resulting in a symmetrical dimer.

Ensifolin K (**49**) obtained as a light yellow, amorphous powder, is a phenanthrene heterodimer with a molecular formula $C_{36}H_{32}O_4$, as inferred by the HRESIMS peak at *m/z* 529.2366 $[M + H]^+$ (calcd for 529.2373) and the 36 carbon resonances detected in the ^{13}C JMOD NMR spectrum (**Table A13** in **Annex II**). It was apparent that one of the building block of compound **49** is ensifolin E (**43**). The other phenanthrene monomer was identified as dehydrojuncuenin B by means of evaluation of the 2D NMR data, and then by comparison of our assignments with reported literature values.[72] Taking into account that H-5 of dehydrojuncuenin B was missing, and a nonprotonated carbon at δ_C 118.6 (C-5) correlated only with the deshielded H-4' (δ_H 7.96, 1H, s) of ensifolin E (**43**), it was concluded that the monomers are connected through a C–C bond formed between C-5 of dehydrojuncuenin B and C-3' of ensifolin E (**43**).

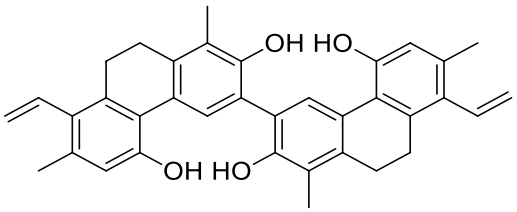

48

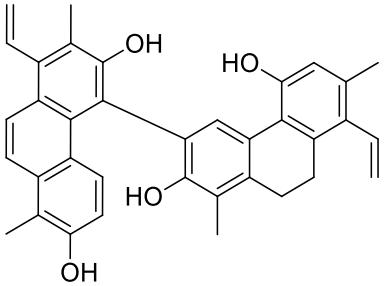

49

Ensifolin L (**50**) possesses a molecular formula $C_{36}H_{34}O_4$ suggested by its protonated molecular peak at *m/z* 529.2437 $[M + H]^+$ (calcd for 529.2435) in the HRESIMS. A brief examination of the ^1H NMR spectrum indicated that ensifolin L is a phenanthrene dimer composed of two ensifolin E (**43**)

monomers (**Table A13** in **Annex II**). Unlike ensifolin J (**48**), ensifolin L is not symmetrical, since its 1D NMR data provided two sets of proton and carbon resonances ascribable to the two constructing subunits. The lack of H-6 and the presence of an upfield shifted singlet at δ_H 7.92 implied that the phenanthrene units are most likely connected by a C–C bond formed between C-6 and C-3' of the corresponding aromatic rings C and A'. This presumption was proven unequivocally by the HMBC correlations from H_3-12 (δ_H 2.03, 3H, s) and H-4' (δ_H 7.92, ring A') to C-6 (δ_C 125.3, ring C), and by a diagnostic NOE cross-peak of H_3-12 with H-4'.

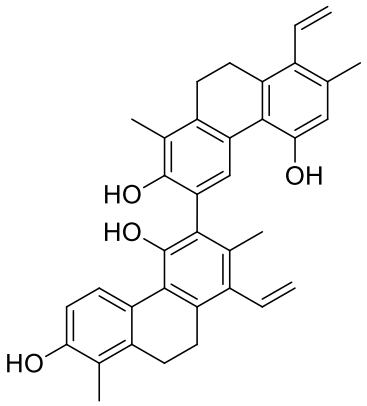

50

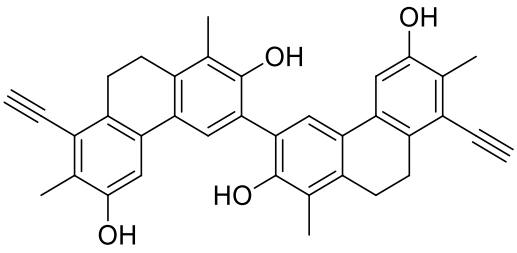

51

The molecular formula $C_{36}H_{30}O_4$ was determined for ensifolin M (**51**) with the aid of a HRESIMS peak at *m/z* 525.2118 $[M + H]^+$ (calcd for 525.2071). The ^{1}H NMR spectrum contained a set of signals reminiscent of juncatrin B (**2**), but only two aromatic singlets were exhibited at δ_H 7.48 and 7.17 instead of three aromatic methines (the mutually coupled H-3/H-4, and H-5) that occur in the original compound (**Table A12** in **Annex II**).[86] This observation, in conjunction with the HRESIMS data indicated ensifolin M to be a symmetrical phenanthrene dimer. The connectivity between C-3 and C-3' was unambiguously determined by the HMBC correlation of H-4 (δ_H 7.48) with a nonprotonated carbon resonating at δ_C 126.8 (C-3,3'), which displayed no heteronuclear correlations with any of the other protons. The nuclear Overhauser effects H-4/H-5 and H_2-10/H_3-11 were in line with the depicted structure **51**.

Besides the new compounds ensifolins A–M (**39–51**), four known phenanthrenes, namely, juncatrin B (**2**),[86] juncuenin B (**3**),[72] gerardiin H (**17**),[89] and sylvaticin A (**52**),[61] and 4-hydroxybenzaldehyde (**53**) and luteolin (**7**) were identified from *J. ensifolius*. The structural characterization was performed by means of HRESIMS and 1D and 2D NMR experiments, and then by comparison of the ^{1}H and ^{13}C assignations with reported literature data. All compounds have been isolated for the first time from this plant.

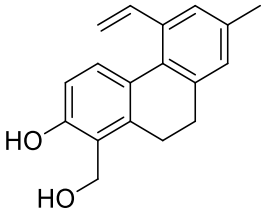

52

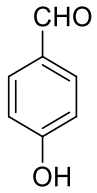

53

6. DISCUSSION

6.1. PHYTOCHEMICAL INVESTIGATION OF *JUNCUS ATRATUS*, *J. GERARDII*, *J. MARITIMUS* AND *J. ENSIFOLIUS*

Chemical investigations of *J. atratus*, *J. gerardii*, *J. maritimus* and *J. ensifolius* resulted in the isolation of 53 compounds, including 31 new (**1**, **2**, **10**–**21**, **32–35** and **39–51**) natural products. The structures were identified by means of spectral methods as phenanthrenes, 9,10-dihydrophenanthrenes, diphenanthrenes, flavonoids, an acyclic diterpene, a fatty acid, a glycerol derivative and benzaldehyde. Pharmacological analysis confirmed that some of the isolated compounds possess biological activity.

6.1.1. Isolation of bioactive compounds

Previous phytochemical investigations of the extracts with different polarity prepared from Juncaceae species showed that mainly the lipophilic CH_2Cl_2 or $CHCl_3$ extracts contain the phenanthrenes. However, it was reported in the literature that phenanthrenes glycosides were isolated from the EtOAc fractions.

The air-dried plant materials were percolated with MeOH at room temperature and then solvent–solvent partition was performed to yield *n*-hexane, CH_2Cl_2/$CHCl_3$ and EtOAc phases. In all cases, the CH_2Cl_2/$CHCl_3$ phases and in case of *J. gerardii* the EtOAc phase too were subjected to a series of chromatographic steps as well as a combination of several chromatographic techniques in order to isolate the compounds. The first fractionation of the organic phases of the plants was carried out by OCC, to afford main fractions; among them, the most interesting ones were further separated. Since these fractions demonstrated great chemical complexity, more selective methods (VLC, MPLC, GF) were applied on normal and reversed phase silica gel and on Sephadex LH-20 gel, and different solvent systems were used for gradient and isocratic elutions. The final purification of the pure compounds was performed by the use of NP- and RP-PLC, GF, and RP-HPLC.

The preparative work was completed with analytical TLC on silica gel with various solvent systems. The detection was carried out in UV light at 254 and 366 nm, followed by spraying with vanillin-sulfuric acid reagent and heating at 120 °C for 5 min.

6.1.2. Structure elucidation

The chemical structures of the isolated compounds were determined by means of spectroscopic methods. The molecular masses and compositions were obtained from MS investigations; optical rotation measurements provided further important information for characterization of the compounds. The most useful data concerning the structures were provided by 1D and 2D NMR spectroscopy. The constitutions of the compounds were elucidated via ^{1}H NMR, JMOD, ^{1}H–^{1}H COSY, HSQC and HMBC experiments, and the relative configurations were then characterized by means of NOESY spectra. As a result of the NMR studies, complete ^{1}H- and ^{13}C-assignments were made for the new compounds and also in the case of some known compounds, where previously published data were incomplete. Enantiomeric purity was checked by chiral HPLC analysis.

Five phenanthrenes were isolated from *J. atratus*. Two compounds (juncatrins A and B, **1**, **2**), are new natural products, substituted with an acetyl or an acetylene group at C-8, respectively, instead of a vinyl group present in juncuenin B (**3**) at the same position. This was the first time that a phenanthrene with an acetylene moiety was isolated from natural source. Regarding the isolation yields of compounds from *J. atratus*, juncuenin B (**3**) is the major phenanthrene of the plant as more than 100 mg was isolated. Most probably, juncatrins A (**1**) and B (**2**) are derived biosynthetically from juncuenin B. Moreover, the phenanthrene dehydroeffusol (**5**) and its 9,10-dihydro analogue effusol (**4**) were also determined from the plant. All identified compounds (phenanthrenes and other components, **1**–**9**) were isolated for the first time from *J. atratus*.

The structure analysis of compounds isolated from *J. gerardii* led to the identification of 23 phenanthrenes, of which 12, members of the gerardiin A-L series, are new natural substances. Gerardiin A (**10**) and gerardiin B (**11**) are substituted with a methoxymethylene group at C-1 (**10**) or C-7 (**11**). The structure of compound **10** is very similar to that of effusol (**4**), with the only difference being the presence of a methoxy group at C-11. Gerardiins C (**12**) and D (**13**) are glycosides of effusol, substituted with a D-glucose unit at C-2 (**12**) or C-7 (**13**), respectively. Gerardiins F (**15**) and G (**16**) are also substituted with a D-glucose moiety at C-2 (**15**) or C-7 (**16**), but instead of a vinyl group a hydroxyethyl group is joined at C-5 to the skeleton. Similarly, gerardiin E (**14**) contains a hydroxyethyl group at the same position as **15** and **16**. The only difference between gerardiin H (**17**) and juncunol (**36**), isolated from *J. maritimus* and other *Juncus* species (*J. acutus*, *J. effusus*, *J. roemerianus*, *J. subulatus*),[74,90-92] is the presence of an unsaturated ring B in the former phenanthrene.

Phenanthrenoid dimers represent a rare class of secondary metabolites; to date, less than 20 have been reported from species in the plant family Juncaceae. In gerardiins I (**18**) and J (**19**), the two effusol (**4**) monomers are connected through their vinyl groups. Gerardiin K (**20**) is composed of two effusol (**4**) monomers that are joined through an ether bond, while in gerardiin L (**21**) an effusol (**4**) and

a dehydroeffusol (**5**) unit is attached via a C–C linkage formed between C-8–C-8'. The individual monomers [effusol (**4**), and dehydroeffusol (**5**)] were also isolated from the plant.

As a result of phytochemical investigation of *J. maritimus* 11 phenanthrenes, among them four new ones [maritins A–D (**32**–**35**)] were identified. The obtained compounds are substituted with hydroxy, methyl, formyl, hydroxymethyl, methoxyethyl, and vinyl groups. From a biosynthetic point of view, maritin C (**34**) was likely formed from a dehydrojuncusol precursor through the modification of its vinylic double bond, followed by a ring closure between C-4 and C-13, forming a rare 4,5-ethanophenanthrene scaffold. The phenanthrene dimer maritin D (**35**) evolves two effusol monomers attached through an ether bond between C-2–C-3', resulted in the formation of a unique diaryl ether skeleton. Seven known phenanthrenes [effusol (**4**), juncusol (**24**), 2,7-dihydroxy-5-formyl-1-methyl-9,10-dihydrophenanthrene (**26)**, juncunol (**36**), 2,7-dihydroxy-1,8-dimethyl-5-vinyl-9,10-dihydrophenanthrene (**37)**, jinflexin A (**38**) and the dimer effususin A (**30**)] were also isolated from the apolar fraction of the plant. All compounds except for effusol (**4**) were isolated for the first time from the plant.

Finally, 19 compounds, including 17 phenanthrenes, were identified from the methanolic extract of *J. ensifolius*. 13 Phenanthrenes, namely ensifolins A–M (**39**–**51**), were obtained for the first time from natural source. Ensifolins A (**39**) and B (**40**) are structurally unique phenanthrenes, considering that they are flavonoid- (luteolin, **7**) or benzaldehyde- (**53**) adducts. Compound **41** is a rare 10-hydroxphenanthrene. Similar compound was isolated previously only from *Luzula sylvatica*. Ensifolin D (**42**) is the 11-methoxy derivative of sylvaticin A (**52**) which was also isolated from the plant. Gerardiin H (**17**) can be served as the biogenetic precursor of both **42** and **52**. The dimers isolated from *J. ensifolius* mainly built up from monomers also isolated from the plant; e.g., in ensifolins J (**48**) and L (**50**), two ensifolin E (**43**) units are connected via their C-3 carbons (**48**) or through C-6 and C-3' carbons (**50**) forming symmetrical or not symmetrical molecules. Similarly, in ensifolin M (**51**) two juncatrin B (**2**) monomers are connected through their C-3 carbons forming a symmetrical dimer, and finally in ensifolin K (**49**) a **43** unit is connected to a dehydrojuncuenin B monomer through a C–C bond formed between C-5–C-3'. Four known phenanthrenes [juncatrin B (**2**), juncuenin B (**3**), gerardiin H (**17**) and sylvaticin A (**52**)], and 4-hydroxybenzaldehyde (**53**) and luteolin (**7**) were also isolated from the plant. All compounds were identified for the first time from *J. ensifolius.*

6.2. BIOACTIVITY OF THE ISOLATED COMPOUNDS

Our investigations are focused on the antiproliferative activity of the isolated phenanthrenes to give as many information as possible. Therefore, the isolated phenanthrenes were evaluated for their antiproliferative activity against different human tumor and normal cell lines by MTT assay. DMSO was used as a negative control and cisplatin or doxorubicin as positive controls.

6.2.1. *Juncus atratus*

Phenanthrenes (**1**–**5**), isolated from *J. atratus*, were tested for their antiproliferative activity against three human tumor cell lines [HeLa and SiHa (cervix adenocarcinoma) and MDA-MB-231 (breast carcinoma)] using the MTT test with cisplatin as positive control. HeLa cell line proved to be the most sensitive with four phenanthrenes (**2**–**5**) being more effective [IC_{50} 3.5 μM (**2**), 2.9 (**3**), 3.7 (**4**), and 7.8 μM (**5**)] than clinically used reference agent cisplatin (IC_{50} 12.4 μM). The compounds with the most pronounced antiproliferative action (**2**–**5**) were additionally tested against NIH-3T3 mouse fibroblasts in order to obtain preliminary data. It was found that all of these agents (**2**–**5**) exerted only negligible action (less than 35% inhibitory activity) on fibroblasts even at 30 μM, and therefore, the antiproliferative action of the tested molecules can be considered cancer selective. Based on these results, some structure-activity relationships could be obtained. Compounds **1**–**3** differ each other in only the substituent at C-8. Since **1** is markedly less effective [on HeLa 55.6 ± 1.9 % (SEM) at 30 μM] than **2** and **3**, presence of an acetyl group instead of a vinyl or an acetylene substituent at the same position seems to be disadvantageous. In case of compounds **4** and **5**, differing only in the saturation of ring B, the dihydrophenanthrene effusol (**4**) proved to be more active. It seems that presence of a methyl group on ring C has no significant effect on the antiproliferative activity of phenanthrenes against HeLa cell line. The other cell lines were substantially less sensitive.

6.2.2. *Juncus gerardii*

In order to gain a deeper insight into the biological effects of the isolated phenanthrenes, 4T1 mouse breast cancer cells were treated with the compounds isolated from *J. gerardii* and changes in the viability and impedance were assessed, which reflects proliferation, degree of adhesion, spreading and viability of the cells. At a concentration of 20 μM, compounds **10**–**17** (gerardiins A–H) had no cytotoxic effects on 4T1 cells, as assessed by a MTT assay.

In contrast to this, the viability of 4T1 cells was reduced significantly in a concentration-dependent manner in response to compounds **18**–**21** (gerardiins I–L). The effect of these phenanthrenes was comparable to that of doxorubicin, which was applied as a positive control to measure cytotoxicity. Since all these compounds are dimers of effusol (**4**) (compounds **18**–**20**) or of effusol and dehydroeffusol (**5**) (compound **21**), the cytotoxic effects of the monomers and dimers in both mouse and human tumor cells and in a non-tumor cell line (D3) were compared. Besides the aforementioned phenanthrenes, effususin A (**30**) was also included in this study, since it is also a dimer of effusol. The results show unequivocally that the dimeric compounds **18**–**21** and **30** comprising effusol (**4**) and dehydroeffusol (**5**) monomers are cytotoxic to both tumor and non-tumor cell lines, while the monomers (**4** and **5**) alone displayed no or very low cytotoxicity. Among the diphenanthrenes tested, effususin A (**30**) exerted the lowest cytotoxicity, while gerardiins I-L (**18**–**21**) proved to be the

most active. Indeed, moderate toxicity of effususin A (**30**) in A2780 human ovarian cancer cells reported by Bús et al.[80] Impedance measurements were in line with the results of the MTT assay, indicating a concentration-dependent toxicity of the dimers.

IC_{50} values of both **18** and **19** were below 10 μM in the two tested tumor cell lines (**Table 3**). In case of compound **20**, the concentration that caused 50% inhibition of cell viability was lower than 10 μM only in the mouse (4T1) (IC_{50} 8.1 μM), but not in the human breast cancer (MDA-MB-231) cell line (10.1 μM). On the other hand, compound **21** was more cytotoxic (IC_{50} 7.3 μM) to the human breast cancer cells (IC_{50} was 11.7 μM on 4T1 cells). D3 endothelial cells were the less sensitive to these diphenanthrenes, all of them having IC_{50} values above 10 μM (21.6 μM for **18**, 15.7 μM for **19**, 10.6 μM for **20**, and 13.7 μM for **21**, respectively).

Table 3. IC_{50} values and their 95% Confidence Intervals [95% CI] for compounds **18**–**21.**

Compound	Cell line	
	MDA-MB-231	4T1
18	8.0 [7.3-8.8]	7.8 [6.5-9.5]
19	6.6 [6.2-7.1]	5.6 [5.1-6.1]
20	>10	8.1 [7.7-8.6]
21	7.3 [6.7-7.9]	>10
doxorubicin	0.8 [0.7-0.9]	3.4 [3.1-3.7]

Considering the already known isolated phenanthrenes, only juncusol (**24**) (in MTT and impedance assays) and jinflexin C (**29**) (in impedance measurements) displayed moderate cytotoxicity, while compounds **22**, **23**, **25**–**28** were not cytotoxic in 4T1 cells at the concentration of 20 μM. The present results are in agreement with previous findings that demonstrated the antiproliferative activity of juncusol (**24**) against HeLa cervical cancer cells.[11]

6.2.3. *Juncus maritimus*

In case of *J. maritimus* the obtained phenanthrenes **4**, **24**, **26**, **30**, **32**–**38**, were tested for their antiproliferative activity against seven human tumor cell lines (HeLa, HTM-26, T-47D, A2780, A2780cis, MCF-7, KCR) and one normal human fetal lung fibroblast (MRC-5) cell line using the 3-(4,5-dimethylthiazol-2-yl)-2,5-diphenyltetrazolium bromide (MTT) assay with cisplatin as a positive control (**Table A14**). Among the tested compounds, dimeric phenanthrenes (**35** and **30**) built up by effusol (**4**) monomers showed substantial antiproliferative activity against all cell lines investigated. The highest activities were detected on T-47D ductal carcinoma cells (IC_{50} 9.1 μM for **35** and 6.2 μM for **30**, respectively) for both compounds. No significant differences were observed between the effects of dimers on different cell lines. In general, T-47D cells were the most sensitive to the phenanthrenes, but some of the isolated compounds [e.g., maritin C (**34**) on MCF-7 cells; maritin B (**33**), juncusol (**24**), and effusol (**4**) on HeLa cells] exerted outstanding inhibitory potential against other malignant cell lines, too.

6.2.4. *Juncus ensifolius*

6.2.4.1. Antiproliferative activity of the compounds

The antiproliferative activity of compounds (**2**, **3**, **7**, **17**, **39**–**53**) was investigated on human cancer cell lines [cervical cancer (HeLa), doxorubicin-sensitive colonic adenocarcinoma COLO 205, multidrug resistant colonic adenocarcinoma COLO 320/MDR-LRP expressing P-gp (MDR1)-LRP, and on human embryonal lung fibroblast MRC-5]. The MTT assay was used for each compound to assess the concentration required for 50% inhibition of viability of the cell population (IC_{50}) (**Table A15**). The luteolin-substituted phenanthrene **39** was found to be the most promising component with substantial antiproliferative effects against all three tested cell lines (IC_{50} values 3.9–12.7 μM) and showed good selectivity (SI = 4.95) in case of COLO 205 cells. It was more than ten-fold as active as the positive control cisplatin in COLO 205 cells. Interestingly, luteolin (**7**) alone, and compound **45**, structurally very similar to the phenanthrene unit of ensifolin A (**39**), were inactive for all tested cell lines.

The lowest IC_{50} values against HeLa cells was found for compounds **3** (IC_{50} 6.67 μM) and **2** (IC_{50} 6.65 μM). The only difference between the two compounds is the substituent at C-8, which is a vinyl group in case of **3**, and an acetylene group in **2**. Ensifolin E (**43**) differing from juncuenin B (**3**) only in the position of the hydroxy group (at C-5 in **43**, and at C-6 in **3**), resulted in a significant decrease in the activity against HeLa cells, while changing of methyl group at C-7 in **43** to hydroxymethylene group in ensifolin F (**44**) led to the loss of the activity. Compounds **46** and **52** possessed moderate antiproliferative activity (IC_{50} values 12.31 μM and 10.56 μM) against HeLa cells. Ensifolin I (**47**) is the dehydroderivative of sylvaticin A (**52**), and this modification resulted in an increased activity in cases of COLO 205 and COLO 320 cell lines, while a twofold decrease at HeLa cells. Finally, dimerization of phenanthrene monomers resulted in the decrease of the activity, as it can be seen in case of compounds **47** and **51**, while in case of **48** and **50** which are the dimers of ensifolin E (**43**), neither the monomer nor its dimers showed antiproliferative activity. The best selectivity was obtained for ensifolins D (**42**, SI > 5.15, HeLa), and H (**46**, SI > 8.13, HeLa), and for compounds **2** (SI > 3.91, HeLa), **3** (SI > 5.37, HeLa), and **52** (SI > 9.43, HeLa).

6.2.4.2. Drug combination assay

Many types of cancers are highly resistant to the currently available chemotherapeutic agents. Therefore, new effective and well-tolerated therapy strategies are needed. One of the possibilities is the identification of new bioactive natural products. Therefore, a chemosensitivity assay was carried out by studying the *in vitro* interactions between the compounds and the antineoplastic drug doxorubicin, known to be transported by P-gp. Therefore, a combination chemotherapy model on human HeLa cervical carcinoma cells was performed. The combination index (CI), based on the Chou

and Talalay method, was the main parameter to assess drug-drug interactions as synergistic (CI < 1), additive (CI = 1) or antagonistic (CI > 1) (**Table A16**).[93,94]

All tested compounds were found to interact synergistically with doxorubicin (CI < 1) on HeLa cell line. Very strong synergisms were observed for ensifolins E (**43**) and H (**46**), with CI values lower than 0.1. Both compounds showed weak or moderated activity (IC_{50} 25.2–31.2 μM for **43**, and 12.3–63.5 μM for **46**) in case of antiproliferative investigation.

7. SUMMARY

The primary aim of the present work was the phytochemical and pharmacological investigation of Juncaceae species occurring in Hungary, and the isolation and structure determination of biologically active compounds from *Juncus atratus*, *J. gerardii*, *J. maritimus* and *J. ensifolius*.

In the preparative work, the lipophilic extracts (CH_2Cl_2, $CHCl_3$ and EtOAc) were purified by multistep separation procedures, including OCC, VLC, MPLC, GF, PLC and HPLC to yield pure compounds. The structures of the isolated compounds were elucidated by means of spectroscopic methods (HR-MS and NMR). In addition, complete ^{1}H and ^{13}C NMR assignments were made for the characterization of the compounds.

As a result of our work, altogether, 53 compounds were isolated from the four investigated *Juncus* species, 47 of them are phenanthrenes (**Annex I**). Five phenanthrenes (**1**–**5**), two flavonoids (**6**, **7**), an acyclic diterpene (**8**) and a fatty acid (**9**) from *J. atratus*, 23 phenanthrenes (**4**, **5**, **10**–**30**) and a glycerol derivative (**31**) from *J. gerardii*, 11 phenanthrenes (**4**, **24**, **26**, **30**, **32**–**38**) from *J. maritimus* and 17 phenanthrenes (**2**, **3**, **17**, **39**–**52**), one flavonoid (**7**) and 4-hydroxybenzaldehyde (**53**) were obtained from *J. ensifolius*. All the isolated compounds except for effusol (**4**) from *J. maritimus* were detected for the first time from the investigated plants. The chemical constituents of *J. atratus*, *J. gerardii* and *J. ensifolius* have not been investigated previously. Among the isolated compounds, phenanthrenes are the most promising ones from phytochemical and pharmacological points of view. 31 of the identified 47 phenanthrenes are new natural products. 37 Compounds are monomers (33 dihydrophenanthrenes and 4 phenanthrenes) and 10 are dimers. The most interesting monomers are the flavonoid- and 4-hydroxybenzaldehyde adducts **39** and **40**. Compounds **34** and **41** are also unique as in case of **34** a ring closure was occurred between C-4 and C-13 resulted in a tetracyclic ring system while **41** is substituted at C-10. Compounds **12**, **13**, **15** and **16** are glucosides. The methyl group at C-1, a hydroxy group at C-2, and vinyl, methyl and hydroxy substitution on ring C are characteristic features of Juncaceae phenanthrenes. In some cases, the methyl group at C-1 was modified to methoxymethylene (**10**, **42**) or hydroxymethyl moiety (**52**), and the hydroxy group at C-2 was changed to methoxy group in **22** and **23**. Moreover, on ring C, hydroxyethyl (**14**–**16**), methoxyethyl (**27**, **38**), formyl (**26**), hydroxymethyl (**32**), acetyl (**1**, **45**) or acetylene (**2**, **46**) group are presented instead of the vinyl unit. In compound **29**, a carbonyl group can be found in the molecule.

In case of the dimers, mostly two effusol (**4**) monomers are connected in different ways forming C–C bond (**30**) or an ether bond (**20**, **35**). In compounds **18** and **19** the two monomers (**4**) joined through their vinyl groups and a heptacyclic ring system is formed. In **21**, an effusol (**4**) and a dehydroeffusol (**5**) unit are connected. In **48** and **50**, two ensifolin E (**43**) units are joined through their 3–3’ or 6–3’

carbons, respectively. Compound **43** also formed a dimer with dehydrojuncuenin B in **49**. And finally, in **51** two juncatrin B (**2**) are joined through their C-3–C-3' resulted in a symmetrical dimer.

Based on the phenanthrene content, *J. gerardii* and *J. ensifolius* are considered to be as good sources of phenanthrenes. Juncusol (**24**) and effusol (**4**) are common constituents of *Juncus* species as they were detected in almost all previously investigated species. They can be served as biogenetic precursors of other Juncaceae phenanthrenes.

Vinyl substituted derivatives can be considered as chemotaxonomic markers for plants belonging to family Juncaceae, since these specifically substituted phenanthrenes were reported only from *Juncus* and *Luzula* species. To date, only two *Luzula* species (*L. luzuloides* and *L. sylvatica*) were investigated thoroughly from phytochemical point of view. Previous investigations focused only on the flavonoid content of the plants. As the phenanthrene content of the investigated *Luzula* and *Juncus* species are very similar it can further confirm the close botanical relationship between the two genera.

From pharmacological point of view the antiproliferative activity and synergistic effect of phenanthrenes with the standard drug doxorubicin can be highlighted. In case of the antiproliferative activity, HeLa cell line proved to be the most sensitive on phenanthrenes. Phenanthrenes **2**–**5**, **24**, **33** and **39** showed remarkable antiproliferative effects [IC_{50} 2.3 μM (**2**), 2.9 μM (**3**), 3.7 μM (**4**), and 7.8 μM (**5**), 0.5 μM (**24**), 11 μM (**33**) and 8.3 μM (**39**)] on HeLa cells. Cytotoxic effect of the dimers of effusol (**18**–**20**), or effusol and dehydroeffusol (**21**) was comparable to that of the positive control doxorubicin to both 4T1 mouse [IC_{50} 7.8 µM (**18**), 5.6 μM (**19**), and 8.1 μM (**20**)] and MDA-MB-231 human breast cancer [IC_{50} 8.0 μM (**18**), 6.6 μM (**19**), and 7.3 μM (**21**)] cells. Interestingly, the monomers **4** and **5** alone displayed no or very low activity. In case of the effusol dimers **30** and **35** remarkable activities were detected in T-47D (IC_{50} 6.2 μM for **30**, and 9.1 μM for **35**) cells. The luteolin-substituted phenanthrene **39** was found to be promising component especially against COLO 205 cells (IC_{50} 3.9 μM). Finally, in the drug combination assay, the interaction of phenanthrenes isolated from *J. ensifolius* was tested with doxorubicin on HeLa cell line and compounds **43** and **46** possessed very strong synergism with the standard drug with CI values lower than 0.1.

Our findings not only enriched the chemical diversity of phenanthrenes but also provided new natural small molecules with antiproliferative activity for further drug developments.

8. REFERENCES

[1] Newman DJ, Cragg GM. *J. Nat. Prod.* **2020**, *83*:770–803.

[2] Abdalla A, Murali C, Amin A. *Front. Oncol*. **2022**, *11*:789172.

[3] Juaid N, Amin A, Abdalla A, Reese K, Alamri Z, Moulay M, Abdu S, Miled N. *Int. J. Mol. Sci*. **2021**, *22*:10774.

[4] Kojima-Yuasa A, Huang X, Matsui-Yuasa I. *Diseases* **2015**, *3*:260–281.

[5] Cao H, Phan H, Yang IX. *Anticancer Res.* **2012**, *32*:1379–1386.

[6] Lagoa R, Silva J, Rodrigues JR, Bishayee A. *Biotechnol. Adv*. **2020**, *38*:107382.

[7] Baig B, Halim SA, Farrukh A, Greish Y, Amin A. *Biomed. Pharmacother*. **2019**, *116*:108852.

[8] Tóth B, Hohmann J, Vasas A. *J. Nat. Prod*. **2018**, *81*:661–678.

[9] Liu W, Meng M, Zhang B, Du L, Pan Y, Yang P, Gu Z, Zhou Q, Cao Z. *Toxicol. Appl. Pharmacol*. **2015**, *287*:98–110.

[10] Zhang B, Han H, Fu S, Yang P, Gu Z, Zhou Q, Cao Z. *Biochem. Pharmacol*. **2016**, *104*:8–18.

[11] Kuo CY, Schelz Z, Tóth B, Vasas A, Ocsovszki I, Chang FR, Hohmann J, Zupkó I, Wang HC. P*hytomedicine* **2019**, *58*:152770.

[12] Bús C, Kulmány Á, Kúsz N, Gonda T, Zupkó I, Mándi A, Kurtán T, Tóth B, Hohmann J, Hunyadi A, Vasas A. *J. Nat. Prod*. **2020**, *83*:3250–3261.

[13] Tóth B, Chang FR, Hwang TL, Szappanos Á, Mándi A, Hunyadi A, Kurtán T, Jakab G, Hohmann J, Vasas A. *Fitoterapia* **2017**, *116*:131–138.

[14] Balslev H. Juncaceae. *Flora Neotropica* **1996**, *68*:1–167.

[15] Tutin TG, Heywood VH, Burges NA, Moore DM, Valentine DH, Walters SM, Webb DA. *Flora Europaea, Vol 5.* Cambridge: University Press **1968**, pp. 102–116.

[16] Simon T. *A magyarországi flóra határozója, Harasztok – virágos növények*. Budapest, Nemzeti Tankönyvkiadó **2000**. pp 701–704.

[17] Watson EB, Wigand C, Cencer M, Blount K. *Aquat. Bot*. **2015**, *121*:52–56.

[18] Soundararajan P, Manivannan A, Jeong BR. Tasks for Vegetation Science. In: *Sabkha Ecosystems,* Vol. VI. *Asia/Pacific*; Springer: Cham, Switzerland **2019**, *49*: 335–347.

[19] Menéndez M. *Aquat. Bot*. **2008**, *89*:365–371.

[20] *Juncus ensifolius* (swordleaf rush). https://www.cabi.org/isc/datasheet/115030 (accessed on 17 May 2022)

[21] Cronquist A. The evolution and classification of flowering plants. **1968**, Thomas Nelson & Sons, London.

[22] Bate-Smith EC. *J. Linn. Soc. (Bot.)* **1968**, *60*:325–356.

[23] Stabursvik A. *Acta Chem. Scand.* **1968**, *22*:2371–2373.

[24] Williams CA, Harborne JB. *Biochem. Syst. Ecol.* **1975**, *3*:181–190.

[25] El-Shamy AI, Abdel-Razek AF, Nassar MI. *Arab. J. Chem*. **2015**, *8*:614–623.

[26] Behery FAA, Naeem ZEM, Maatooq GT, Amer MMA, Ahmed AF. *Nat. Prod. Res.* **2013**, *27*:155–163.

[27] Park S, Yang S, Ahn D, Yang JH, Kim DK. *J. Korean Soc. Appl. Biol. Chem.* **2011**, *54*:685–692.

[28] Della Greca M, Fiorentino A, Isidori M, Previtera L, Temussi F, Zarrelli A. *Tetrahedron* **2003**, *59*:4821–4825.

[29] Stabursvik A. *Acta Chem. Scand.* **1968**, *22*:2056–2057.

[30] Dong-Zhe J, Zhi-Da M, Chiou GCY, Inuma M, Tanaka T. *Phytochemistry* **1996**, *41*:545–547.

[31] Della Greca M, Fiorentino A, Monaco P, Previtera L. *Phytochemistry* **1994**, *35*:1017–1022.

[32] Corsaro MM, Della Greca M, Fiorentino A. *Phytochemistry* **1994**, *37*:515–519.

[33] Awaad AS. *Chem. Nat. Compd.* **2006**, *42*:152–155.

[34] Shi QW, Su XH, Kiyota H. *Chem. Rev*. **2008**, *108*:4295–4327.

[35] Vasas A. Phenanthrenes from Orchidaceae and Their Biological Activities. In: *Orchids Phytochemistry, Biology and Horticulture – Fundamentals and Applications*. Reference Series in Phytochemistry. Eds Jean-Michel Merillon, Hippolyte Kodja, Springer, **2021**, pp. 1-41.

[36] Bús C, Tóth B, Stefkó D, Hohmann J, Vasas A. *Phytochem. Rev*. **2018**, *17*:833–851.

[37] Abdel-Shafy HI, Mansour MSM. *Egypt. J. Pet*. **2016**, *25*:107–123.

[38] Andreoni V, Gianfreda L. PAH bioremediation by microbial communities and enzymatic activities. In: *Handbook of Green Chemistry: Online* Vol. 3. Biocatalysis **2015**, 243–268.

[39] Menichini E, Bocca B. Polycyclic aromatic hydrocarbons. In: *Encyclopedia of Food Sciences and Nutrition* (2nd Eds.) **2003**.

[40] Skupinska K, Mislewicz I, Kasprzycka-Guttman T. *Acta Pol. Pharm*. **2004**, *61*:233–240.

[41] Alagić SČ, Maluckov BS, Radojičić VB. *Clean Techn. Environ. Policy* **2015**, *17*:597–614.

[42] Chong J, Poutaraud A, Hugueney P. *Plant Sci.* **2009**, *177*:143–155.

[43] Long L, Lee SK, Chai HB, Rasoanaivo P, Gao Q, Navarro H, Wall ME, Wani MC, Farnsworth NR, Cordell GA, Pezzuto JM, Kinghorn AD. *Tetrahedron* **1997**, *53*:15663–15670.

[44] Vasas A, Hohmann J. *Chem. Rev*. **2014**, *114*:8579–8612.

[45] Merves ML, Goldberger BA. Heroin. In: *Encyclopedia of Analytical Science* (2nd Ed.), **2005**.

[46] Kovács A, Vasas A, Hohmann J. *Phytochemistry* **2008**, *69*:1084–1110.

[47] Li JY, Kuang MT, Yang L, Kong QH, Hou B, Liu ZH, Chi XQ, Yuan MY, Hu JM, Zhou J. *Fitoterapia* **2018**, *127*:74–80.

[48] Sun MH, Ma XJ, Shao SY, Han SW, Jiang JW, Zhang JJ. *Phytochemistry* **2021**, *182*:112609.

[49] Cheng L, Guo DL, Zhang MS, Linghu L, Fu SB, Deng Y, He YQ, Xiao SJ. *Fitoterapia* **2020**, *143*:104586.

[50] Zhao GY, Deng BW, Zhang CY, Cui YD, Bi JY. *J. Nat. Med*. **2018**, *72*:246–251.

[51] Ranong SN Likhitwitayawuid K, Mekboonsonglarp W, Sritularak B. *Nat. Prod. Res*. **2019**, *33*:420–426.

[52] Sun J, Zhang Y, Chen L, Zhan R, Chen Y. *Nat. Prod. Res*. **2018**, *32*:2447–2451.

[53] Liu L, Yin QM, Yan X, Hu C, Wang W, Wang RK, Luo X, Zhang XW. *J. Agric. Food Chem*. **2019**, *67*:7274–7280.

[54] Zhao Y, Kongstad KT, Liu Y, He C, Staerk D. *Faraday Discuss*. **2019**, *218*:202–218.

[55] Maffo T, Melong R, Nganteng DND, Wafo P, Ali MS, Ngadjui BT. *Nat. Prod. Res*. **2018**, *32*:85–90.

[56] Pang X. Yin SS, Yu HY, Zhang Y, Wang T, Hu LM, Han LF. *Nat. Prod. Res*. **2017**, DOI: 10.1080/14786419.2017.1405410.

[57] Huang SZ, Kong FD, Chen G, Cai XH, Zhou LM, Ma QY, Wang Q, Mei WL, Dai HF, Zhao YX. *Phytochemistry* **2019**, *159*:208–215.

[58] Xiao J, Wang Y, Yang Y, Liu J, Chen G, Lin B, Hou Y. *Bioorg. Chem*. **2021**, *107*:104597.

[59] Shao SY, Wang C, Han SW, Sun MH, Li S. *Org. Biomol. Chem*. **2019**, *17*:567–572.

[60] Liu L, Yin QM, Gao Q, Li J, Jiang Y, Tu PF. *Nat. Prod. Res*. **2021,** *35*:750–756.

[61] Gainche M, Ripoche I, Senejoux F, Cholet J, Ogeron C, Decombat C, Danton O, Delort L, Vareille-Delarbre M, Berry A, Vermerie M, Fraisse D, Felgines C, Ranouille E, Berthon JY, Priam J, Saunier E, Tourrette A, Troin Y, Caldefie-Chezet F, Chalard P*Molecules* **2020**, *25*:2372.

[62] Oliveira M, Sales Jr PA, Rodrigues MJ, DellaGreca M, Barreira L, Murta SMF, Romanha AJ, Custódio L. *Asian Pac. J. Trop. Med*. **2016**, *9*:735–741.

[63] Sahli R, Rivière C, Siah A, Smaoui A, Samaillie J, Hennebelle T, Roumy V, Ksouri R, Halama P, Sahpaz S. *Environ. Sci. Pollut. Res*. **2018**, *25*:29775–29783.

[64] Sahuc ME, Sahli R, Rivière C, Pène V, Lavie M, Vandeputte A, Brodin P, Rosenberg AR, Dubuisson J, Ksouri R, Rouillé Y, Sahpaz S, Séron K. *J. Virol*. **2019**, *93*:e02009-18.

[65] Song JI, Kang YJ, Yong HY, Kim YC, Moon A. *Oncol. Rep*. **2012**, *27*:813–818.

[66] Sánchez-Duffhues G, Calzado MA, de Vinuesa AG, Appendino G, Fiebich BL, Loock U, Lefarth-Risse A, Krohn K, Muñoz E. *Biochem. Pharmacol*. **2009**, *77*:1401–1409.

[67] Lu TL, Han CK, Chang YS, Lu TJ, Huang HC, Bao BY, Wu HY, Huang CH, Li CY, Wu TS. *Am. J. Chin. Med*. **2014**, *42*:1539–1554.

[68] Boudjada A, Touil A, Bensouici C, Bendif H, Rhouati S. *Nat. Prod. Res*. **2019**, *33*:3278–3282.

[69] Lee W, Jeong SY, Gu MJ, Lim JS, Park EK, Baek MC, Kim JS, Hahn D, Bae JS. *J. Toxicol. Environ. Health Part A* **2019**, *82*:727–740.

[70] Li Q, Li K, Hu T, Liu F, Liao S, Zou Y. *J. Agric. Food Chem*. **2021**, *69*:4720–4731.

[71] Sangdee A, Sangdee K, Bunchalee P, Seephonkai P. *Trop. Biomed*. **2021**, *38*:484–490.

[72] Wang XY, Ke CQ, Tang CP, Yuan D, Ye Y. *J. Nat. Prod*. **2009**, *72*:1209–1212.

[73] Tóth B, Liktor-Busa E, Kúsz N, Szappanos Á, Mándi A, Kurtán T, Urbán E, Hohmann J, Chang FR, Vasas A. *J. Nat. Prod.* **2016**, *79*:2814–2823.

[74] DellaGreca M, Fiorentino A, Mangoni L, Molinaro A, Monaco P, Previtera L. *Tetrahedron Lett*. **1992**, *33*:5257–5260.

[75] Shima K, Toyota M, Asakawa Y. *Phytochemistry* **1991**, *30*:3149–3151.

[76] Shen CC, Chang YS, Ho LK. *Phytochemistry* **1993**, *34*:843–845.

[77] Lin LC, Pai YF, Tsai TH. *J. Agric. Food Chem*. **2015**, *63*:7700–7706.

[78] Ahrens EH, Williams DC, Battersby AR. *J. Chem. Soc. Perkin Trans. I*. **1977**, 2540–2545.

[79] Waridel P, Wolfender JL, Lachavanne JB, Hostettmann K. *Phytochemistry* **2004**, *65*:945–954.

[80] Bús C, Kúsz N, Jakab G, Tahaei SAS, Zupkó I, Endrész V, Bogdanov A, Burián K, Csupor-Löffler B, Hohmann J, Vasas A. *Molecules* **2018**, *23*:2085.

[81] DellaGreca M, Isidori M, Lavorgna M, Monaco P, Previtera L, Zarrelli A. *J. Chem. Ecol*. **2004**, *30*:867–879.

[82] DellaGreca M, Monaco P, Previtera L, Zarrelli A, Pollio A, Pinto G, Fiorentino A. *J. Nat. Prod.* **1997**, *60*:1265–1268.

[83] Wang YG, Wang YL, Zhai HF, Liao YJ, Zhang B, Huang JM. *Nat. Prod. Res.* **2012**, *26*:1234–1239.

[84] Ishiuchi K, Kosuge Y, Hamagami H, Ozaki M, Ishige K, Ito Y, Kitanaka S. *J. Nat. Med*. **2015**, *69*:421–426.

[85] Cooper R, Gottlieb HE, Lavie D. *Phytochemistry* **1978**, *17*:1673–1675.

[86] Stefkó D, Kúsz N, Barta A, Kele Z, Bakacsy L, Szepesi Á, Fazakas C, Wilhelm I, Krizbai IA, Hohmann J, Vasas A. *J. Nat. Prod.* **2020**, *83*:3058–3068.

[87] Resnick SM, Gibson DT. *Appl. Environ. Microbiol*. **1996**, *62*:3355–3359.

[88] Stefkó D, Kúsz N, Csorba A, Jakab G, Bérdi P, Zupkó I, Hohmann J, Vasas A. *Tetrahedron* **2019**, *75*:116–120.

[89] Della Greca M, Fiorentino A, Monaco P, Pinto G, Pollio A, Previtera L. *J. Chem. Ecol*. **1996**, *22*:587–603.

[90] DellaGreca M, Fiorentino A, Isidori M, Lavorgna M, Monaco P, Previtera L, Zarrelli A. *Phytochemistry* **2002**, *60*:633–638.

[91] Sarkar H, Zerchi M, Bhattacharya J. *Phytochemistry* **1988**, *27*:3006–3008.

[92] Abdel-Razik AFI, Elshamy ASI, Nassar MI, El-Kousy SM, Hamdy H. *Rev. Latinoamer. Quim*. **2009**, *37*:70–84.

[93] Chou TC. *Pharmacol. Rev*. **2006**, *58*:621–681.

[94] Ferreira MJU, Duarte N, Rei, M, Madureira AM, Molnar J. *Phytochemistry Rev*. **2014**, *13*:915–935.

ACKNOWLEDGEMENTS

This work was carried out at the Department of Pharmacognosy, University of Szeged, during the period 2016-2021. I am indebted to Professor Judit Hohmann, Director of the Department of Pharmacognosy, for placing the facilities of the department at my disposal.

I would like to express my sincere thanks to my supervisor, Andrea Vasas, for introducing me to the world of phenanthrenes. She was always there to answer questions, give advice and encourage work. Her professional knowledge and humanity are outstanding. I wouldn't have gotten this far without her. I have always admired her perseverance and diligence. She is a real role model for me.

Special thanks to László Bakacsy (Department of Plant Biology, University of Szeged, Faculty of Science and Informatics) and Gusztáv Jakab (Institute of Environmental Sciences, Faculty of Water and Environmental Management, Szent István University) for the identification and collection of plant materials.

I am grateful to Norbert Kúsz (Department of Pharmacognosy, Interdisciplinary Center of Excellence, University of Szeged) for the NMR measurements and evaluations; to Attila Csorba (Department of Pharmacognosy, University of Szeged) Zoltán Kele and Róbert Berkecz (Institute of Pharmaceutical Analysis, University of Szeged) for the MS measurements; to Péter Bérdi (Department of Pharmacodynamics and Biopharmacy, University of Szeged), István Zupkó (Department of Pharmacodynamics and Biopharmacy, University of Szeged), Csilla Fazakas, Imola Wilhelm, István A. Krizbai (Laboratory of Molecular Neurobiology, Institute of Biophysics, University of Szeged), Annamária Kincses, Nikoletta Szemerédi, Gabriella Spengler (Department of Medical Microbiology, Albert Szent-Györgyi Health Center and Albert Szent-Györgyi Medical School, University of Szeged) for the antiproliferative and cytotoxicity investigations.

Special thanks to Orsolya Éles, who introduced me in the world of laboratory work providing knowledge for successful research work and for being honored with her friendship.

I am grateful to all the staff of the Department for their help in my research and for the pleasant, good atmosphere.

I am especially grateful to my family for providing me with a supportive and encouraging background.

ANNEX

Annex I. Isolation of compounds from *J. atratus*, *J. gerardii*, *J. maritimus* and *J. ensifolius*

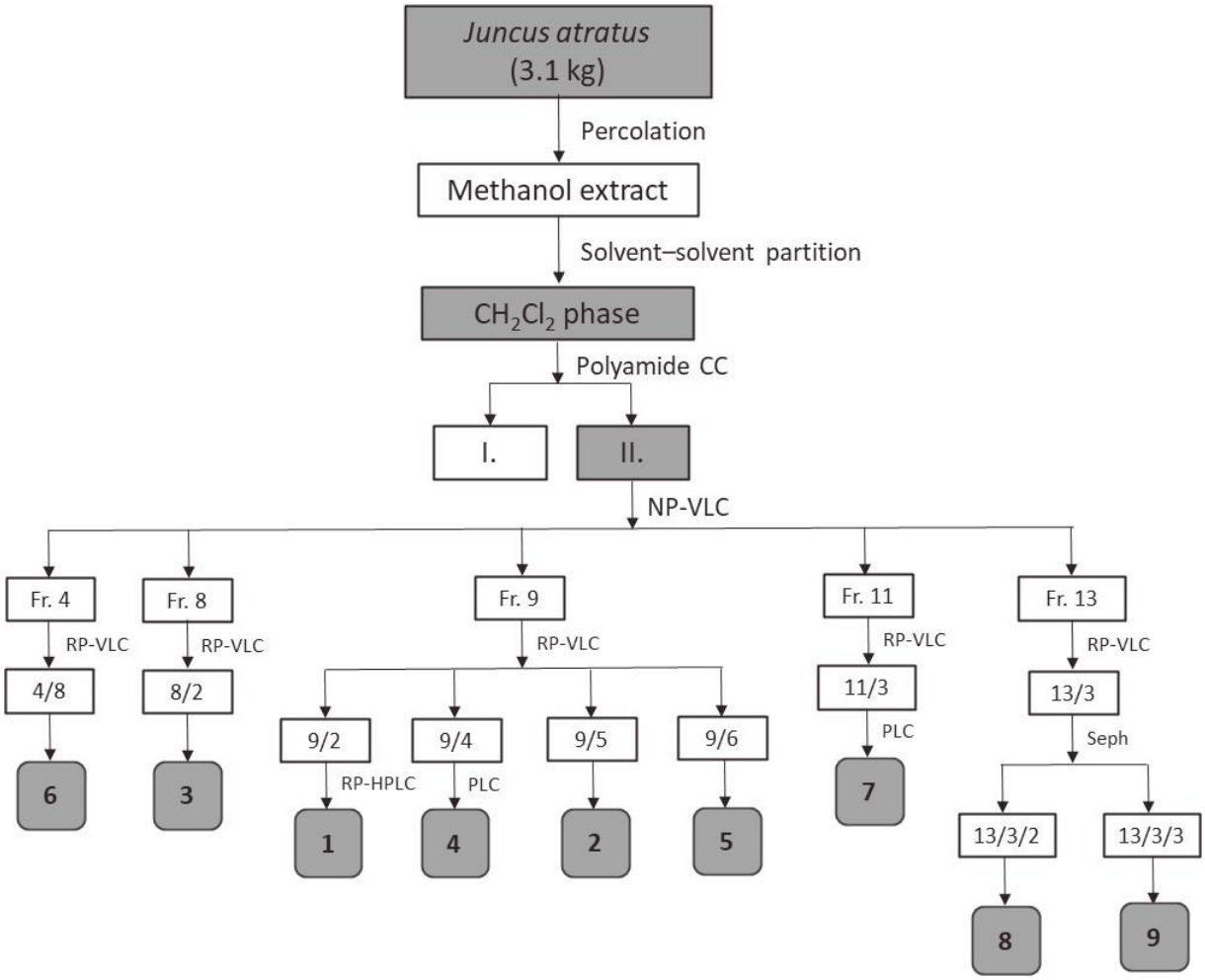

Isolation of compounds from *J. atratus*

Isolation of compounds from *J. gerardii*

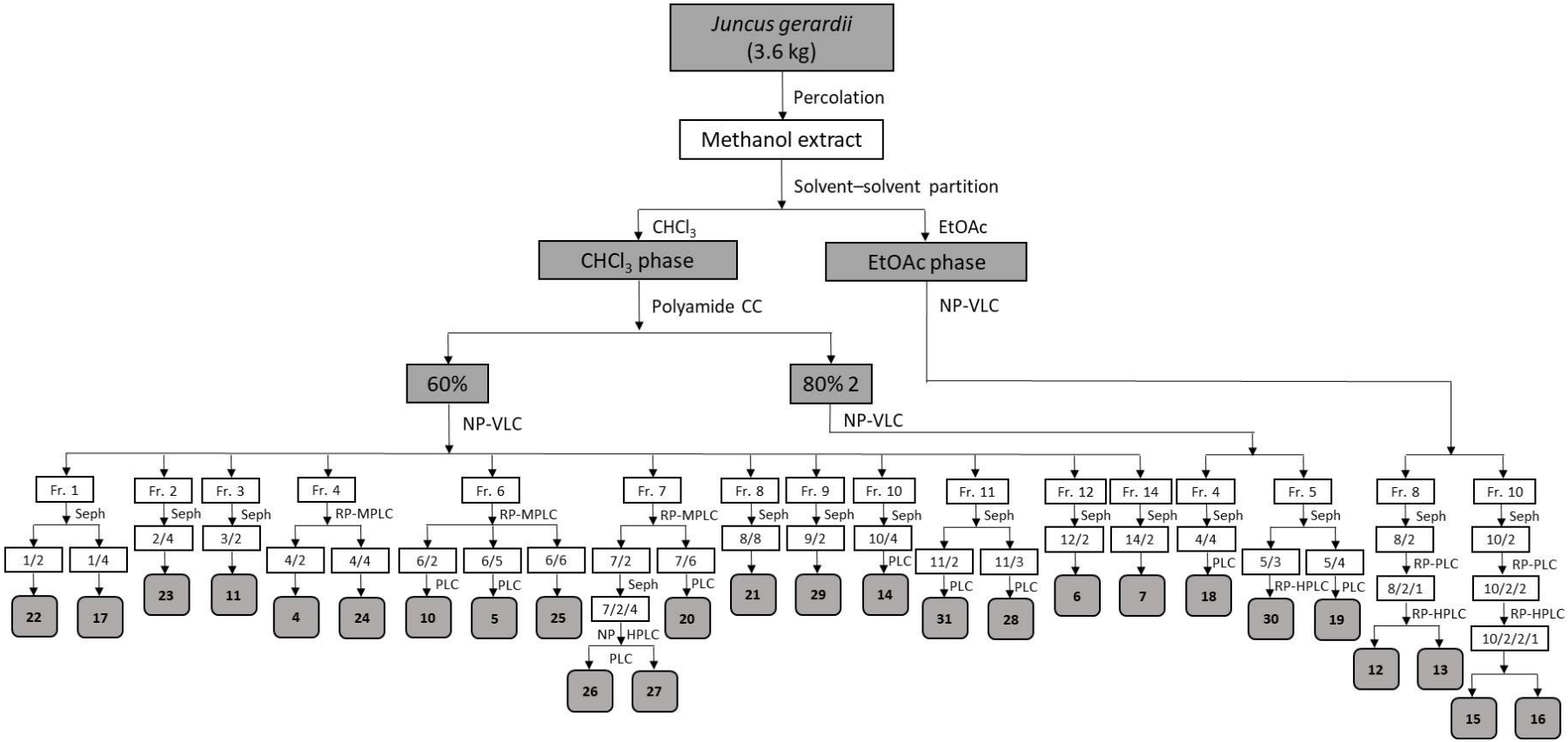

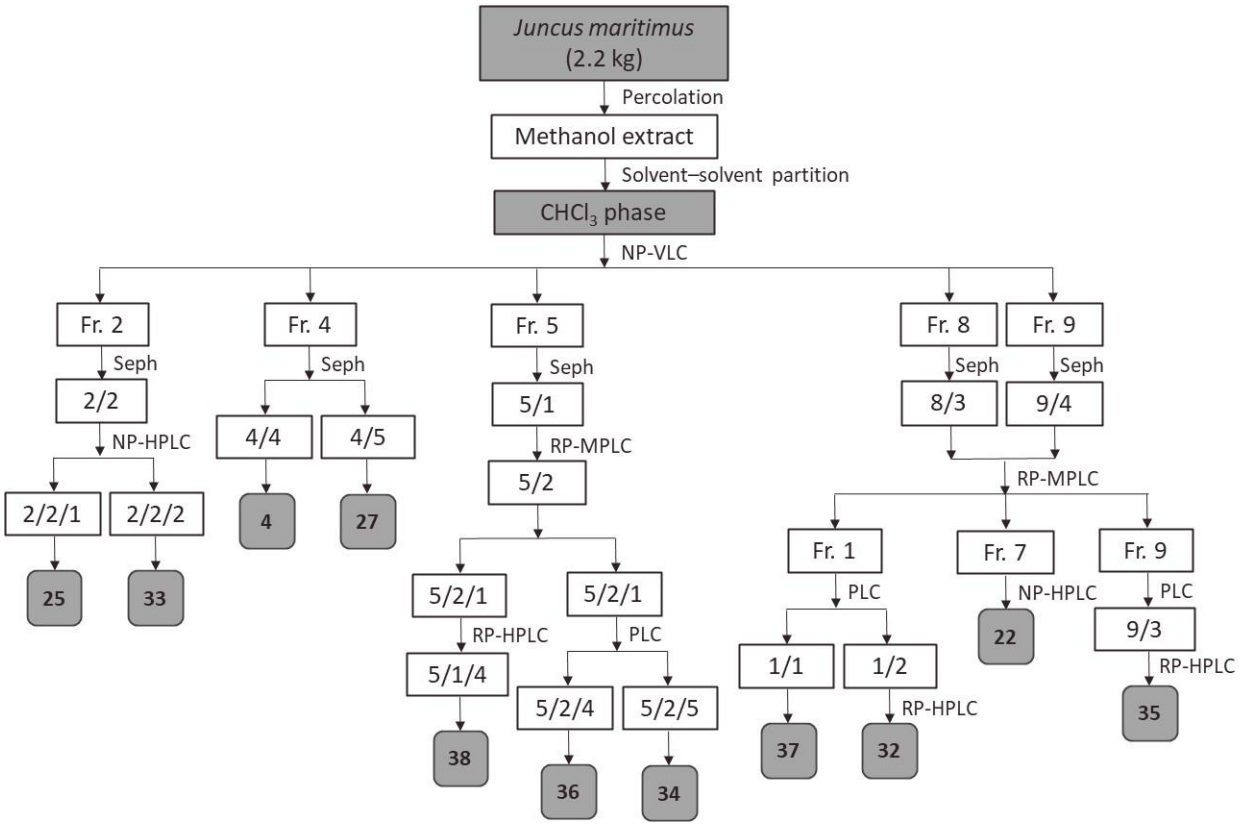

Isolation of compounds from *J. maritimus*

Isolation of compounds from *J. ensifolius*

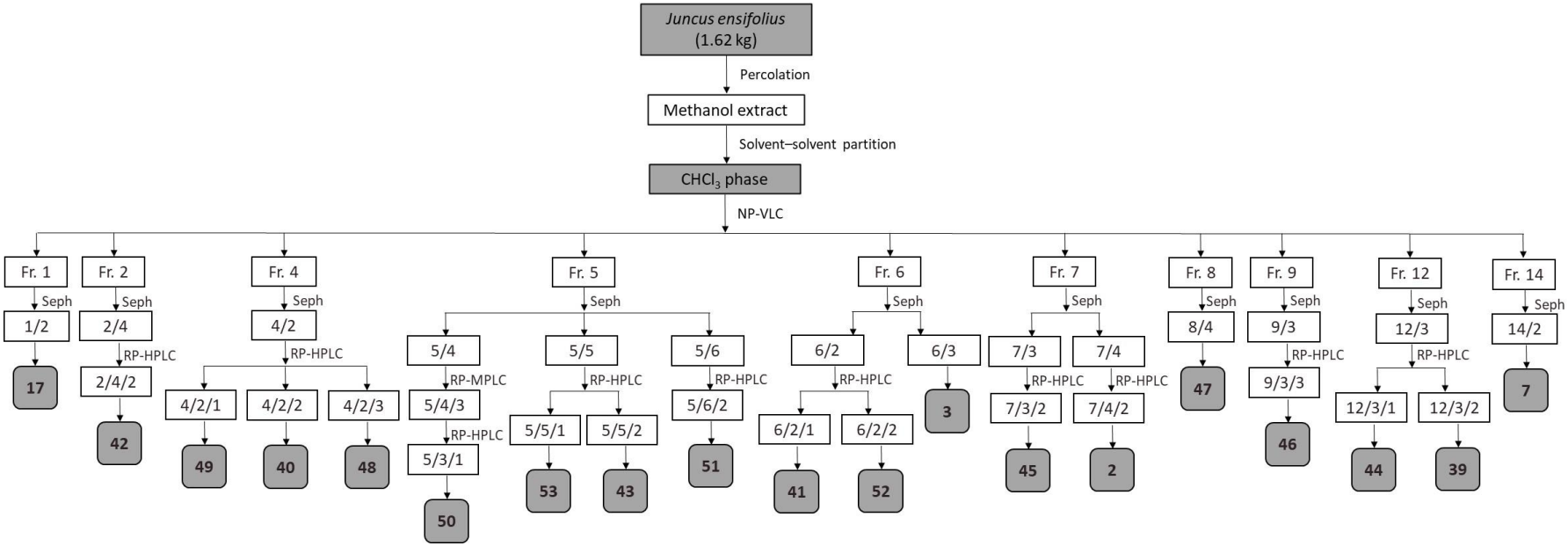

Annex II. ^{1}H and ^{13}C NMR data of new compounds [500 MHz (^{1}H), 125 MHz (^{13}C), δ in ppm]

Table A1. NMR spectroscopic data for juncatrins A (**1**) and B (**2**), and juncuenin B in CD_3OD

Position	**1**		**2**		**3**	
	δ_H (*J* in Hz)	δ_C, type	δ_H (*J* in Hz)	δ_C, type	δ_H (*J* in Hz)	δ_C, type
1		122.5, C		122.5, C		122.9, C
1a		138.2, C		138.4, C		139.1, C
2		156.2, C		156.0, C		155.8, C
3	6.70, d (8.4)	114.0, CH	6.70, d (8.3)	113.8, CH	6.69, d (8.4)	113.8, CH
4	7.35, d (8.4)	123.0, CH	7.33, d (8.3)	122.8, CH	7.33, d (8.4)	122.2, CH
4a		127.1, C		127.3, C		126.2, CH
5	7.11, s	110.9, CH	7.11, s	111.3, CH	7.03, s	109.8, CH
5a		135.9, C		135.0, C		138.5, C
6		155.5, C		154.7, C		154.8, C
7		117.7, C		126.1, C		121.4
8		143.7, C		122.8, C		136.9
8a		122.3, C		131.0, C		128.2
9	2.53, m (2H)	26.2, CH_2	2.89, dd (6.4, 6.9) (2H)	27.3, CH_2	2.65, m (2H)	26.7, CH_2
10	2.73, m (2H)	26.2, CH_2	2.71, dd (6.5, 6.9) (2H)	26.1, CH_2	2.71, m (2H)	26.9, CH_2
11	2.17, s	11.6, CH_3	2.16, s	11.6, CH_3	2.16, s	13.1, CH_3
12	2.07, s	12.4, CH_3	2.33, s	14.1, CH_3	2.15, s	11.6, CH_3
13		211.4, C		82.2, C	6.74, dd (11.4, 17.8)	135.0, CH
14	2.48, s	32.9, CH_3	3.78, s	86.0, CH	5.54, d (11.3) 5.12, d (17.8)	120.1, CH_2

Table A2. ^{1}H and ^{13}C NMR data of compounds **10–12**

	10[a]		**11**[a]		**12**[b]	
position	δ_H (*J* in Hz)	δ_c, type	δ_H (*J* in Hz)	δ_c, type	δ_H (*J* in Hz)	δ_c, type
1		121.8, C		122.3, C		123.5, C
1a		142.2, C		137.2, C*		138.3, C
2		156.0, C		156.2, C		154.2, C
3	6.69, d (8.5)	112.9, CH	6.72, d (8.5)	114.0, CH	7.00, d (8.6)	111.7, CH
4	7.32, d (8.5)	131.1, CH	7.43, d (8.5)	123.5, CH	7.18, d (8.6)	126.5, CH
4a		127.4, C		127.7, C		127.4, C
5		137.3, C	7.53, d (8.0)	123.1, CH		135.7, C
5a		127.2, C		136.8, C		124.9, C
6	6.84, d (2.4)	113.6, CH	7.25, d (8.0)	128.6, CH	6.80, d (2.2)	112.6, CH
7		156.7, C		134.3, C		155.8, C
8	6.64, d (2.4)	115.0, CH		138.5, C*	6.66, br s	114.3, CH
8a		141.8, C		135.1, C		140.3, C
9	2.62, m	31.4, CH_2	2.82, m	27.1, CH_2	2.59, m	29.7, CH_2
10	2.75, m	26.5, CH_2	2.70, m	26.2, CH_2	2.64, m	25.1, CH_2
11	4.65, s	66.5, CH_2	2.18, s	11.6, CH_3	2.21, s	11.9, CH_3
11-OCH_3	3.40, s	58.1, CH_3				
12	6.91, dd (17.4, 10.8)	140.2, CH	4.44, s	74.3, CH_2	6.84, dd (17.3, 10.8)	138.4, CH
12-OCH_3			3.36, s	58.1, CH_3		
13	5.65, dd (17.4, 1.3) 5.21, dd (10.8, 1.3)	113.9, CH_2	6.85, dd (17.9, 11,5)	135.4, CH	5.64, d (17.3) 5.27, d (10.8)	114.1, CH_2
14			5.57, dd (11.5, 2.1) 5.25, dd (17.9, 2.1)	120.9, CH_2		

[a] Measured in CD_3OD; [b] Measured in DMSO-d_6; glucose part of compound **12**: δ_H – 4.79 (H-1'; 1H, d, *J* = 7.1 Hz), 3.28 (H-2'; 1H, m), 3.26 (H-3'; 1H, m), 3.16 (H-4'; 1H, m), 3.31 (H-5'; 1H, m), 3.70 (H-6'; 1H, br d, *J* = 11.4 Hz), 3.46 (H-6'; 1H, m); δ_C (with types of carbons) – 101.3 (C-1'; CH), 73.4 (C-2'; CH), 76.7 (C-3'; CH), 69.8 (C-4'; CH), 77.1 (C-5'; CH), 60.8 (C-6'; CH_2).

Table A3. ^{1}H and ^{13}C NMR data of compounds **13–15** in DMSO-d_6

	13		**14**		**15**	
position	δ_H (*J* in Hz)	δ_c, type	δ_H (*J* in Hz)	δ_c, type	δ_H (*J* in Hz)	δ_c, type
1		120.7, C		120.3, C		123.4, C
1a		138.9, C		138.9, C		138.8, C
2		154.3, C		153.7, C		153.9, C
3	6.72, d (8.4)	111.6, CH	6.71, d (8.4)	111.6, CH	7.00, d (8.6)	111.8, CH
4	7.10, d (8.4)	126.9, CH	7.13, d (8.4)	125.9, CH	7.26, d (8.6)	125.9, CH
4a		124.3, C		125.0, C		127.7, C
5		135.0, C		144.2, C		144.6, C
5a		128.0, C		124.8, C		124.4, C
6	7.06, d (2.1)	113.6, CH	6.92, d (2.2)	112.0, CH	6.94, d (2.2)	112.1, CH
7		155.4, C		155.4, C		155.8, C
8	6.92, d (2.1)	115.1, CH	6.56, d (2.2)	113.1, CH	6.58, d (2.2)	113.1, CH
8a		139.9, CH		139.4, C		139.8, C
9	2.59-2.65, m	29.9, CH_2	2.48-2.55, m	30.5, CH_2	2.51-2.57, m	30.4, CH_2
10	2.59-2.65, m	25.0, CH_2	2.59, m 2.49, m	25.4, CH_2	2.61, m 2.51-2.57, m	25.3, CH_2
11	2.13, s	11.7, CH_3	2.12, s	11.7, CH_3	2.22, s	12.0, CH_3
11-OCH_3						
12	6.85, dd (17.3, 10.8)	138.0, CH	5.05, q (6.2)	64.2, CH	5.04, q (5.9)	64.2, CH
12-OCH_3						
13	5.74, d (17.4) 5.26, d (10.8)	114.4, CH_2	1.39, d (6.2)	25.6, CH_3	1.40, d (5.9)	25.6, CH_3
14						
1′	4.88, d (7.4)	100.7, CH			4.81, d (7.1)	101.2, CH
2′	3.23, m	73.3, CH			3.27, m[a]	73.4, CH
3′	3.26, m	76.7, CH			3.27, m[a]	76.7, CH
4′	3.14, dd (8.9, 8.3)	69.9, CH			3.16, m	69.8, CH
5′	3.33, m	77.2, CH			3.31, m (overlaps with H_2O)	77.0, CH
6′	3.70, br d (11.4) 3.45, m	60.8, CH_2			3.70, br d (11.4) 3.47, dd (11.4, 5.5)	60.8, CH_2

[a] Interchangeable signals

Table A4. ^{1}H and ^{13}C NMR data of compounds **16** and **17**

	16[a]		**17**[b]	
position	δ_H (*J* in Hz)	δ_c, type	δ_H (*J* in Hz)	δ_c, type
1		120.5, C		118.7, C
1a		139.4, C		134.9, C
2		154.0, C		154.1, C
3	6.73, d (8.4)	111.6, CH	7.10, d (9.1)	115.8, CH
4	7.21, d (8.4)	126.2, CH	8.58, d (9.1)	128.1, CH
4a		124.6, C		126.0, C
5		144.0, C		138.2, C
5a		127.6,C		128.7, C
6	7.13, d (2.3)	113.6, CH[c]	7.42, br s	131.3, CH
7		155.5, C		135.7, C
8	6.88, d (2.3)	113.6, CH[c]	7.59, br s	129.2, CH
8a		139.8, C		133.3, C
9	2.54-2.64, m	30.6, CH_2	7.65, d (9.1)	128.4, CH
10	2.54-2.64, m	25.3, CH_2	7.89, d (9.1)	124.0, CH
11	2.13, s	11.7, CH_3	2.56, s	11.4, CH_3
OCH_3-11				
12	5.07 m, (overlaps with H_2O)	64.3, CH	7.48, dd (17.2, 11.0)	143.6, CH
OCH_3-12				
13	1.39, d (6.0)	25.5, CH_3	5.73, dd (17.2, 1.7) 5.40, dd (16.9, 1.7)	114.3, CH_2
14			2.51, s	21.3, CH_3
1′	4.85, d (7.5)	100.7, CH		
2′	3.24, m	73.3, CH		
3′	3.27, m	76.7, CH		
4′	3.18, m	69.7, CH		
5′	3.30, m	77.1, CH		
6′	3.68, br d (11.4) 3.49, m	60.7, CH_2		

[a] Measured in DMSO-d_6; [b] Measured in CD_3OD; [c] Interchangeable signals

Table A5. ^{1}H and ^{13}C NMR data of compounds **18** and **19** in DMSO-d_6

	18		**19**	
position	δ_H (*J* in Hz)	δ_c, type	δ_H (*J* in Hz)	δ_c, type
1		120.1, C		120.6, C[a]
1a		139.2, C		139.3, C
2		153.3, C		153.7, C
3	6.74, d (8.4)	111.7, CH	6.68 (d, overlaps with H-8′)	111.6, CH
4	7.62, d (8.4)	125.1, CH	7.03, d (7.8)	125.1, CH
4a		126.2, C		125.1, C
5		142.5, C		142.8, C
5a		125.1, C		125.9, C
6	6.12, d (2.0)	114.2, CH	6.76, d (2.2)	113.7, CH
7		154.3, C		155.2, C
8	6.40, d (2.0)	111.9, CH	6.57, d (2.2)	112.7, CH
8a		139.9, C		140.1, C
9	2.47, m	31.0, CH_2	2.52-2.58, m	30.7, CH_2
10	2.53, m	25.7, CH_2	2.64, m	25.4, CH_2
			2.52, m[a]	
11	2.15, s	11.7, CH_3[a]	2.12, s	11.7, CH_3
12	5.19, d (9.3)	30.8, CH	4.13, m	35.4, CH
13	2.62, m	30.0, CH_2	3.17, m	30.7, CH_2
	2.20, m		2.59, m[a]	
14				
1′		120.5, C		120.5, C[a]
1a′		138.6, C		133.7, C
2′		153.6, C		153.8, C
3′	6.72, d (8.4)	111.5, CH	6.72, d (8.1)	111.6, CH
4′	7.04, d (8.4)	126.7, CH	7.05, d (8.1)	126.6, CH
4a′		124.9, C		124.7, C
5′		130.5, C		129.5, C
5a′		124.3, C		124.5, C
6′		123.9, C		119.4, C
7		152.3, C		151.9, C
8′	6.56, s	113.4, CH	6.67 (s, overlaps with H-3)	113.8, CH
8a′		137.3, C		137.1, C
9′	2.59, m	29.7, CH_2	2.59, m[a]	29.7, CH_2
	2.42, m		2.44, m	
10′	2.87, m	25.3, CH_2	2.80, m	25.3, CH_2
	2.40, m		2.42, m	
11′	2.14, s	11.9, CH_3[a]	2.13, s	11.8, CH_3
12′	6.77, dd (9.7, 2.6)	127.5, CH	6.78, dd (9.8, 2.0)	127.0, CH
13′	5.76, m	124.2, CH	5.93, br d (9.8)	132.3, CH

[a] Interchangeable signals

Table A6. ^{1}H and ^{13}C NMR data of compounds **20** and **21** in CD_3OD

	20		**21**	
position	δ_H (*J* in Hz)	δ_c, type	δ_H (*J* in Hz)	δ_c, type
1		121.9, C		118.1, C
1a		140.2, C		133.1, C[a]
2		155.1, C		153.1,C
3	6.56, d (8.6)	112.2, CH	6.96, d (9.1)	115.2, CH
4	7.02, d (8.6)	128.4, CH	8.36, d (9.1)	127.8, CH
4a		126.7, C[a]		126.3, C
5		136.5, C		137.1, C
5a		128.2, C		124.9, C
6	6.25, d (1.9)	112.7, CH	7.22, s	118.6, CH
7		156.9, C		152.8, C
8	6.33, br s	115.6, CH		122.9, CH
8a		141.0, C		133.2, C[a]
9	2.36-2.44, m	31.3, CH_2	8.02, d (9.6)	125.3, CH
10	2.63, m	26.5, CH_2	7.68, d (9.6)	123.2, CH
	2.48, m			
11	2.14, s	11.7, CH_3	2.46, s	11.1, CH_3
12	6.70, dd (17.4, 10.9)	139.8, CH	7.36, dd (17.2, 10.7)	143.4, CH
13	5.00, br d (17.4)	113.3, CH_2	5.74, dd (17.2, 1.3)	113.1, CH_2
	4.92, br d (10.9)		5.33, dd (10.7, 1.3)	
14			4.58, s	22.8, CH
1′		122.7, C		121.3, C
1a′		141.4, C		140.0, C
2′		155.5, C		154.7, C
3′	6.79, d (8.6)	112.6, CH[a]	6.50, d (8.4)	112.1, CH
4′	7.04, d (8.6)	127.3, CH	6.98, d (8.4)	128.5, CH
4a′		126.7, C[a]		127.4, C[a]
5′		141.8, C		134.7, C
5a′		128.6, C		128.7, C
6′	6.94, d (2.1)	112.6, CH[a]	7.00, s	112.7, CH
7		156.9, C		154.1, C
8′	6.58, d (2.1)	114.7, CH		127.5, CH[a]
8a′		141.3, C		141.3, C
9′	2.65, m	31.8, CH_2	2.42, m	27.2, CH_2
	2.52, m			
10′	2.98, br d (14.6)	27.2, CH_2	2.47, m	26.4, CH_2
	2.30, m			
11′	2.27, s	12.1, CH_3	2.09, s	11.6, CH_3
12′	5.80, q (6.2)	72.1, CH	6.85, dd (17.4, 10.8)	140.4, CH
13′	1.86, d (6.2)	24.1, CH_3	5.65, dd (17.4, 1.2)	112.5, CH_2
			5.13, dd (10.8, 1.2)	

[a] Interchangeable signals

Table A7. ^{1}H and ^{13}C NMR data of compounds **32**–**34**

Atom	**32**[a]		**33**[b]		**34**[a]	
	δ_H (*J* in Hz)	**δc, Type**	**δ_H (*J* in Hz)**	**δc, Type**	**δ_H (*J* in Hz)**	**δc, Type**
1	-	121.6, C	-	120.9, C	-	116.3, C
1a	-	140.1, C	-	137.7, C	-	131.5, C
2	-	155.1, C	-	153.3, C	-	153.4, C
3	6.63, d (8.4)	112.2, CH	6.73, d (8.2)	113.3, CH	7.02, s	117.0, CH
4	7.13, d (8.4)	128.6, CH	7.47, d (8.2)	122.52*, CH	-	130.9, C
4a	-	127.2, C	-	128.4, C	-	122.47*, C
5	-	136.6, C	7.49, d (8.4)	122.49*, CH	-	134.6, C
5a	-	128.3, C	-	133.3, C	-	122.52*, C
6	6.92, s	113.0, CH	7.11, d (8.4)	128.2, CH	-	125.6, C
7	-	155.3, C	-	134.4, C	-	155.1, C
8	-	124.4, C	-	136.8, C	7.17, s	111.1, CH
8a	-	141.2, C	-	134.1, C	-	130.5, C
9	2.76, m (2H)	26.9, CH_2	2.88, m (2H)	26.3, CH_2	7.56, d (9.2)	126.9, CH
10	2.68, m (2H)	26.4, CH_2	2.74, m (2H)	25.5, CH_2	7.79, d (9.2)	123.1, CH
11	2.21, s	11.7, CH_3	2.24, s	11.5, CH_3	2.49, s	10.7, CH_3
12	6.90, dd (17.4, 10.9)	140.4, CH	2.32, s	20.8, CH_3	5.45, br s	67.4, CH
13	5.65, dd (17.4, 1.2) 5.18, dd (10.9, 1.2)	113.2, CH_2	6.77, dd (17.9, 11.4)	135.1, CH	3.38, br d (16.4) 3.29[+]	38.3, CH_2
14	4.79, s (2H)	56.6, CH_2	5.59, dd (11.4, 2.0) 5.22, dd (17.9, 2.0)	120.1, CH_2	2.50, s	11.4, CH_3

[a] measured in CD_3OD; [b] measured in $CDCl_3$; * interchangeable signals; [+] overlapped with residual H_2O signal

Table A8. ^{1}H and ^{13}C NMR data of compound **35** in CD_3OD

Effusol Monomer			**OH-2 Effusol Monomer**		
Atom	**δ_H (*J* in Hz)**	**δc, Type**	**Atom**	**δ_H (*J* in Hz)**	**δc, Type**
1	-	127.7, C	1′	-	123.4, C
1a	-	140.8, C	1′a	-	133.5, C
2	-	154.4, C	2′	-	144.6, C
3	6.83, d (8.4)	117.8, CH	3′	-	156.6 [#], C
4	7.38, d (8.4)	128.7, CH	4′	6.66, s	116.1, CH
4a	-	131.4, C	4′a	-	127.06 *, C
5	-	137.9, C	5′	-	137.4, C
5a	-	126.7, C	5′a	-	126.98 *, C
6	6.88, d (2.2)	113.8[#], CH	6′	6.68, br s	113.8 [#], CH
7	-	157.2, C	7′	-	156.6 [#], C
8	6.69 d (2.2)	115.1, CH	8′	6.61, br s	115.0, CH
8a	-	142.1, C	8′a	-	141.7, C
9	2.68, m (2H)	31.4, CH_2	9′	2.63[#], m (2H)	31.6, CH_2
10	2.78, m (2H)	26.7, CH_2	10′	2.64[#], m (2H)	26.1, CH_2
11	2.28, s	12.4, CH_3	11′	2.30, s	12.0, CH_3
12	6.96, dd (17.4, 10.9)	140.1, CH	12′	6.64 dd (17.3, 11.4)	140.2, CH
13	5.67, d (17.4) 5.23, d (10.9)	114.2, CH_2	13′	5.33, dd (17.3, 0.9) 4.78, d (11.4)	113.7, CH_2

[#] overlapping signals; * interchangeable signals

Table A9. ^{1}H and ^{13}C NMR data of compounds **39–41**

position	**39**[a]		**40**[b]		**41**[a]	
	δ_H (*J* in Hz)	δ_C, type	δ_H (*J* in Hz)	δ_C, type	δ_H (*J* in Hz)	δ_C, type
1		121.1, C		117.5, C		123.5, C
1a		139.5, C		135.9, C		139.4, C
2		155.0, C		152.4, C		155.9, C
3	6.66, d (8.6)	112.8, CH	6.86, d (8.6)	114.1, CH	6.76, d (8.4)	114.3, CH
4	7.97, d (8.6)	128.1, CH	7.53, d (8.6)	129.3, CH	7.38, d (8.4)	129.2, CH
4a		125.8, C		127.6, C		126.4, C
5a		123.2, C		130.6, C		132.0, C
5		155.3, C		135.3, C		136.0, C
6	6.67, s	118.5, CH	7.25, br s	127.7, CH	7.21, br s	128.5, CH
7		136.8, C		136.3, C		136.8, C
8		122.1, C	7.02, br s	127.9, CH	7.03, br s	130.5, CH
8a		140.9, C		138.5, C		134.8, C
9	2.77, m 2.87, m	27.8, CH_2	2.73, m (2H)	29.6, CH_2	2.84, dd (16.0, 3.0) 3.05, dd (16.0, 2.8)	39.1, CH_2
10	2.64, m (2H)	26.5, CH_2	2.54, m (2H)	24.1, CH_2	5.10, br t (2.8)	64.3, CH
11	2.18, s (3H)	11.6, CH_3	5.09, d (14.5) 5.19, d (14.5)	66.2, CH_2	2.33*, s (3H)	11.1, CH_3
OCH_3–11						
12	2.38, s (3H)	20.7, CH_3	6.98, dd (17.4, 10.9)	138.9, CH	7.02, dd (17.4, 10.9)	140.9, CH
13	5.65, dd (9.9, 2.9)	75.6, CH	5.28, dd (10.9, 1.3) 5.72, dd (17.4, 1.3)	114.7, CH_2	5.21, dd (10.9, 1.4) 5.66, dd (17.4, 1.4)	113.6, CH_2
14	4.32, dd (11.9, 2.9) 4.42, dd (11.9, 9.9)	67.1, CH_2	2.37, s (3H)	21.2, CH_3	2.33*, s (3H)	21.1, CH_3

[a] measured in CD_3OD; [b] measured in $CDCl_3$; * overlapping signals; luteolin part of compound **1**: δ_H – 6.63 (H-3'; 1H, s), 6.23 (H-6'; 1H, d, *J* = 2.1 Hz), 6.47 (H-8'; 1H, d, *J* = 2.1 Hz), 7.57 (H-2"; 1H, d, *J* = 2.2 Hz), 7.06 (H-5"; 1H, d, *J* = 8.6 Hz), 7.53 (H-6"; 1H, dd, *J* = 8.6 and 2.2 Hz); δ_C (with types of carbons) – 165.5 (C-2'; C), 104.9 (C-3'; CH), 183.9 (C-4'; C), 105.5 (C-4a'; C), 163.3 (C-5'; C), 100.3 (C-6'; CH), 166.3 (C-7'; C), 95.2 (C-8'; CH), 159.5 (C-8a'; C), 125.6 (C-1"; C), 116.6 (C-2"; CH), 145.0 (C-3"; C), 148.6 (C-4"; C), 119.2 (C-5"; CH), 121.3 (C-6"; CH); hemiacetal part originated from 4-hydroxybenzaldehyde of compound **2**: δ_H – 5.94 (H-1'; 1H, s), 7.50 (H-3'/H-7'; 2H, d, *J* = 8.5 Hz), 6.89 (H-4'/H-6'; 2H, d, *J* = 8.5 Hz); δ_C (with types of carbons) – 98.7 (C-1'; CH), 129.8 (C-2'; C), 2 x 128.2 (C-3'/C-7'; 2 x CH), 2 x 115.5 (C-4'/C-6'; 2 x CH), 156.7 (C-5'; C)

Table A10. ^{1}H and ^{13}C NMR data of compounds **42–44** in CD_3OD

position	**42**		**43**		**44**	
	δ_H (*J* in Hz)	δ_C, type	δ_H (*J* in Hz)	δ_C, type	δ_H (*J* in Hz)	δ_C, type
1		121.9, C		121.2, C		121.2, C
1a		142.8, C		139.5, C		139.7, C
2		156.5, C		154.7, C		154.9, C
3	6.71, d (8.5)	113.0, CH	6.65, d (8.6)	112.7, CH	6.65, d (8.6)	112.7, CH
4	7.40, d (8.5)	131.6, CH	7.98, d (8.6)	127.9, CH	8.03, d (8.6)	128.1, CH
4a		127.2, C		126.5, C		126.2, C
5a		132.4, C		121.7, C		123.0, C
5		135.9, C		153.8, C		154.2, C
6	7.22, br s	128.0, CH	6.61, s	117.0, CH	6.91, s	114.9, CH
7		136.8, C		135.6, C		138.54[#], C
8	7.00, br s	128.5, CH		129.4, C		128.5, C
8a		140.0, C		138.4, C		138.57[#], C
9	2.66, m (2H)	31.0, CH_2	2.72, m (2H)	28.5, CH_2	2.74, m (2H)	28.2, CH_2
10	2.77, m (2H)	26.5, CH_2	2.60, m (2H)	26.7, CH_2	2.63, m (2H)	26.6, CH_2
11	4.66, s (2H)	66.5, CH_2	2.18, s (3H)	11.7, CH_3	2.19, s (3H)	11.7, CH_3
OCH_3–11	3.40, s (3H)	58.1, CH_3				
12	6.92, dd (17.5, 10.9)	140.3, CH	2.22, s (3H)	20.8, CH_3	4.58, s (2H)	63.3, CH_2
13	5.21, dd (10.9, 1.6) 5.68, dd (17.5, 1.6)	113.8, CH_2	6.72, dd (17.9, 11.3)	136.5, CH	6.79, dd (17.8, 11.3)	135.5, CH
14	2.33, s (3H)	21.1, CH_3	5.09, dd (17.9, 2.3) 5.48, dd (11.3, 2.3)	119.5, CH_2	5.17, dd (17.8, 2.2) 5.51, dd (11.3, 2.2)	120.1, CH_2

[#] interchangeable signals

Table A11. ^{1}H and ^{13}C NMR data of compounds **45–47**

position	**45**[a]		**46**[a]		**47**[b]	
	δ_H (J in Hz)	δ_C, type	δ_H (J in Hz)	δ_C, type	δ_H (J in Hz)	δ_C, type
1		121.5, C		122.7, C		121.5, C
1a		139.1, C		138.7, C		139.1, C
2		155.1, C		156.5, C		155.1, C
3	6.66, d (8.6)	112.9, CH	6.72, d (8.4)	114.1, CH	6.66, d (8.6)	112.9, CH
4	8.03, d (8.6)	128.1, CH	7.38, d (8.4)	123.2, CH	8.03, d (8.6)	128.1, CH
4a		125.5, C		127.0, C		125.5, C
5a		121.8, C		137.5, C		121.8, C
5		155.5, C	7.16, s	112.2, CH		155.5, C
6	6.61, s	117.4, CH		156.1, C	6.61, s	117.4, CH
7		132.4, C		127.2, C		132.4, C
8		134.3, C		122.2, C		134.3, C
8a		135.8, C		131.3, C		135.8, C
9	2.55, m (2H)	28.3, CH_2	2.94, m (2H)	27.2, CH_2	2.55, m (2H)	28.3, CH_2
10	2.68, m (2H)	26.3, CH_2	2.76, m (2H)	26.1, CH_2	2.68, m (2H)	26.3, CH_2
11	2.18, s (3H)	11.7, CH_3	2.19, s (3H)	11.5, CH_3	2.18, s (3H)	11.7, CH_3
12	2.17, s (3H)	19.1, CH_3	4.93, s (2H)	60.1, CH_2	2.17, s (3H)	19.1, CH_3
13		211.4, C		81.1, C		211.4, C
14	2.46, s (3H)	33.1, CH_3	3.85, s	86.4, CH	2.46, s (3H)	33.1, CH_3

[a] measured in CD_3OD; [b] measured in $CDCl_3$

Table A12. ^{1}H and ^{13}C NMR data of symmetric dimers **48** and **51** in CD_3OD

position	**48**		**51**	
	δ_H (J in Hz)	δ_C, type	δ_H (J in Hz)	δ_C, type
1, 1’		122.9, C		124.5, C
1a, 1a’		139.0, C		137.7, C
2, 2’		151.4, C		153.3^{+}, C
3, 3’		124.9, C		126.8, C
4, 4’	8.12, s	130.3, CH	7.48, s	125.3, CH
4a, 4a’		127.4, C		128.3^{+}, C
5a, 5a’		121.5, C		134.9, C
5, 5’		153.9, C	7.17, s	111.3, CH
6, 6’	6.60, s	117.0, CH		155.0, C
7, 7’		136.0, C		126.4, C
8, 8’		129.5, C		123.0, C
8a, 8a’		138.6, C		131.2, C
9, 9’	2.82, m (2H)	28.5, CH_2	2.99, m (2H)	27.5, CH_2
10, 10’	2.70, m (2H)	26.9, CH_2	2.84, m (2H)	26.4, CH_2
11, 11’	2.32, s (3H)	12.4, CH_3	2.32, s (3H)	12.3, CH_3
12, 12’	2.23, s (3H)	20.8, CH_3	2.33, s (3H)	14.1, CH_3
13, 13’	6.76, dd (17.9, 11.3)	136.5, CH		82.2, C
14, 14’	5.13, dd (17.9, 2.2) 5.52, dd (11.3, 2.2)	119.6, CH_2	3.85, s	86.1, C

$^{+}$ only seen in the HMBC spectrum

Table A13. ^{1}H (500 MHz) and ^{13}C (125 MHz) NMR data of compounds **49** and **50** in CD_3OD

position	**49**		**50**	
	δH (J in Hz)	δC, type	δH (J in Hz)	δC, type
1		117.4, C		121.2, C
1a		134.9, C		139.82#, C
2		153.47#, C		154.9, C
3	6.53, d (9.4)	115.4, CH	6.64, d (8.6)	112.7, CH
4	7.56, d (9.4)	127.1, CH	8.02, d (8.6)	128.2, CH
4a		125.82, C		126.5, C
5a		131.0, C		122.1, C
5		118.6, C		151.3, C
6		153.37#, C		125.3, C
7		123.3, C		135.4, C
8		138.8, C		130.49, C
8a		125.5, C		137.9, C
9	8.04, d (9.5)	125.80, CH	2.87, m (2H)	28.4, CH_2
10	7.72, d (9.5)	120.9, CH	2.69*, m (2H)	26.8, CH_2
11	2.47, s (3H)	11.2, CH_3	2.21, s (3H)	11.7, CH_3
12	2.44, s (3H)	14.5, CH_3	2.03, s (3H)	18.5, CH_3
13	7.19, dd (17.9, 11.4)	136.9, CH	6.82, dd (17.8, 11.2)	137.3, CH
14	5.41, dd (17.9, 2.2)	121.8, CH_2	5.16, dd (17.8, 2.4)	119.9, CH_2
	5.85, dd (11.4, 2.2)		5.54, dd (11.2, 2.4)	
1’		123.4, C		122.7, C
1a’		140.5, C		139.89#, C
2’		152.2, C		152.6, C
3’		123.6, C		120.8, C
4’	7.96, s	130.0, CH	7.92, s	130.38, CH
4a’		128.6, C		127.3, C
5a’		121.2, C		121.4, C
5’		153.9, C		153.9, C
6’	6.55, s	117.0, CH	6.61, s	117.1, CH
7’		136.2, C		136.0, C
8’		129.4, C		129.5, C
8a’		138.4, C		138.5, C
9’	2.77, m	28.6, CH_2	2.78*, m (2H	28.8, CH_2
	3.05, ddd (15.1, 6.9, 4.3)			
10’	2.67, m	27.1, CH_2	2.67*, m	27.0, CH_2
	2.94, ddd (11.1, 6.9, 4.3)		2.77*, m	
11’	2.32, s (3H)	12.4, CH_3	2.30, s (3H)	12.3, CH_3
12’	2.22, s (3H)	20.8, CH_3	2.23, s (3H)	20.8, CH_3
13’	6.78, dd (17.9, 11.3)	136.4, CH	6.76, dd (17.8, 11.3)	136.4, CH
14’	5.16, dd (17.9, 2.2)	119.7, CH_2	5.13, dd (17.8, 2.2)	119.6, CH_2
	5.54, dd (11.3, 2.2)		5.52, dd (11.3, 2.2)	

* overlapping signals; # interchangeable signals reflects the chemical diversity of phenanthrenes

Table A14. Antiproliferative activity (IC_{50}) of phenanthrenes **4**, **24**, **26**, **30**, **32**–**38**

Compound	IC_{50} (μM) ± SD							
	HeLa	**HTB-26**	**T-47D**	**A2780**	**A2780cis**	**MCF-7**	**KCR**	**MRC-5**
4	2.3 ± 0.7	57.0 ± 2.73	24.6 ± 1.9	33.1 ± 3.1	30.4 ± 0.4	48.6 ± 3.4	39.3 ± 1.6	60.1 ± 5.1
24	0.5 ± 0.0	41.7 ± 3.5	25.0 ± 0.4	23.8 ± 1.3	37.1 ± 2.8	37.1 ± 1.1	35.8 ± 1.7	40.9 ± 2.0
26	24.7 ± 0.5	85.3 ± 4.5	26.6 ± 1.1	30.0 ± 3.6	32.3 ± 2.3	38.0 ± 2.0	70.6 ± 3.1	71.1 ± 1.3
30	25.2 ± 0.6	24.7 ± 2.1	6.2 ± 0.1	25.6 ± 2.4	16.3 ± 0.3	14.0 ± 0. 6	19.6 ± 0.9	20.1 ± 1.6
32	57.0 ± 1.3	48.7 ± 1.6	12.8 ± 0.9	21.5 ± 0.4	40.1 ± 0.4	34.7 ± 3.0	57.6 ± 0.7	75.4 ± 1.8
33	11.0 ± 0.9	>100	>100	>100	>100	97.0 ± 0.3	>100	>100
34	43.2 ± 0.7	35.9 ± 1.5	17.0 ± 0.6	23.7 ± 0.1	18.6 ± 0.1	9.8 ± 0.6	>100	15.0 ± 0.2
35	22.5 ± 1.2	25.1 ± 0.3	9.1 ± 0.4	14.1 ± 1.3	13.3 ± 0.1	14.2 ± 0.3	16.2 ± 0.6	17.1 ± 3.1
36	76.7 ± 1.8	75.0 ± 5.0	41.4 ± 5.8	43.5 ± 1.1	52.8 ± 2.4	45.7 ± 2.4	68.4 ± 2.5	78.4 ± 3.7
37	>100	>100	57.0 ± 7.1	>100	>100	69.5 ± 1.7	>100	>100
38	24.7 ± 0.3	22.8 ± 0.2	14.2 ± 1.1	22.3 ± 2.7	16.9 ± 4.7	12.9 ± 0.2	24.2 ± 2.1	18.9 ± 4.0
cisplatin	2.3 ± 0.1	20.1 ± 2.3	5.9 ± 0.1	3.6 ± 0.3	7.3 ± 0.2	0.9 ± 0.0	6.5 ± 0.3	0.6 ± 0.0

Table A15. Antiproliferative activity (IC_{50} values) of the isolated compounds (**2**, **3**, **7**, **17**, **39–53**) (SI means selectivity index)

Compound	IC_{50} (μM) ± SD				SI	SI	SI
	COLO 205	**COLO 320**	**HeLa**	**MRC-5**	**MRC-5/COLO 205**	**MRC-5/COLO 320**	**MRC-5/HeLa**
2	34.42 ± 0.57	32.48 ± 0.75	6.65 ± 0.10	26.03 ± 0.85	0.76	0.80	3.91
3	37.08 ± 0.57	30.54 ± 0.93	6.67 ± 0.03	35.85 ± 1.23	0.97	1.17	5.37
7	>100	>100	>100	>100			
17	32.92 ± 0.59	52.36 ± 0.77	58.09 ± 1.20	60.89 ± 0.25	1.85	1.16	1.05
39	3.86 ± 0.08	12.71 ± 0.05	8.25 ±0.51	19.29 ± 0.54	5.00	1.52	2.34
40	45.64 ± 0.50	37.24 ± 0.11	33.49 ± 0.29	51.87 ± 0.14	1.14	1.39	1.55
41	>100	>100	>100	>100			
42	65.61 ± 0.78	61.56 ± 9.95	19.40 ± 0.33	>100	>1.52	>1.62	>5.15
43	31.23 ± 0.66	25.17 ± 0.92	27.46 ± 1.19	44.31 ± 0.61	1.42	1.76	1.61
44	>100	93.71 ± 0.14	74.32 ± 2.98	>100		>1.07	>1.35
45	>100	>100	75.57 ± 0.94	>100			>1.32
46	>100	63.46 ± 2.70	12.31 ± 0.13	>100		>1.58	>8.12
47	18.21 ± 0.28	18.52 ± 0.06	24.09 ± 0.11	49.14 ± 0.83	2.70	2.65	2.04
48	44.48 ± 1.22	42.76 ± 1.28	33.54 ± 1.89	57.75 ± 1.32	1.30	1.35	1.72
49	31.38 ± 0.72	37.84 ± 1.05	29.53 ± 0.31	33.16 ± 0.05	1.06	0.88	1.12
50	26.91 ± 1.19	37.36 ± 2.13	30.22 ± 0.21	50.36 ± 1.30	1.87	1.35	1.67
51	42.72 ± 0.92	37.27 ± 0.55	31.51 ± 0.53	72.54 ± 1.56	1.70	1.95	2.30
52	56.73 ± 0.75	57.66 ± 0.92	10.56 ± 0.09	>100	>1.76	>1.73	>9.47
53	>100	>100	>100	>100			
DMSO	>1%	>1%	>1%	>1%			
cisplatin	41.67 ± 1.62	2.14 ± 0.32	3.62 ± 0.16	2.36 ± 0.33			
doxorubicin	1.36 ± 0.36	0.22 ± 0.004	0.04 ± 0.004	0.53 ± 0.06			

Four parallel measurements were applied for all tested compounds. SI: selectivity index; The selectivity indexes (SI) were calculated as the ratio of the IC_{50} value in the non-tumor cells and the IC_{50} in the cancer cell lines. The compound's activity towards cancer cells is considered as strongly selective if the selectivity index (SI) value is higher than 6, moderately selective if 3 < SI < 6, slightly selective if 1 < SI < 3, and non-selective if SI is lower than 1.

Table A16. Interaction type between doxorubicin and phenanthrenes (**2**, **3**, **17**, **39**–**52**) on HeLa cells.

Compound	CI	SD	Ratio	Interaction
2	0.682	0.3743	13.92:1	synergism
3	0.864	0.2338	27.84:1	slight synergism
17	0.579	0.0855	92.8:1	synergism
39	0.272	0.2124	9.28:1	strong synergism
40	0.584	0.0510	23.2:1	synergism
41	0.580	0.0387	13.92:1	synergism
42	0.643	0.1623	55.68:1	synergism
43	0.001	0.0003	9.28:1	very strong synergism
44	0.159	0.1414	23.2:1	strong synergism
45	0.568	0.0268	46.4:1	synergism
46	0.033	0.0106	185.6:1	very strong synergism
47	0.180	0.0675	9.28:1	strong synergism
48	0.454	0.0269	38.4:1	synergism
49	0.112	0.0387	10.44:1	strong synergism
50	0.120	0.0418	11.6:1	strong synergism
51	0.445	0.1202	46.4:1	synergism
52	0.279	0.0574	13.92:1	strong synergism

Combination index (CI) values are expressed as the average of CI values calculated based on different drug ratios ± standard deviation (SD), for an inhibitory concentration of 50% (IC_{50}). CI < 0.1: very strong synergism; 0.1 < CI < 0.3: strong synergism; 0.3 < CI < 0.7: synergism; 0.7 < CI < 0.9: moderate to slight synergism; 0.9 < CI < 1.1: nearly additive; 1.1 < CI < 1.45: slight to moderate antagonism; 1.45 < CI < 3.30: antagonism.

Annex III. Structure of the isolated compounds (phenanthrene monomers)

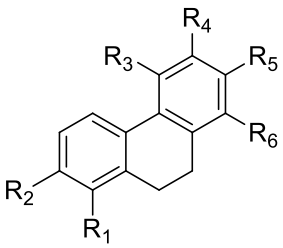

	R_1	R_2	R_3	R_4	R_5	R_6
1	CH_3	OH	H	OH	CH_3	$COCH_3$
2	CH_3	OH	H	OH	CH_3	CCH
3	CH_3	OH	H	OH	CH_3	$CHCH_2$
4	CH_3	OH	$CHCH_2$	H	OH	H
10	CH_2OCH_3	OH	$CHCH_2$	H	OH	H
11	CH_3	OH	H	H	CH_2OCH_3	$CHCH_2$
12	CH_3	O-glc	$CHCH_2$	H	OH	H
13	CH_3	OH	$CHCH_2$	H	O-glc	H
14	CH_3	OH	$CH(CH_3)OH$	H	OH	H
15	CH_3	O-glc	$CH(CH_3)OH$	H	OH	H
16	CH_3	OH	$CH(CH_3)OH$	H	O-glc	H
22	CH_3	OCH_3	$CHCH_2$	CH_3	OH	H
23	CH_3	OCH_3	$CHCH_2$	H	OH	H
24	CH_3	OH	$CHCH_2$	CH_3	OH	H
25	CH_3	OH	$CHCH_2$	H	CH_2OH	H
26	CH_3	OH	CHO	H	OH	H
27	CH_3	OH	$CH(CH_3)OCH_3$	H	OH	H
28	CH_3	OH	CH_2OH	H	OH	H
32	CH_3	OH	$CHCH_2$	H	OH	CH_2OH
33	CH_3	OH	H	H	CH_3	$CHCH_2$
36	CH_3	OH	H	CH_3	$CHCH_2$	H
37	CH_3	OH	$CHCH_2$	H	OH	CH_3
38	CH_3	OH	$CH(CH_3)OCH_3$	H	OH	H
42	CH_2OCH_3	OH	$CHCH_2$	H	CH_3	H
43	CH_3	OH	OH	H	CH_3	$CHCH_2$
44	CH_3	OH	OH	H	CH_2OH	$CHCH_2$
45	CH_3	OH	OH	H	CH_3	$COCH_3$
46	CH_3	OH	H	OH	CH_2OH	CCH
52	CH_2OH	OH	$CHCH_2$	H	CH_3	H

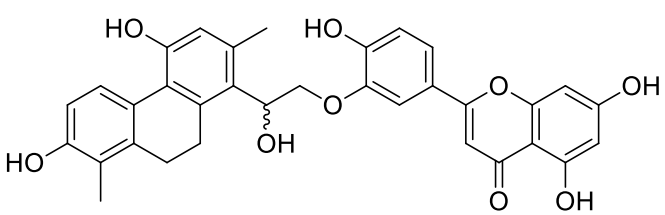

39

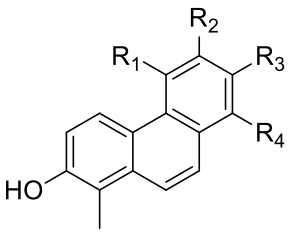

	R_1	R_2	R_3	R_4
5	$CHCH_2$	H	OH	H
17	$CHCH_2$	H	CH_3	H
47	H	OH	CH_3	CCH

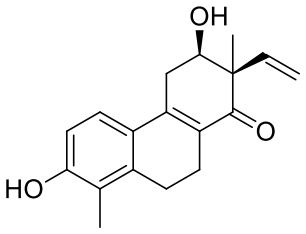

29

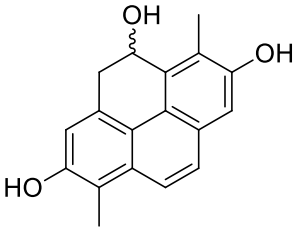

34

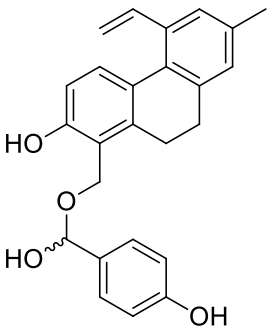

40

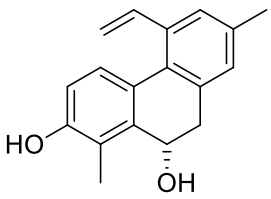

41

Annex III. *Cont.*

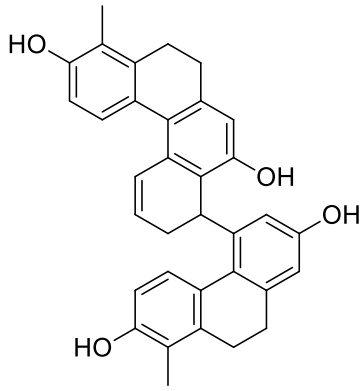

18

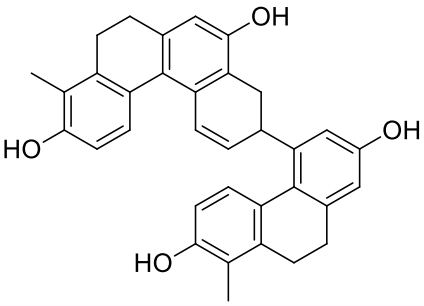

19

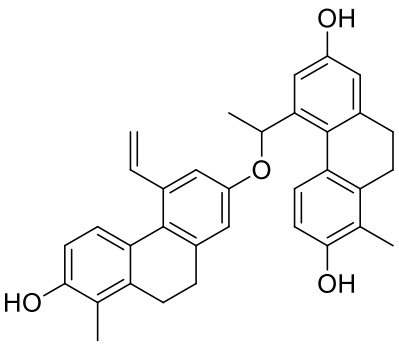

20

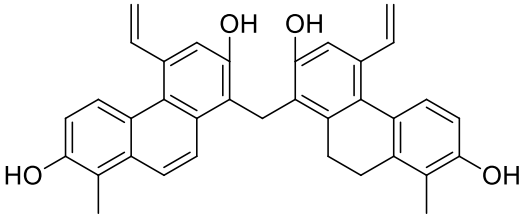

21

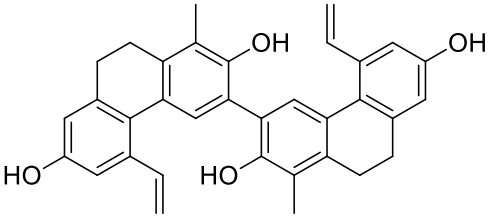

30

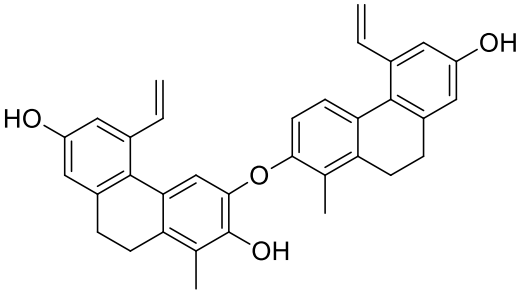

35

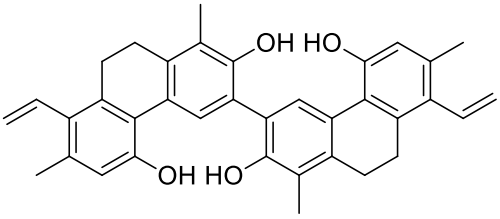

48

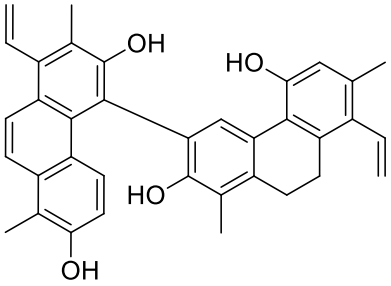

49

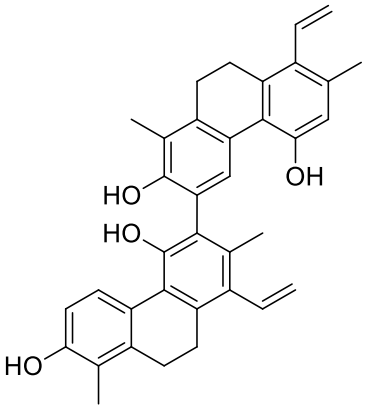

50

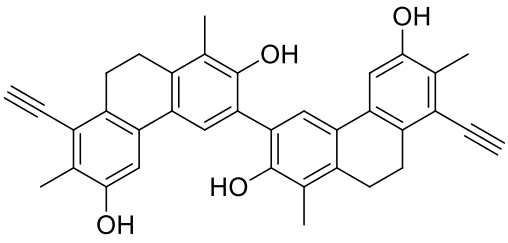

51

Annex III. *Cont*.

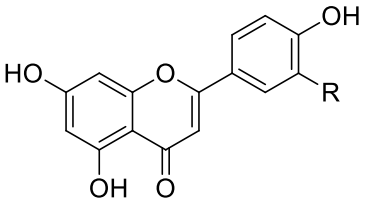

	R
6	H
7	OH

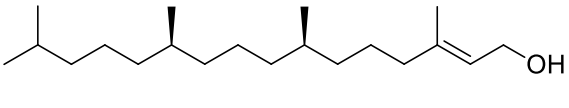

8

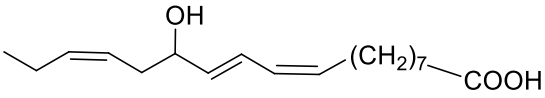

9

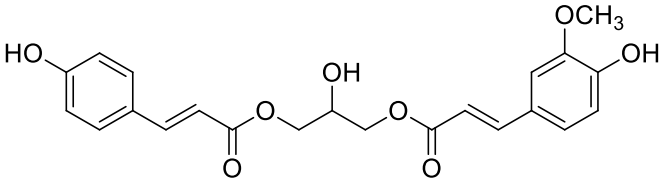

31

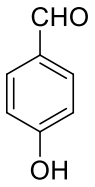

53

APPENDIX

The thesis is based on the following publications:

I. **Stefkó D**, Kúsz N, Csorba A, Jakab G, Bérdi P, Zupkó I, Hohmann J, Vasas A.
Phenanthrenes from *Juncus atratus* with antiproliferative activity
Tetrahedron 2019, **75**: 116-120.

II. **Stefkó D**, Kúsz N, Barta A, Kele Z, Bakacsy L, Szepesi Á, Fazakas Cs, Wilhelm I, Krizbai I. A, Hohmann J, Vasas A.
Gerardiins A–L and structurally related phenanthrenes from the halophyte plant *Juncus gerardii* and their cytotoxicity against triple-negative breast cancer cells
Journal of Natural Products 2020, **83**: 3058-3068.

III. Kúsz N, **Stefkó D***, Barta A, Kincses A, Szemeredi N, Spengler G, Hohmann J, Vasas A.
Juncaceae species as promising sources of phenanthrenes: antiproliferative compounds from *Juncus maritimus* Lam.
Molecules 2021, **26**: 999.

IV. **Stefkó D**, Kúsz N, Szemerédi N, Barta A, Spengler G, Berkecz R, Hohmann J, Vasas A.
Unique phenanthrenes from *Juncus ensifolius* and their antiproliferative and synergistic effects with the conventional anticancer agent doxorubicin against human cancer cell lines
Pharmaceutics 2022, **14**: 608.

* shared first authorship